GULF STATES UTILITIES COMPANY
POST OFFICE BOX 2951 • BEAUMONT, TEXAS 77704
AREA CODE 409 838-6631

May 22, 1985
RBG - 21090
File Code: G9.5

Mr. Harold R. Denton, Director
Nuclear Reactor Regulation
U.S. Nuclear Regulatory Commission
Washington, D.C. 20555

Dear Mr. Denton:

River Bend Station - Unit 1
Docket No. 50-458

Provided for your information are Gulf States Utilities Company (GSU) Final Safety Analysis Report (FSAR) changes that were identified during GSU's indepth review of the River Bend Station Technical Specifications. These changes are provided to ensure consistency between the Technical Specifications and the FSAR.

This letter will complete our response referenced in a letter dated May 6, 1985 (RBG-20903) from W. J. Cahill, Jr. to H. R. Denton.

Sincerely yours,

J. E. Booker

J. E. Booker
Manager - Engineering
Nuclear Fuels & Licensing
River Bend Nuclear Group

JEB/WJR/JEP

B001
1/40

Replace with Insert

4.3.2.1 Nuclear Fuel Design Description

The initial fuel loading is composed of three distinct bundle types, each with a unique rod-by-rod enrichment distribution. The bottom and top of each fuel rod in two of these bundles consists of 6 in of natural uranium. The third bundle type contains only natural uranium fuel rods. The three unique bundle types are distributed in the initial core based on the principal of minimizing radial power peaking and maximizing core reactivity for the EOC state. This same strategy is carried into the reload cores. A diagram of the initial core fuel bundle loading is shown in Fig. 4.3-1.

The peripheral core zone is composed of bundles containing only natural uranium fuel rods. The interior of the core is divided into two zones: an inner zone which comprises about 50 percent of the core area, and an outer zone, a ring, which comprises about 35 percent of the core area. The outer zone consists entirely of the high enrichment bundles. The inner zone is an array of high and medium enrichment bundles arranged in a checkerboard fashion.

Each bundle contains 62 fuel rods and 2 water rods. The water rods have a slightly larger diameter than the fuel rods. The layout and dimensions are presented in Fig. 4.3-2. Gadolinia, in the form of Gd_2O_3, is selectively placed in fuel rods in the high and medium enrichment bundles to provide reactivity control, and is distributed axially to flatten the axial power distribution. The reactivity variations of the high and medium enrichment bundles are designed to complement each other. The low enrichment bundle is composed entirely of natural uranium rods. The fuel rod distributions for the high and medium enrichment bundles are shown in Fig. 4.3-3 and 4.3-4. The axial distribution of enrichment and gadolinia in rods for the high and medium enrichment bundles is shown in Fig. 4.3-5 and 4.3-6, respectively. The natural uranium bundles do not contain gadolinia rods.

The fuel bundle can be represented by axial segments of uniquely defined fuel types. Each fuel type is defined by its average percent by weight U-235 enrichment, and the number and percent by weight of gadolinia rods.

The dominant fuel is that which comprises the greatest volume of fuel of one type in the bundle. The behavior of the dominant fuel type is often used to characterize the typical behavior of the bundle as a whole. The same basic zonal concept of fuel loading is carried into the reload

Replace with Insert

cycles. The lowest reactivity fuel is loaded on the periphery, a high reactivity ring is loaded adjacent to the periphery, and a medium reactivity zone forms the central part of the core.

The bundle reactivity is a complex function of several important physical properties. The important properties consist of the average bundle enrichment, the gadolinia rod location and gadolinia concentration, the void fraction, and the accumulated exposure. The variation in reactivity of the infinite lattice data (k-infinity as a function of void fraction and exposure) for the dominant gadolinia segment of the high enrichment bundle is presented in Fig. 4.3-7. At low exposure the reactivity effect due to void formation is readily apparent; however, at higher exposure, due to the effect of void history, the curves cross. The primary reason for this behavior is the greater rate of plutonium formation at the higher void fraction. The isotopic concentrations as a function of exposure for the high enrichment, dominant fuel type are presented in Fig. 4.3-8 for the important heavy element isotopes.

Early in the fuel bundle life approximately 93 percent of the power is produced by fissions in U-235 with the remainder coming from fast fissions in U-238. At high exposures typical of discharge, the power production due to plutonium exceeds that of the U-235. The fraction of fissions in the important isotopes is shown in Fig. 4.3-9 for the high enrichment, dominant fuel type. Data and discussion concerning plutonium buildup are presented in Reference 5. 2

Other bundle parameters, such as neutron generation time and delayed neutron fraction as a function of exposure at core average voids, are shown in Fig. 4.3-10 and 4.3-11, respectively.

The variation of the core-wide nuclear characteristics is a function of the characteristics of each bundle in the core. With the three unique initial core bundles and the various reload situations, any description of the gross core characteristics can only be expressed in terms of the overall core performance.

4.3.2.2 Power Distribution

The core is designed such that the resultant operating power distributions meet the plant Technical Specifications. The two primary criteria for thermal limits are the maximum

Insert (page 4.3-4)

The River Bend initial core contains five fuel assembly types which are arranged in the loading pattern shown in Fig. 4.3-1.

Each bundle contains 62 fuel rods and 2 water rods. The water rods have a slightly larger diameter than the fuel rods. The layout and dimensions are presented in Fig. 4.3-2. Gadolinia, in the form of Gd_2O_3, is selectively placed in fuel rods in the 1.63 $\bar{e}$, 2.48 $\bar{e}$, and 2.78 $\bar{e}$ bundles to provide reactivity control, and is distributed axially to flatten the axial power distribution. The fuel rod distributions for the five bundle types are shown in Fig. 4.3-3a through 4.3-3e. The axial distribution of enrichment and gadolinia in rods are shown in Fig. 4.3-4a through 4.3-4e. The natural Uranium peripheral bundles and the 0.94 $\bar{e}$ control cell bundles do not contain gadolinia rods.

The fuel bundle can be represented by axial segments of uniquely defined fuel types. Each fuel type is defined by its average percent by weight

Insert (Cont.)

U-235 enrichment, and the number and percent by weight of gadolinia rods.

The bundle reactivity is a complex function of several important physical properties. The important properties consist of the average bundle enrichment, the gadolinia rod location and gadolinia concentration, the void fraction, and the accumulated exposure. The variation in reactivity of the infinite lattice data (k-infinity as a function of void fraction and exposure) for the dominant gadolinia segment of the typical enrichment bundle is presented in Fig. 4.3-5. The isotopic concentrations as a function of exposure for the typical bundle, dominant fuel type, are presented in Fig. 4.3-6 for the important heavy element isotopes.

Early in the fuel bundle life approximately 93 percent of the power is produced by fissions in U-235 with the remainder coming from fast fissions in U-238. At high exposures typical of discharge, the power production due to plutonium exceeds that of the U-235. The fraction of fissions in the important

Insert (Cont.)

isotopes is shown in Fig. 4.3-7 for the typical bundle, dominant fuel type. Data and discussion concerning plutonium buildup are presented in Reference 5.

Delayed neutron fraction as a function of exposure at core average voids is shown in Fig. 4.3-8.

The variation of the core-wide nuclear characteristics is a function of the characteristics of each bundle in the core. With the five unique initial core bundles and the various reload situations, any description of the gross core characteristics can only be expressed in terms of overall core performance.

stringent than the MLHGR limit. Each of these is a function of both the gross three-dimensional power distribution and the local rod-to-rod power distribution. Sufficient design calculations are performed to ensure that the core meets these criteria. For design convenience, separate target peaking factors are used for the local and the gross power distributions. The local peaking factor is defined as the ratio of the power density in the highest power rod in the lattice, at a cross section through the bundle, to the average power density in the lattice at that location. In addition, the local effects on the critical power ratio (CPR) are characterized by a quantity designated as R-Factor[2,17]. For the BWR 6 core design the target local peaking factor is 1.13 and the target R-Factor is 1.05. The gross power peaking is defined as the ratio of the maximum power density in any axial segment of any bundle in the core to the average power density in the core. The target gross power peaking limit for the BWR 6 fuel design is 2.06.

11

Variations from these target peaking factors are considered acceptable providing the technical specifications are not exceeded anywhere in the core. Appropriate design allowances are included at the design stage to ensure that these limits are met. During operation of the plant the power distributions are measured by the incore instrumentation system and thermal margins are calculated by the process computer.

4.3.2.2.1 Local Power Distribution

The local rod-to-rod power distribution and the associated R-Factor distribution are direct functions of the lattice fuel rod enrichment distribution. Near the outside of the lattice, where the thermal flux peaks due to interbundle water gaps, low enrichment fuel rods are utilized to minimize power peaking. Closer to the center of the bundle, higher enrichment fuel rods are used to increase the power generation and flatten the power distribution. In addition, two water tubes containing unvoided water are at the center of the lattice in order to increase the thermal flux and produce more power in the center of the lattice. The combination of these factors results in the relatively flat local power distribution. The fuel rods which contain gadolinia produce relatively little power early in bundle life; however, as the gadolinia is depleted, the power in these rods increases to approximately 90 percent of the lattice average.

Insert

The local power distributions at beginning-of-cycle (BOC) at the core average void condition for the dominant gadolinia

Insert (page 4.3-6)

The uncontrolled and controlled local power distributions at 40 percent voids as a function of exposure for the typical fuel type are shown in Figures 4.3-9 and 4.3-10 respectively.

Figures 4.3-11 and 4.3-12 present the uncontrolled and controlled R-Factor respectively for the typical fuel type at 40 percent voids as a function of exposure.

designs are shown in Fig. 4.3-12 and 4.3-13 for the high and medium enrichment lattices for the initial core. Although the enrichment distribution and gadolinia design vary between the two bundles, it can be seen from these data that the design target is not exceeded in either case. The variation of the maximum local peaking factor as a function of exposure at core average conditions is shown in Fig. 4.3-14. The high power rods deplete at a greater rate and the local power peaking factor decreases with exposure. For the high enrichment bundle, the local power distribution for core average voids at BOC, at an exposure typical of EOC-one, and end-of-bundle life is shown in Fig. 4.3-15. For the high enrichment bundle (dominant fuel type), the variation in local power distribution for various lattice void fractions is shown in Fig. 4.3-16. The local power distribution tends to flatten with increasing void fraction. The presence of a control blade adjacent to the bundle significantly perturbs the local power distribution. The controlled local power distribution for the high enrichment bundle (dominant fuel type) is shown in Fig. 4.3-17. Although the local peaking factor is quite large in this case, the gross power in a controlled bundle is sufficiently low such that a controlled lattice is never limiting.

Fig. 4.3-18 presents the R-Factor for each fuel rod at a particular planar elevation, that of the dominant fuel/gadolinia type, through the high enrichment bundle at BOC for core average conditions. The variation of the maximum bundle-integrated R-Factor with exposure is presented in Fig. 4.3-19. The behavior shown is typical of any bundle. This demonstrates that the 1.05 target limit is met for the exposure range of interest.

4.3.2.2.2 Radial Power Distribution

The integrated bundle power, commonly referred to as the radial power, is the primary factor for determining MCPR. At rated conditions the MCPR is directly proportional to the radial power peaking. The radial power distribution is a complex function of the control rod pattern in the core, the fuel bundle type and distribution, and the void condition for that bundle and power. A three-dimensional BWR simulator is used to calculate the three-dimensional power distribution in the core and the power is axially integrated to determine average bundle power[3]. The bundle radial power distributions for typical BOC and EOC conditions are presented in Fig. 4.3-20. Radial peaking factors of approximately 1.30 at BOC and approximately 1.25 at EOC are typical.

The radial distribution is controlled by both the radial reactivity zones and the control rods. The control rods are selectively inserted, or withdrawn, to flatten the radial power distribution consistent with the reactivity control needed. Near EOC the ring of high enrichment bundles adjacent to the periphery provides radial power flattening without recourse to control rods.

4.3.2.2.3 Axial Power Distribution

The axial power distributions obtained in a BWR are a function of the control rod pattern, the axial gadolinia distribution, and the exposure distribution. The effect of voids is to skew the power toward the bottom of the core; the effect of the bottom entry control rods is to reduce the power in the bottom of the core; and the effect of the axial gadolinia shaping is to flatten the power near the bottom. Since the void distribution is determined primarily from the power shape, the two mechanisms available for optimizing the axial power shape are the control rods and the gadolinia. Detailed three-dimensional calculations are performed to determine the axial gadolinia distribution which provides the desired axial power flattening. The combination of the control rod patterns and axial gadolinia help to achieve an EOC exposure distribution which approximates the Haling shape[15]. This in turn provides a relatively flat axial power shape with all control rods withdrawn.

A typical BOC axial power shape is shown in Fig. 4.3-21 13 along with the optimal EOC power shape.

For a reload condition, the exposure shape existing in the bundles which remain from previous cycles provides the necessary power shaping. Current reload bundle designs contain axially uniform gadolinia.

4.3.2.2.4 Power Distribution Calculations

A full range of calculated power distributions along with the resultant exposure shapes and the corresponding control rod patterns are shown in Appendix 4A for a typical BWR 6.

2 The process computer calculates the power distribution at a frequency set by the operator, typically at 1-hr intervals. However, this may be extended to longer periods for very steady-state operation, or the operator may make on-demand calls during certain maneuvers of particular interest.

In order to assure optimum plant performance determined by the predicted plant transient response, design limits have been established on those nuclear parameters which have a significant effect on the plant transients. Specifically, design limits have been established for the void coefficient, the Doppler coefficient, and the scram reactivity response. These limits were established such that the proper balance was made between the nuclear design and the plant design. The design limits presented herein represent the extreme values expected to occur during normal operation of the core over the lifetime. The plant transient analyses reported in Chapter 15 use these design limits for the void coefficient, Doppler coefficient, and scram reactivity. The nominal calculated values for these parameters in this core demonstrate margins to these design limits which are greater than or equal to the standard safety conservatism factors applied to these parameters for the transient analysis.

4.3.2.3.1 Void Reactivity Coefficients

The most important of these coefficients is the void reactivity coefficient. The void coefficient must be large enough to prevent power oscillation due to spatial xenon changes yet small enough that pressurization transients do not unduly limit plant operation. In addition, the void coefficient in a BWR has the ability to flatten the radial power distribution and to provide ease of reactor control due to the void feedback mechanism. The overall void coefficient is always negative over the complete operating range since the BWR design is undermoderated. The reactivity change due to the formation of voids results from the reduction in neutron moderation due to the decrease in the water-to-fuel ratio.

A detailed discussion of the methods used to calculate void reactivity coefficients, their accuracy and their application to plant transient analysis is presented in Reference 7. A comparison of a detailed model using spatial variation of the important parameters and the point model is also shown.

The moderator void reactivity coefficient as a function of percent voids is presented in Fig. 4.3-22 for the exposure at which the void coefficient reaches its maximum. Also shown in this figure is the design limit used for hydrodynamic stability analysis. It is clear that the magnitude of the void coefficient is less than the design limit. The most limiting transient response occurs at EOC.

The variation of the calculated dynamic void reactivity coefficient, as a function of core average void percent, is shown in Fig. 4.3-23 for the EOC condition. Also shown is the comparison of the design limit used for transient analysis and the calculated nominal value at rated conditions multiplied by 1.25, the standard transient safety conservatism factor. These data demonstrate that the design limit value is not exceeded.

4.3.2.3.2 Moderator Temperature Coefficient

The moderator temperature coefficient is the least important of the reactivity coefficients since its effect is limited to a very small portion of the reactor operating range. Once the reactor reaches the power producing range, boiling begins and the moderator temperature remains essentially constant. As with the void coefficient, the moderator temperature coefficient is associated with a change in the moderating power of the water. The temperature coefficient is negative for most of the operating cycle; however, near the EOC the overall moderator temperature coefficient becomes slightly positive, due to the fact that the uncontrolled BWR lattice is slightly overmoderated near the EOC. This, combined with the fact that more control rods must be withdrawn from the reactor core near the EOC to establish criticality, results in the slightly positive overall moderator temperature coefficient.

The range of values of moderator temperature coefficients encountered in current BWR lattices does not include any that are significant from the safety point of view. Typically, the temperature coefficient may range from $+4 \times 10^{-5}$ $\Delta k/k^{\circ}F$ to -14×10^{-5} $\Delta k/k^{\circ}F$, depending on base temperature and core exposure. The small magnitude of this coefficient, relative to that associated with steam voids and combined with the long time-constant associated with transfer of heat from the fuel to the coolant, makes the reactivity contribution of moderator temperature change insignificant during rapid transients.

For the reasons stated previously, current core design criteria do not impose limits on the value of the temperature coefficient, and effects of minor design changes on the coefficient in members of the same class of core usually are not calculated. A measure of design control over the temperature coefficient is exercised, however, by applying a design limit to the void coefficient. This constraint implies control over the water-to-fuel ratio of the lattice; this, in turn, controls the temperature coefficient. Thus, imposing a quantitative limit on the

void coefficient effectively limits the temperature coefficient.

4.3.2.3.3 Doppler Reactivity Coefficient

The Doppler reactivity coefficient is the change in reactivity due to a change in the temperature of the fuel. This change is due to the broadening of the resonance absorption cross sections as the temperature increases. At beginning-of-life the Doppler contribution is primarily due to U-238; however, the buildup of Pu-240 with exposure adds to the Doppler coefficient. A detailed discussion of the methods used to calculate the Doppler coefficient, their accuracy, and application to plant transient analyses is presented in Reference 7. The application of the Doppler coefficient to the analysis of the rod drop accident is discussed in Reference 8.

The variation in the core average Doppler reactivity coefficient as a function of average lattice fuel temperature at EOC-one is shown in Fig. 4.3-24. Also shown is the design limit for the Doppler coefficient. These data demonstrate that the design limit on the Doppler coefficient is not violated.

4.3.2.3.4 Power Coefficient

The power coefficient is determined from the composite of all the significant individual sources of reactivity change associated with a differential change in reactor thermal power assuming xenon reactivity remains constant. At end of initial cycle, the power coefficient at rated conditions is approximately -0.045 $\Delta k/k \div \Delta P/P$. This value is well within the range required for adequately damping power and spatial-xenon disturbances.

4.3.2.4 Control Requirements

The core and fuel design in conjunction with the reactivity control system provide an inherently stable system for BWRs.

The control rod system is designed to provide adequate control of the maximum excess reactivity anticipated during the equilibrium fuel cycle operation. The initial core loading, however, has an excess reactivity somewhat higher than that of the equilibrium core. Thus, the basis for design of the initial burnable poison loading is that it shall compensate for the reactivity difference between the control rod system capability and the initial core fuel. Because fuel reactivity is a maximum and control is a

minimum at ambient temperature, the shutdown capability is evaluated assuming a cold, xenon-free core. The safety design basis requires that the core, in its maximum reactivity condition, be subcritical with the control rod of the highest worth fully withdrawn and all others fully inserted. This limit allows control rod testing at any time in core life and assures that the reactor can be made subcritical by control rods alone.

4.3.2.4.1 Shutdown Reactivity

To assure that the safety design basis is satisfied, an additional design margin is adopted: k-effective (k_{eff}) is calculated to be less than or equal to 0.99 with the rod of highest worth fully withdrawn. The shutdown reactivity as a function of fuel exposure is shown in Fig. 4.3-25. margin 17

The shutdown reactivity curve shows the calculated values of k_{eff} for the shutdown condition (20°C, highest worth rod withdrawn, no xenon). The initial drop in k_{eff} shows the effect of the transition from clean core to equilibrium samarium. The presence of the burnable poison, Gd_2O_3, is apparent from the rise in k_{eff} as the poison depletes. The k_{eff} peak and the point of burnable poison depletion are a function of the fuel nuclear design (enrichment level, gadolinia concentration, etc). margin

The cold (20°C) reactor condition is the most limiting with regard to shutdown criteria. Heating the reactor to hot conditions will increase the shutdown margin by 0.02 Δk to 0.03 Δk. For this reason, shutdown margin calculations are not generally performed for hot conditions.

Reduction of control rod effectiveness during the operating cycle is not a major concern with the BWR. Using normal control rod sequencing, the control rod worth remains essentially constant over the BWR operating cycle.

The accuracy with which shutdown reactivity is calculated is discussed in Reference 6. Basically, the accuracy is characterized as a bias and an uncertainty. The bias is a reactivity correction applied directly to the calculated results. For example:

$$k_{eff}\,(\text{expected}) = k_{eff}\,(\text{calculated}) + \Delta k\ (\text{bias})$$

This bias has been 17 incorporated into the shutdown curves shown in Fig. 4.3-25. The 1 percent design margin is satisfied after the bias correction is applied.

k_{eff}, for various cold, xenon-free conditions. For the purposes of this table middle-of-cycle (MOC) is defined as the most reactive point in the cycle. The reactivity and control fraction (CF) values for a variety of operating conditions are listed in Table 4.3-3. The worth of various reactivity effects can be estimated by taking the differences between reactivity states with all but one variable constant. Estimates of the temperature defect, the power defect, the xenon defect, and the excess reactivity can be inferred.

Figure 4.3-24 is based on point model calculations. Nuclear parameters are volume weighted and power shape is not assumed to change with void fraction and leakage effects. Integrating this curve over large void fraction changes is not representative of true change in reactivity because the basic assumption of the point model basis is violated (e.g., power shape changes). 11

4.3.2.5 Control Rod Patterns and Reactivity Worths

A detailed core simulation study for a typical BWR 6 is provided in Appendix 4A showing that the BWR core meets design performance criteria. Typical BWR control rod positions are utilized in the study. The rod patterns described represent only one feasible sequence which results in power distributions well within design limits. Actual operating reactor rod patterns are based upon the measured distributions in the plant and together with the rod worth minimizing systems, limit the amount and rate of reactivity insertion in the event of a control rod drop accident in such a way that the peak fuel pellet enthalpy is less than the 280 cal/gm design limit. Rod worth minimizing systems also assure that the 170 cal/gm fuel enthalpy limit is not exceeded for any cold rod withdrawal error event. 2

For BWR plants, control rod patterns are not uniquely specified in advance; rather, during normal operation the control rod patterns are selected based on the measured core power distributions, within the constraints imposed by the systems indicated in the following sections.

Typical control rod patterns are calculated during the design phase to ensure that all safety and performance criteria are satisfied. Control rod patterns and the associated power distributions for a typical BWR are presented in Appendix 4A. These control rod patterns are calculated with the BWR core simulator[3]. The ability of this model to predict control rod worth can be inferred from the detailed reactivity data presented in Reference 6. The

At lower power levels the increment is allowed to increase, until full withdrawals (144 in) are allowed at very low power levels.

4.3.2.5.4 Control Rod Operation

The control rods can be operated either individually or in a gang composed of up to four rods. The purpose of the ganged rods is to reduce the time required for plant startup or recovery from a scram. The RCIS provides regulation of control rod operation regardless of whether rods are being moved in single or ganged mode. The assignment of control rods to RCIS groups is shown in Fig. 4.3-27 and 4.3-28 for the A pattern and Fig. 4.3-29 and 4.3-30 for the B pattern. Also shown in these figures is the division of the groups into gangs of one to four rods which can be moved simultaneously.

20 21 22 19

4.3.2.5.5 Scram Reactivity

18

The RPS responds to some abnormal operational transients by initiating a scram. The RPS and the CRD system act quickly enough to prevent the initiating disturbance from driving the fuel beyond transient limits. The scram reactivity curve at the EOC-one is shown in Fig. 4.3-26. Also shown is the calculated value multiplied by 0.80, the standard transient safety conservatism factor, and the design limit scram curve. These data show that the design limit curve is not violated. In particular, the design limit curve is not violated for control fractions between 0.0 and 0.6, the range of importance for transient analyses.

At the hot operating condition the control rod, power, delayed neutron, and void distributions must all be properly accounted for as a function of time. Therefore, the scram reactivity is calculated using a one-dimensional (axial), finite-difference, space-time model which is coupled with a single channel, thermal-hydraulic model. The finite-difference, space-time model uses three prompt and six delayed neutron energy groups, and has been compared to, and verified by, analysis of published results obtained using the industry standard computer code[10].

The transient thermal-hydraulic model employed for this calculation is described in detail in Reference 11. The coupled neutronics and thermal-hydraulics properly account for the redistribution of the power, neutron flux, and voids during scram.

4.3.2.6 Criticality of Reactor During Refueling

The maximum allowable value of k_{eff} is <1.000 at any time. For each reload cycle the maximum core reactivity is calculated with the highest worth rod withdrawn to show at least 1.0 percent Δk margin. A control rod system interlock prevents the withdrawal of more than one rod while in the REFUEL mode.

4.3.2.7 Stability

4.3.2.7.1 Xenon Transients

BWRs do not have instability problems due to xenon. This has been demonstrated by operating BWRs for which xenon instabilities have never been observed, (such instabilities would readily be detected by the LPRMs), by special tests which have been conducted on operating BWRs in an attempt to force the reactor into xenon instability, and by calculations. All these indicators have proven that xenon transients are highly damped in a BWR due to the large negative power coefficient.

Analysis and experiments conducted in this area are reported in Reference 12.

4.3.2.7.2 Thermal-hydraulic Stability

This subject is covered in Section 4.4.4.6.

4.3.2.8 Vessel Irradiations

The neutron flux at the vessel have been calculated using the one-dimensional discrete ordinates transport code described in Section 4.1.4.5. The discrete ordinates code was used in a distributed source mode with cylindrical geometry. The geometry described six regions from the center of the core to a point beyond the vessel. The core region was modeled as a single, homogenized, cylindrical region. The coolant water region between the fuel channel and the shroud was described containing saturated water at 550°F and 1,050 psi. The material compositions for the stainless steel in the shroud and the carbon steel in the vessel contain the mixtures by weight as specified in the ASME material specifications for ASME SA240, 304L, and ASME SA533 Grade B. In the region between the shroud and the vessel, the presence of the jet pumps was ignored. A simple diagram showing the regions, dimensions, and weight fractions is shown in Fig. 4.3-31.

23

The distributed source used for this analysis was obtained from the gross radial power description. The distributed source at any point in the core is the product of the power from the power description and the neutron yield from fission. By using the neutron energy spectrum, the distributed source is obtained for position and energy. The integral over position and energy is normalized to the total number of neutrons in the core region. The core region is defined as a 1-cm thick disc with no transverse leakage. The power in this core region is set equal to the maximum power in the axial direction. The radial and optimum axial power distributions are shown in Fig. 4.3-32 (24) and 4.3-21 (13).

The neutron fluence is determined from the calculated flux by assuming that the plant is operated 90 percent of the time at 90 percent power level for 40 yr or equivalent to 1×10^9 full power sec. The calculated flux and fluence are listed in Table 4.3-5. The calculated neutron flux leaving the cylindrical core is listed in Table 4.3-6.

4.3.3 Analytical Methods

The analytical methods and nuclear data used to determine the nuclear characteristics are similar to those in use for design and analysis of water-moderated reactors.

The Lattice Physics Model is used to calculate lattice reactivity characteristics, few group flux averaged cross sections, and local rod-to-rod power and exposure distributions[13]. These data are generated for various temperature, void, exposure, and control conditions as required to represent the reactor core behavior.

The 3WR core simulator is a large, three-dimensional code which provides for spatially varying voids, control rods, burnable poisons, xenon, and exposure[3]. This code is used to calculate three-dimensional power and exposure distributions, control rod patterns, and thermohydraulic characteristics throughout core life.

These methods have been compared extensively to experiments and plant operating data. The results are presented in References 5 and 6.

reduction in hot-to-cold swing can be used to increase hot excess reactivity to provide additional margin against uncertainties in nuclear predictions and to provide more power shaping flexibility early in the cycle.

4.3.4.1.4 Fuel Rod Diameter Reduction

To maintain standardization of design and fabrication, the fuel rod diameter is reduced from 0.493 to 0.483 in. The 10-mil reduction in fuel rod diameter was accomplished by reducing the pellet diameter by 6 mils and decreasing the cladding thickness by 2 mils. The revisions to the fuel rod design are listed in Table 4.3-4.

The MLHGR rate is preserved at 13.4 kW/ft as a design basis; therefore, the maximum fuel centerline temperature at full power remains very nearly the same. Although the fuel time-constant is slightly decreased as a consequence of the reduction in fuel rod diameter, analyses of core transient response have indicated the MCPR, peak fuel temperature, and system pressure will be maintained below limits.

A summary of fuel bundle design changes can be found in Table 4.3-4. The new fuel bundle design is also illustrated in Fig. 4.3-2.

4.3.4.1.5 Standardization

The BWR 6 core design is limited to a number of discrete, standardized initial and reload bundle enrichments. Three of these bundle average enrichments are used in any initial core design.

The interior of each initial core consists of a central checkerboard of medium and high enrichment fuel bundles surrounded by a zone containing only bundles of high enrichment. The number of medium enrichment bundles in the checkerboard approximates the reload batch size which results in a smooth and efficient transition from the first cycle of operation to the equilibrium state. The periphery is loaded with natural uranium assemblies. With this type of loading it is possible to maintain the same radial power peaking as in a single enrichment core while at the same time minimizing neutron leakage. The net result is that the total enrichment inventory needed to achieve a given cycle energy is decreased with no power peaking penalty.

Fuel will also be better utilized in this multiple enrichment core since fuel bundles will be discharged with an initial enrichment which is consistent with the discharge

exposure. At the EOC-one, the natural uranium bundles will be discharged, resulting in a greater reactivity carryover into the transition cycle. The natural uranium bundles, when discharged at EOC, will be replaced with the lowest reactivity fuel remaining in the core. The planned reload fuel bundles will contain natural uranium segments at both ends. The initial core loading pattern is shown in Fig. 4.3-1. The octant symmetry maximizes symmetry relative to incore instrumentation.

NOTE LOADING PATTERN IS PRESENTED FOR QUARTER CORE ONLY. REFLECTIVE SYMMETRY APPLIES TO REMAINDER OF CORE

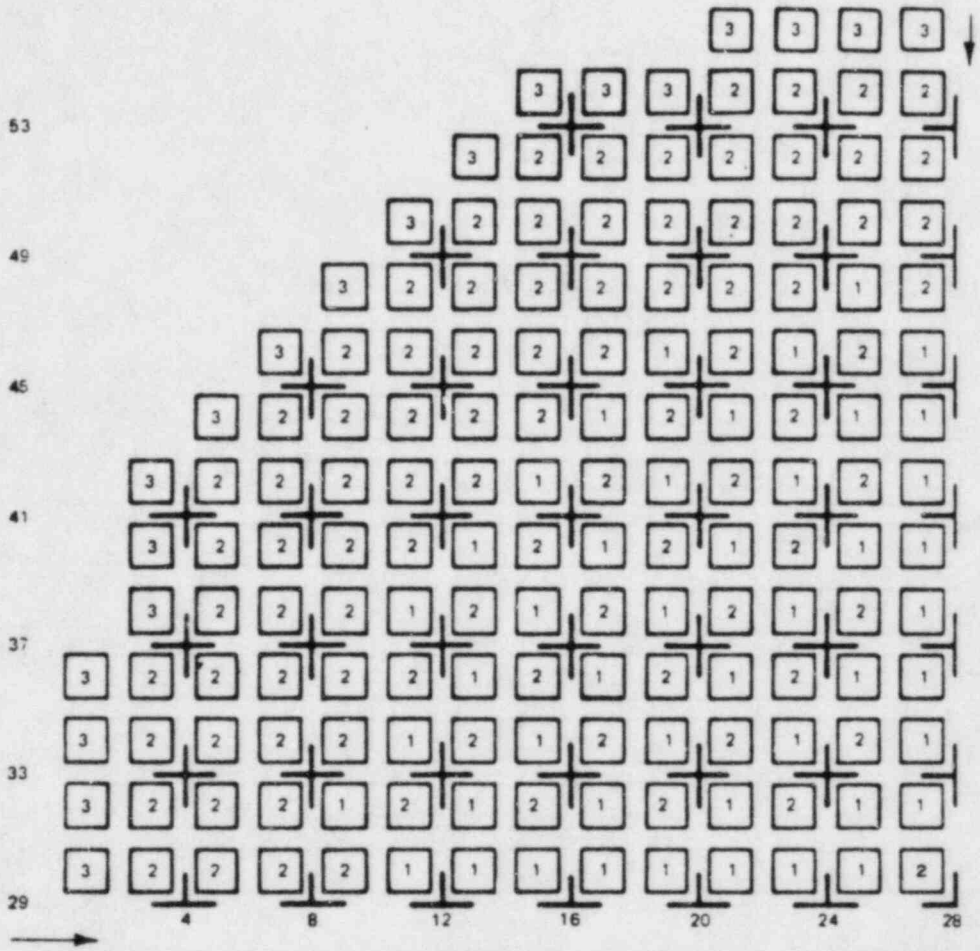

BUNDLE TYPE	NO. OF BUNDLES	BUNDLE AVERAGE ENRICHMENT
1 MEDIUM ENRICHMENT	188	1.54
2 HIGH ENRICHMENT	360	2.00
3 NATURAL URANIUM	76	0.711

Replace with attached

FIGURE 4.3-1

INITIAL CORE LOADING MAP

RIVER BEND STATION
FINAL SAFETY ANALYSIS REPORT

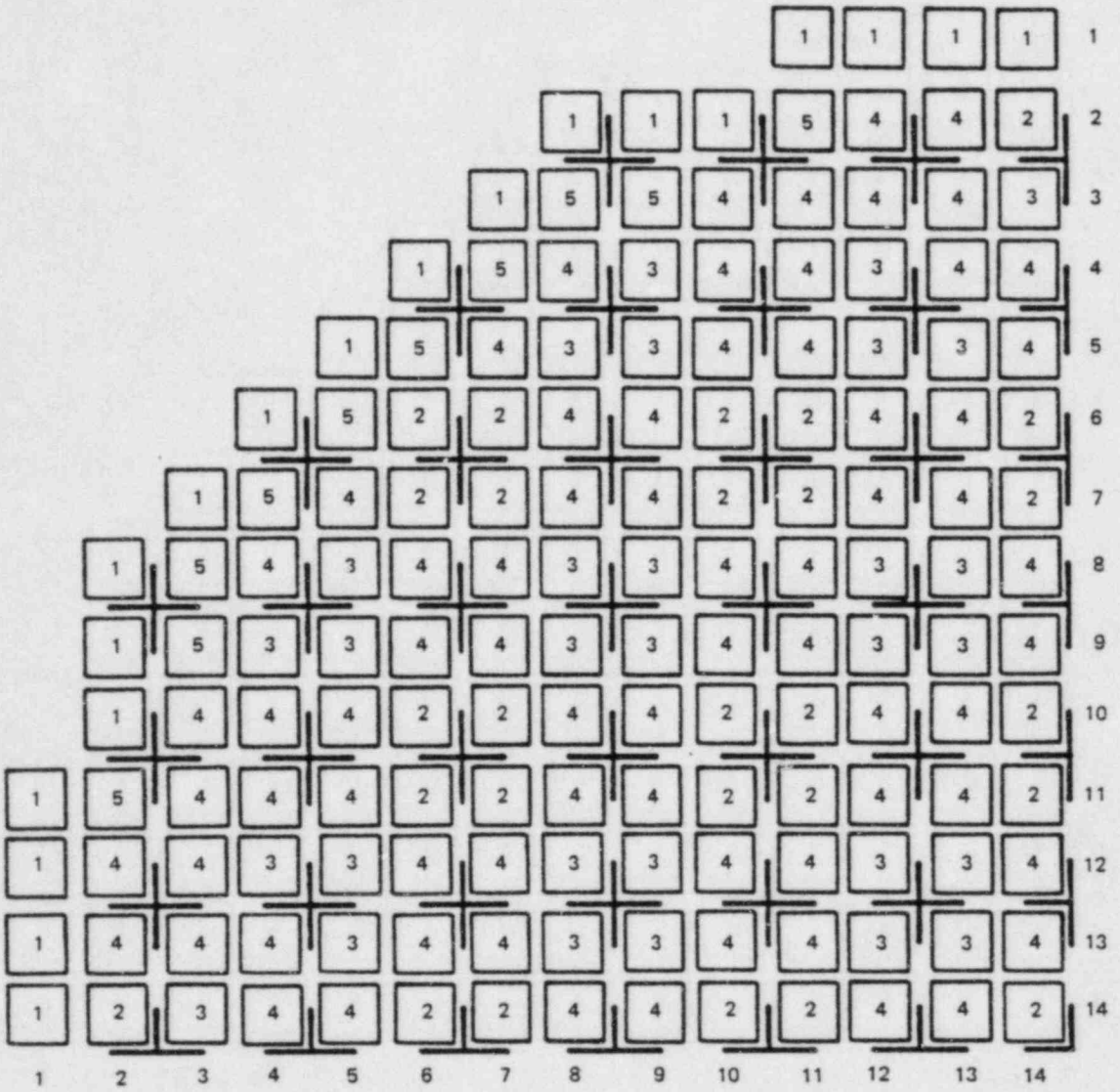

BUNDLE TYPE	NUMBER OF BUNDLES	BUNDLE AVG. ENRICHMENT
1 P8SRB071	76	0.711
2 P8SRB094	108	0.94
3 P8SRB163	120	1.63
4 P8SRB248	280	2.48
5 P8SRB278	40	2.78

NOTE: LOADING PATTERN IS SHOWN FOR ONE-QUARTER CORE ONLY. MIRROR SYMMETRY APPLIES TO REMAINDER OF CORE.

Figure 4.3-1 RIVER BEND STATION – FSAR INITIAL CORE LOADING MAP

85-201-18

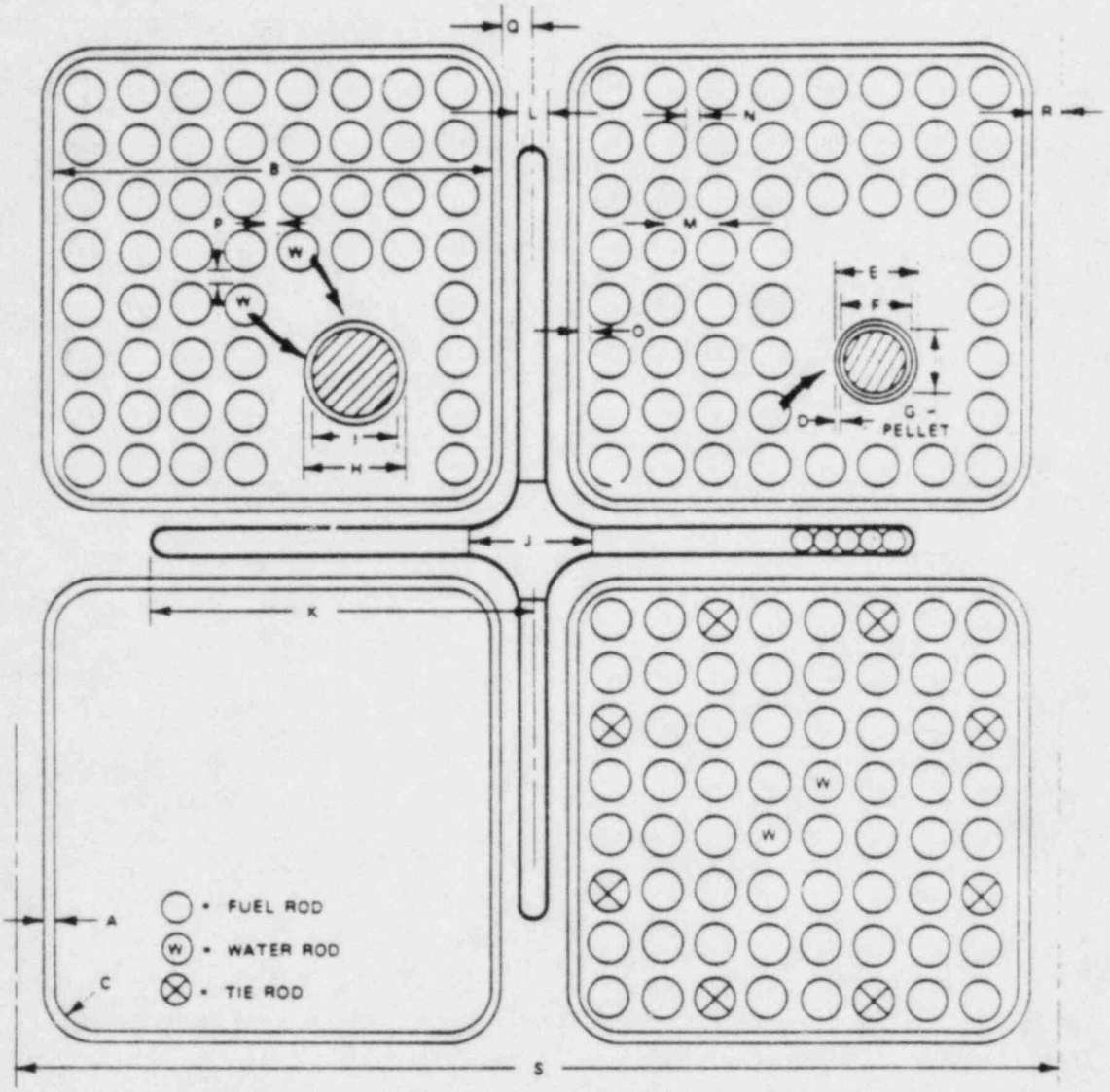

	CHANNEL			FUEL ROD			PELLET	WATER ROD	
DIM I.D.	A	B	C	D	E	F	G	H	I
DIM INCHES	0.120	5.215	0.380	0.032	0.483	0.419	0.410	0.591	0.531

	CONTROL ROD			BUNDLE LATTICE				CELL		
DIM I.D.	J	K	L	M	N	O	P	Q	R	S
DIM INCHES	1.55	4.902	0.328	0.636	0.153	0.140	0.099	0.2725	0.2725	12.00

FIGURE 4.3-2

S

C LATTICE 120-MIL CHANNEL

RIVER BEND STATION

FINAL SAFETY ANALYSIS REPORT

THIS FIGURE IS GE COMPANY
PROPRIETARY AND IS SUBMITTED
UNDER SEPARATE PROPRIETARY COVER.

Replace

FIGURE 4.3-5

AXIAL ENRICHMENT AND GADOLINIA
DISTRIBUTION, HIGH ENRICHMENT
BUNDLE (GE COMPANY PROPRIETARY)

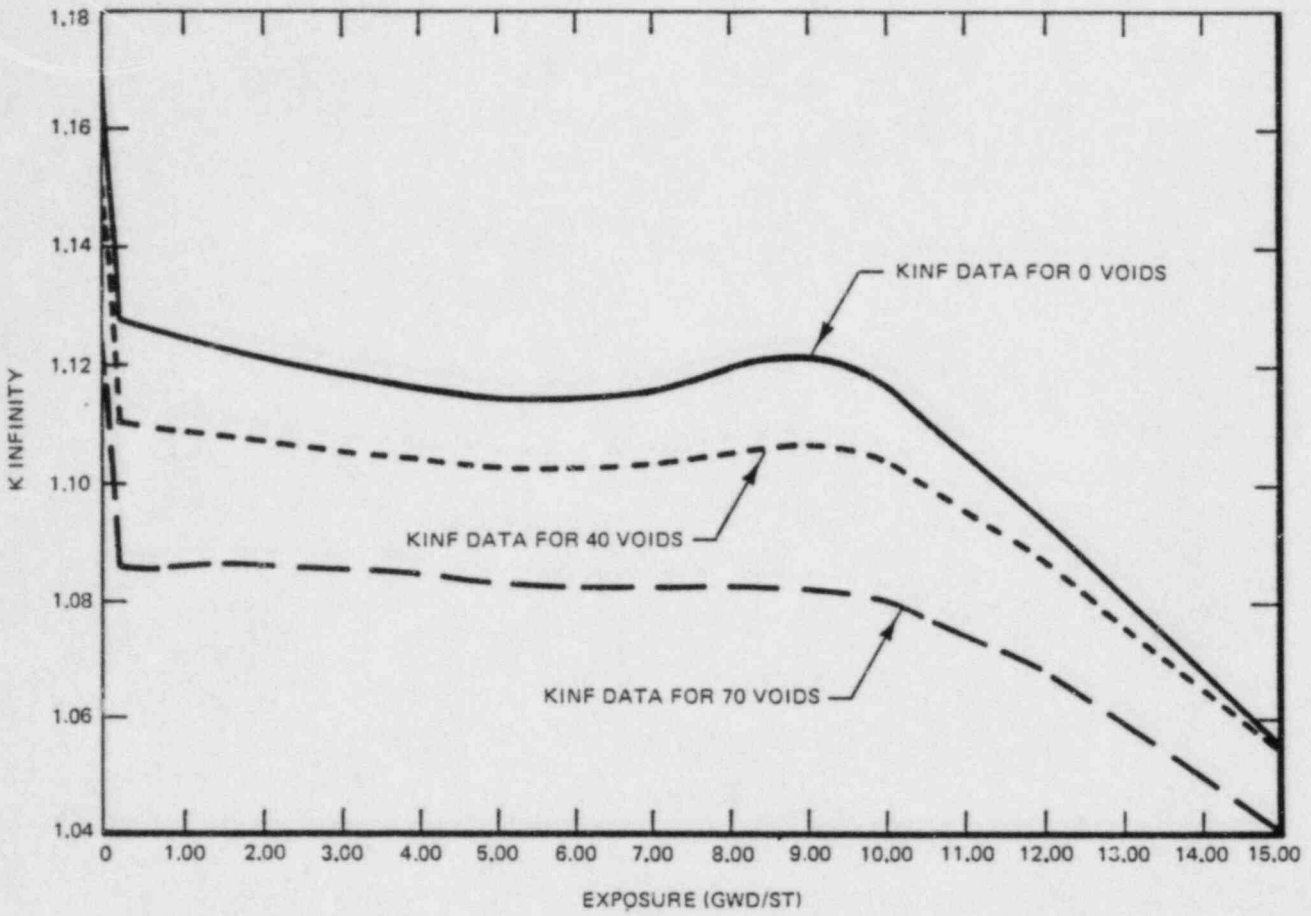

Figure 4.3-5 RIVER BEND STATION – FSAR K-INFINITY AS A FUNCTION AT VARIOUS VOID FRACTIONS, UNCONTROLLED, TYPICAL FUEL TYPE

85-201-26

THIS FIGURE IS GE COMPANY
PROPRIETARY AND IS SUBMITTED
UNDER SEPARATE PROPRIETARY COVER.

Replace

FIGURE 4.3-6

AXIAL ENRICHMENT AND GADOLINIA DISTRIBUTION, MEDIUM ENRICHMENT BUNDLE (GE COMPANY PROPRIETARY)

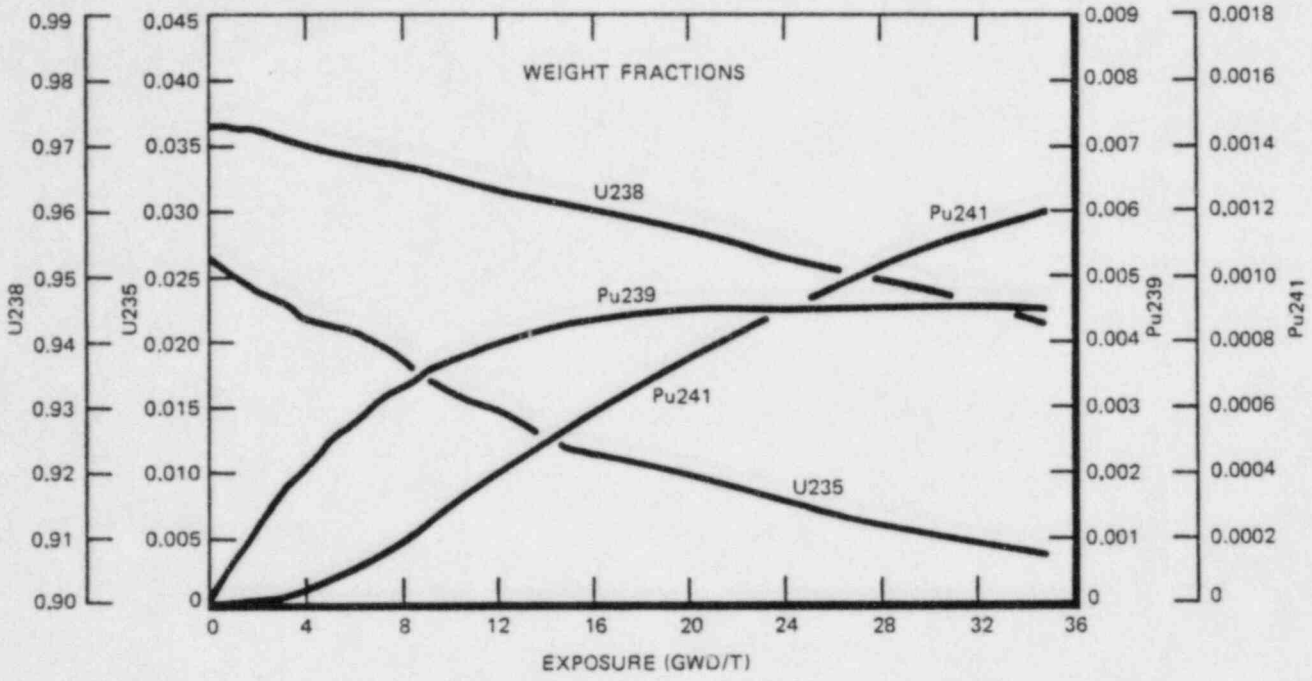

Figure 4.3-6 RIVER BEND STATION – FSAR WEIGHT FRACTION AS A FUNCTION OF EXPOSURE, 40% VOIDS FOR THE TYPICAL FUEL TYPE

85-201-19

Replace

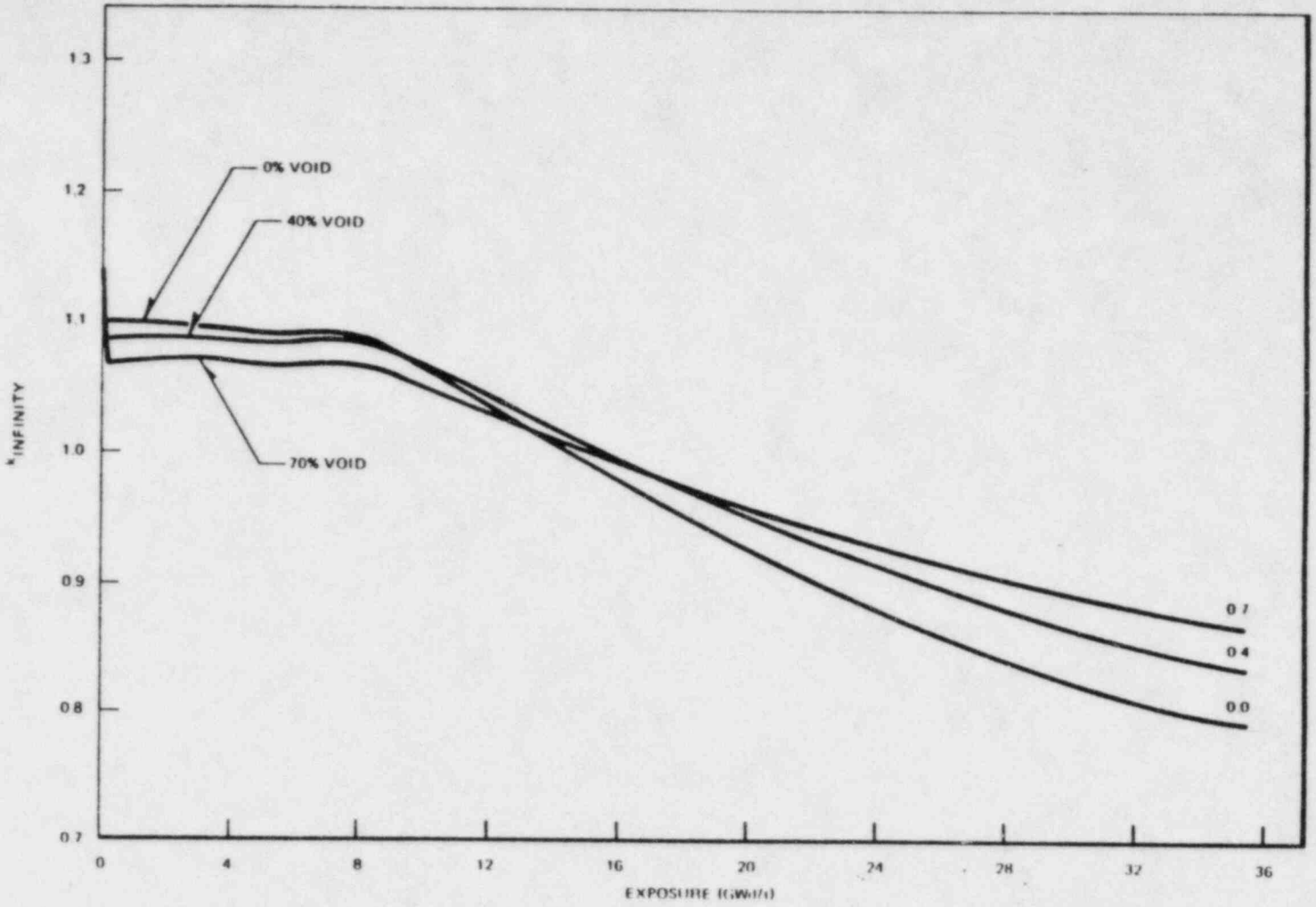

FIGURE 4.3-7

K-INFINITY AS A FUNCTION AT VARIOUS VOID FRACTIONS; HIGH ENRICHMENT, DOMINANT FUEL TYPE

RIVER BEND STATION

FINAL SAFETY ANALYSIS REPORT

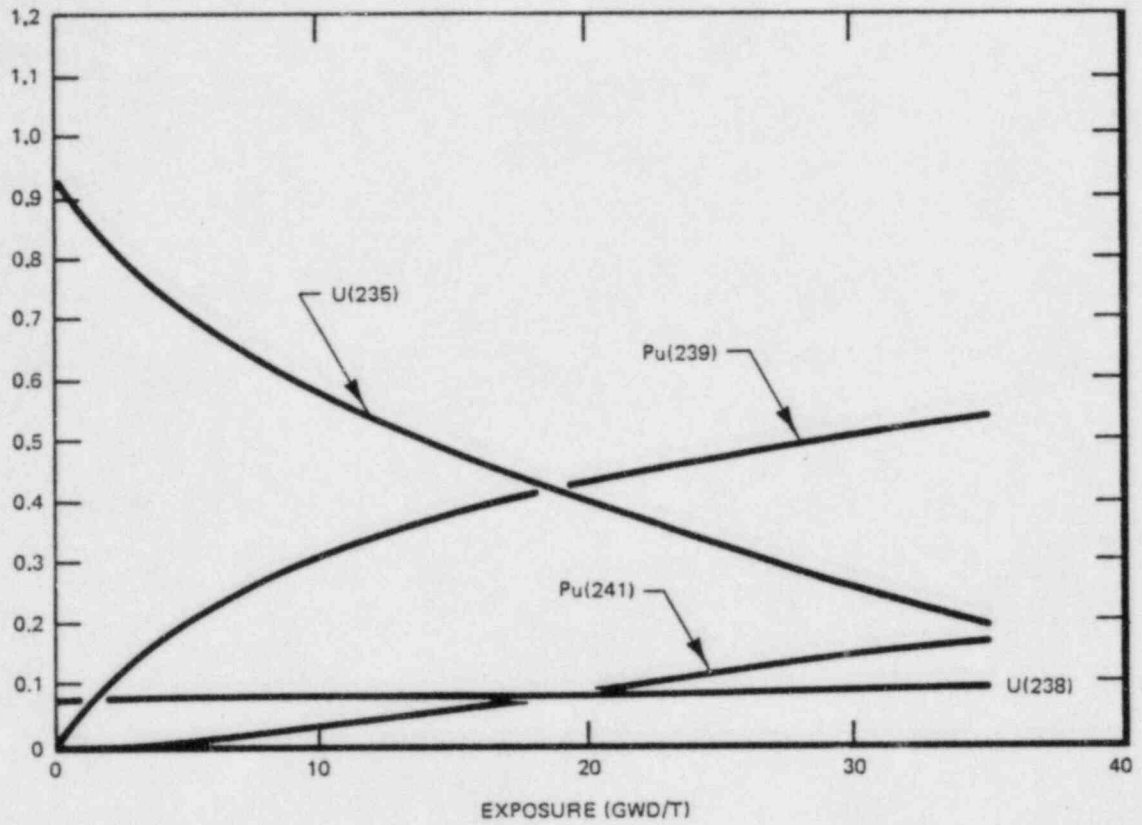

Figure 4.3-7 RIVER BEND STATION – FSAR FISSION FRACTION AS A FUNCTION OF EXPOSURE, 40% VOIDS FOR THE TYPICAL FUEL TYPE

85-201-06

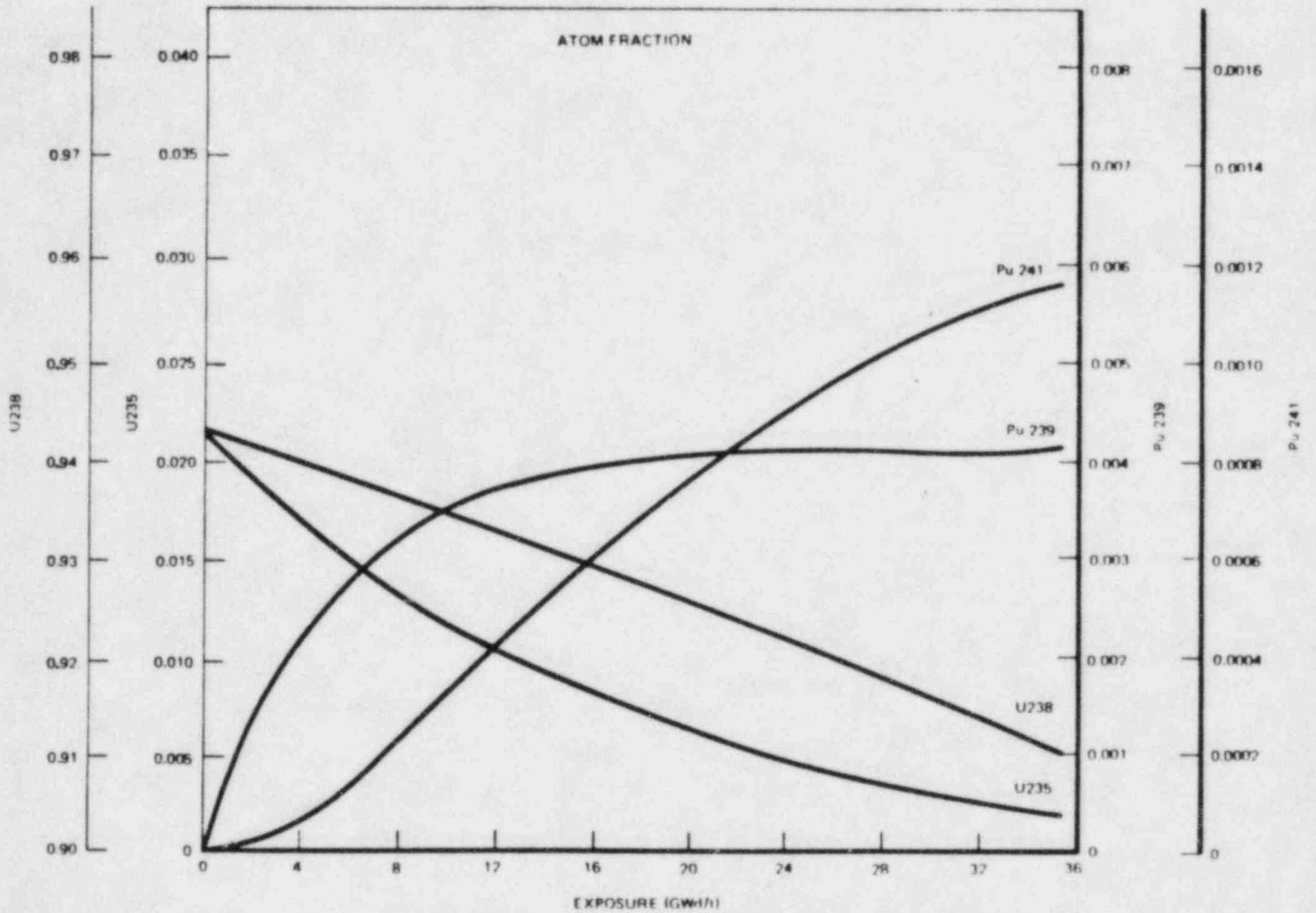

Replace

FIGURE 4.3-8

ATOM FRACTION AS A FUNCTION OF EXPOSURE; HIGH ENRICHMENT, DOMINANT FUEL TYPE; 40 PERCENT VOIDS

RIVER BEND STATION

FINAL SAFETY ANALYSIS REPORT

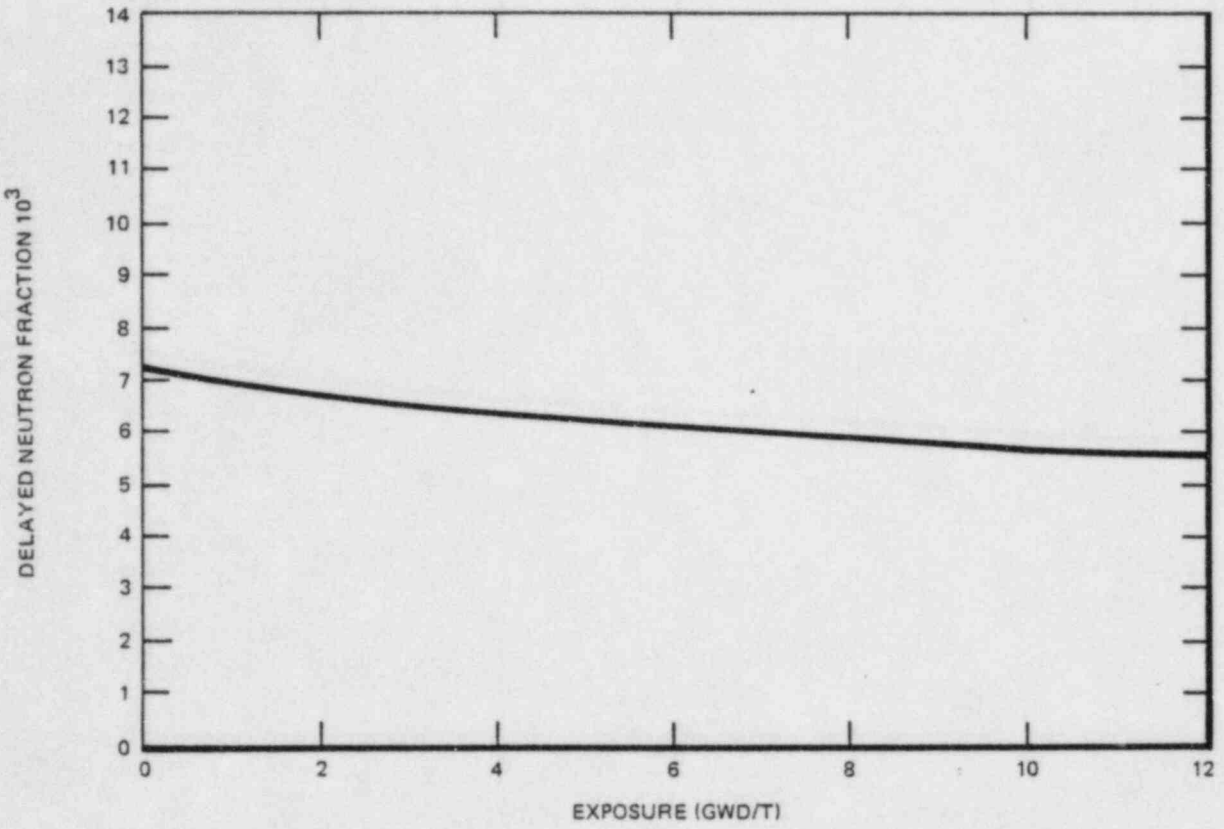

Figure 4.3-8 RIVER BEND STATION – FSAR DELAYED NEUTRON FRACTION AS A FUNCTION OF EXPOSURE AT 40% VOIDS, TYPICAL FUEL TYPE

85-201-07

THIS FIGURE IS GE COMPANY
PROPRIETARY AND IS SUBMITTED
UNDER SEPARATE PROPRIETARY COVER.

Replace

FIGURE 4.3-13

UNCONTROLLED LOCAL POWER
DISTRIBUTION AT 40% VOIDS
--BEGINNING OF CYCLE--
MEDIUM ENRICHMENT DOMINANT FUEL
TYPE (GE COMPANY PROPRIETARY)

RIVER BEND STATION
FINAL SAFETY ANALYSIS REPORT

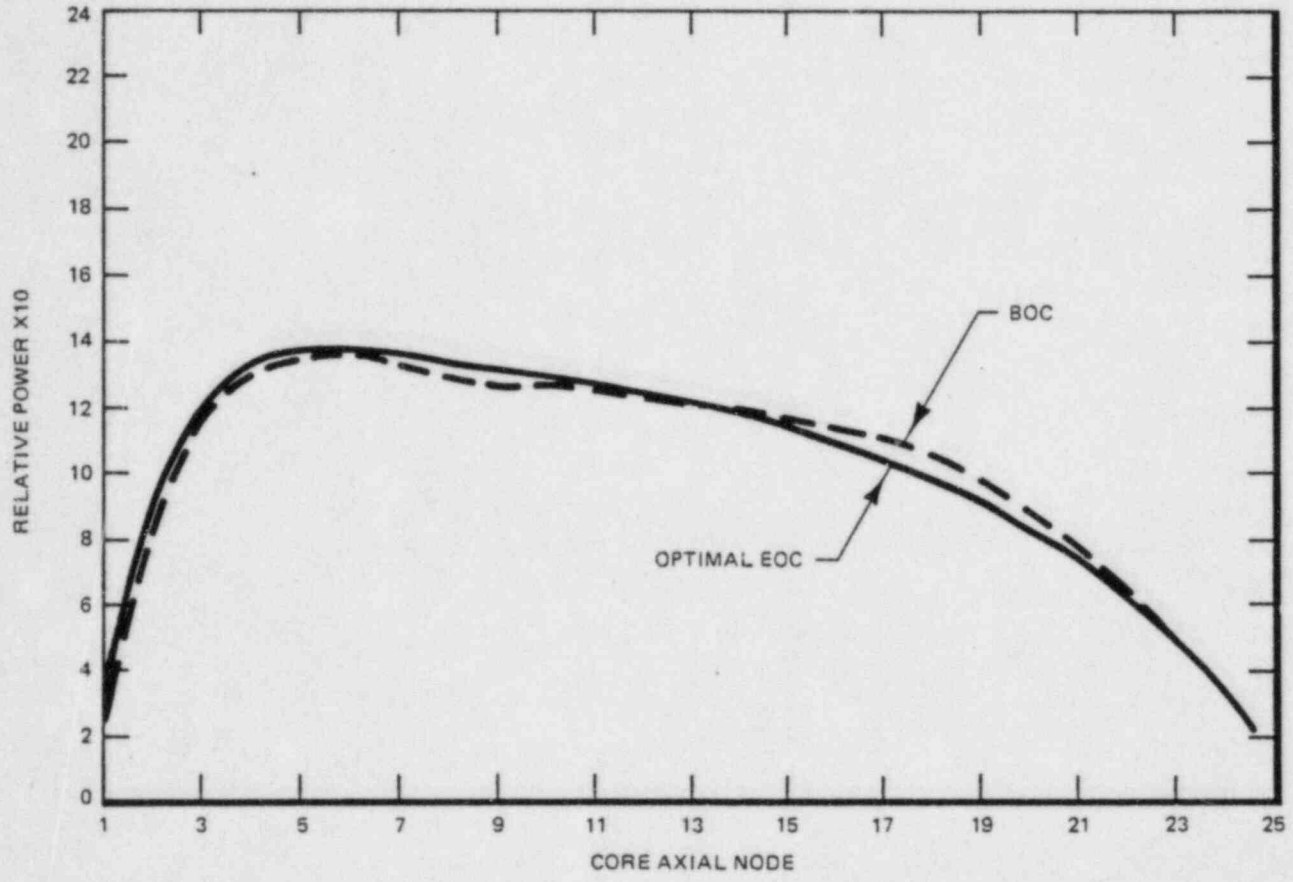

Figure 4.3-13 RIVER BEND STATION – FSAR BEGINNING OF CYCLE AND OPTIMAL END OF CYCLE CORE AVERAGE AXIAL POWER

85-201-20

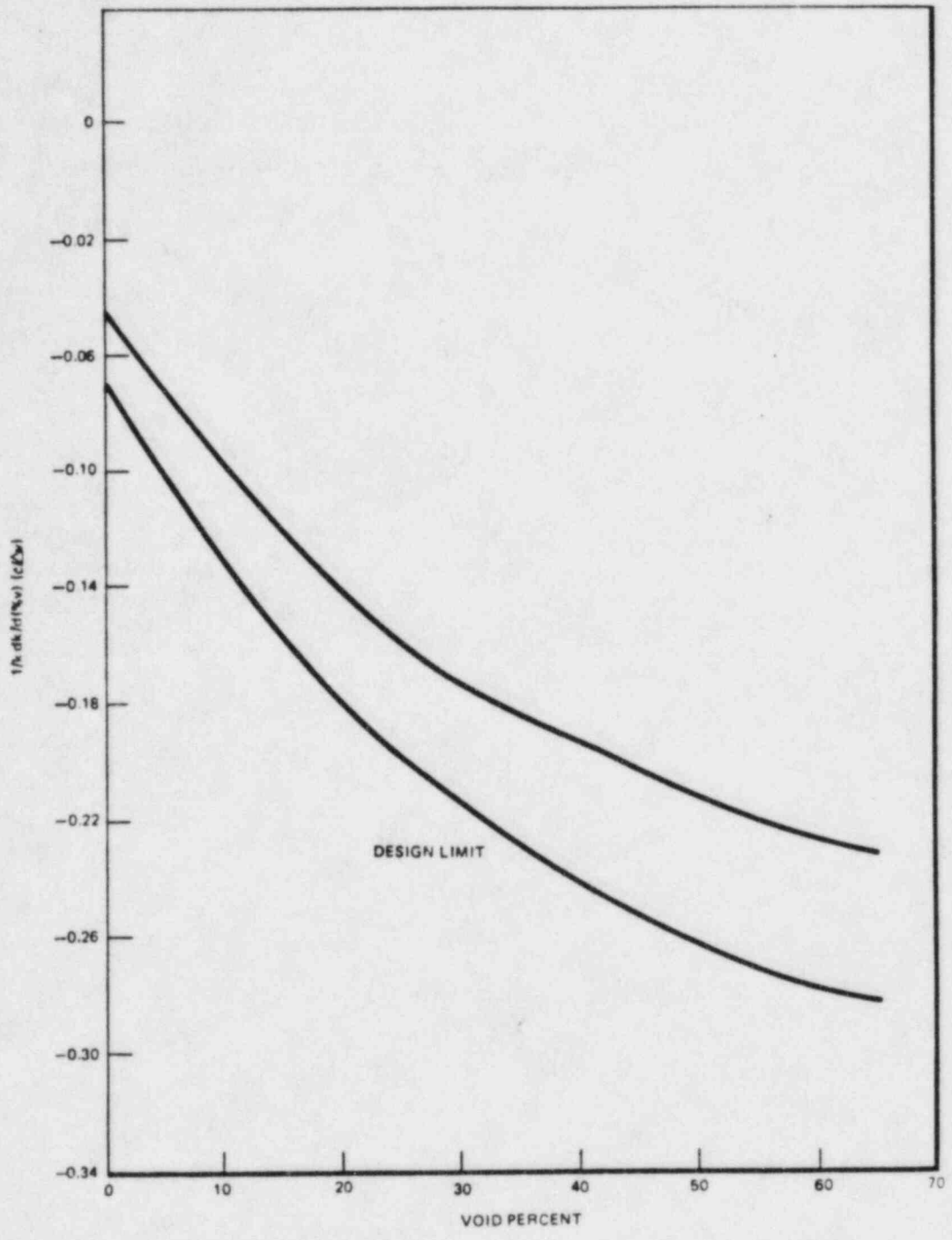

Replace with attached

FIGURE 4.3-~~22~~ 14

FIRST CYCLE MODERATOR VOID COEFFICIENT (FOR STABILITY ANALYSIS) AS A FUNCTION OF VOIDS

RIVER BEND STATION
FINAL SAFETY ANALYSIS REPORT

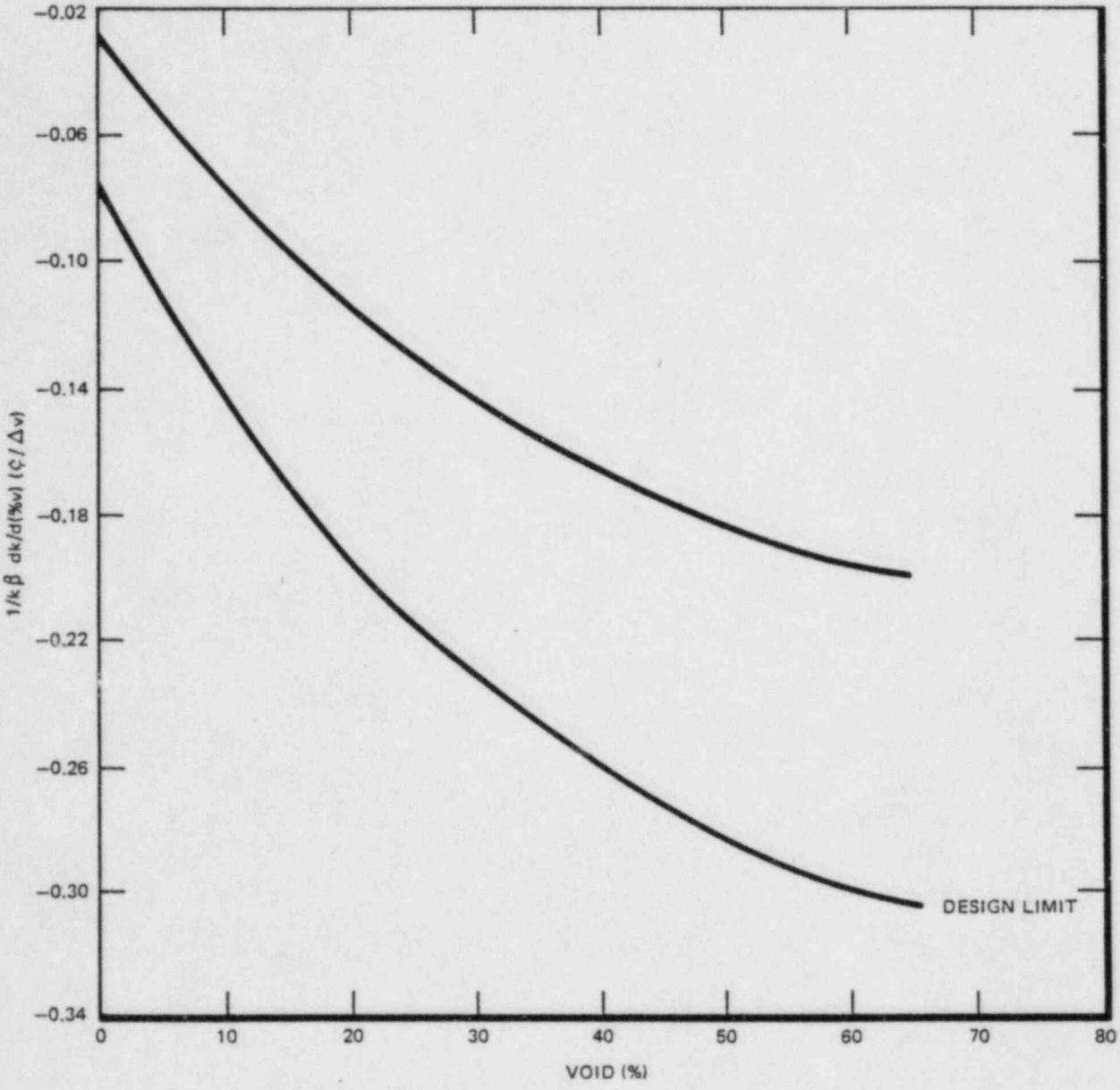

Figure 4.3-14 RIVER BEND STATION – FSAR FIRST CYCLE MODERATOR VOID COEFFICIENT (FOR STABILITY ANALYSIS) AS A FUNCTION OF VOIDS

85-201-05

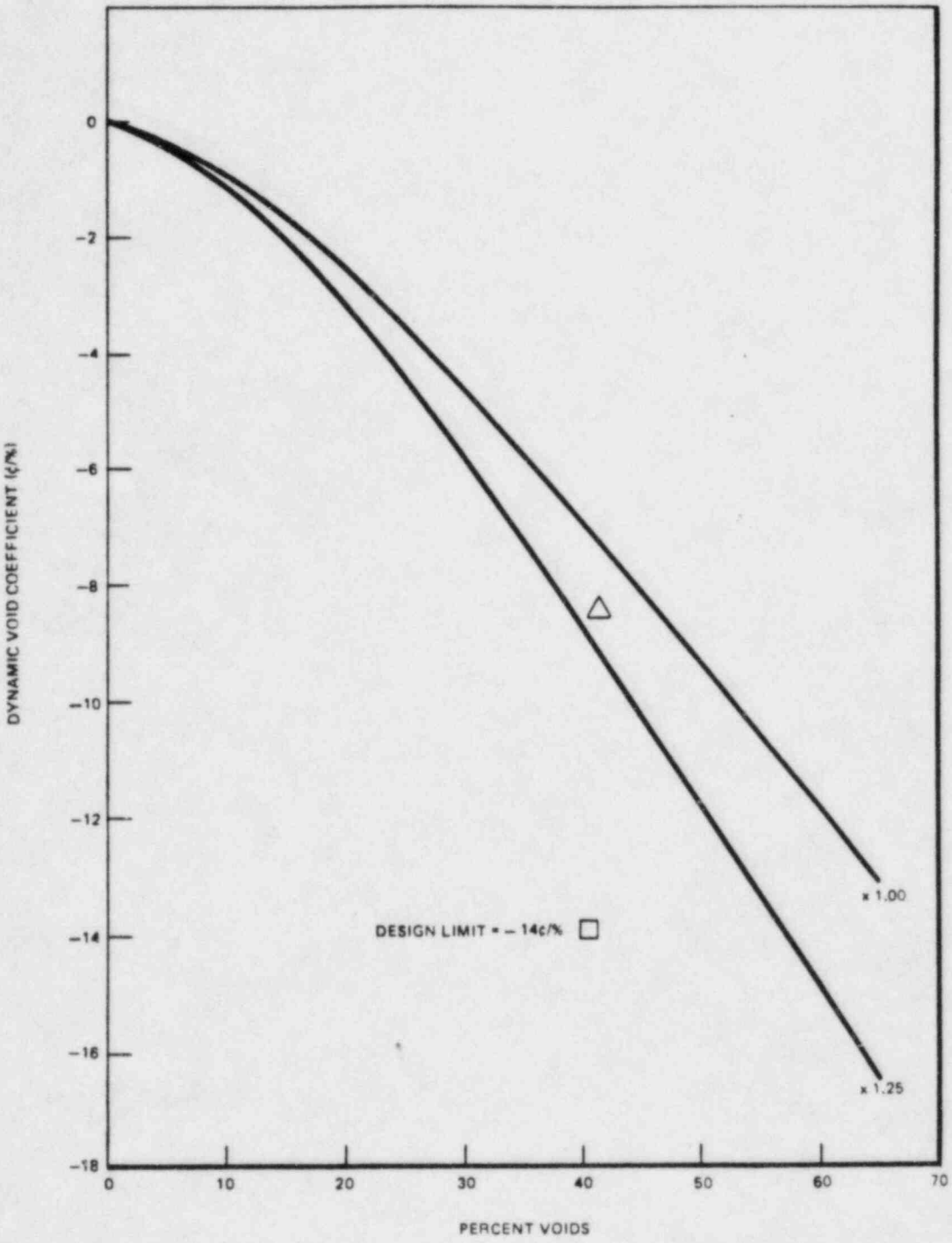

Replace with attached

FIGURE 4.3-~~23~~ 15

DYNAMIC MODERATOR VOID REACTIVITY COEFFICIENT AS A FUNCTION OF PERCENT VOIDS AT END-OF-CYCLE

RIVER BEND STATION
FINAL SAFETY ANALYSIS REPORT

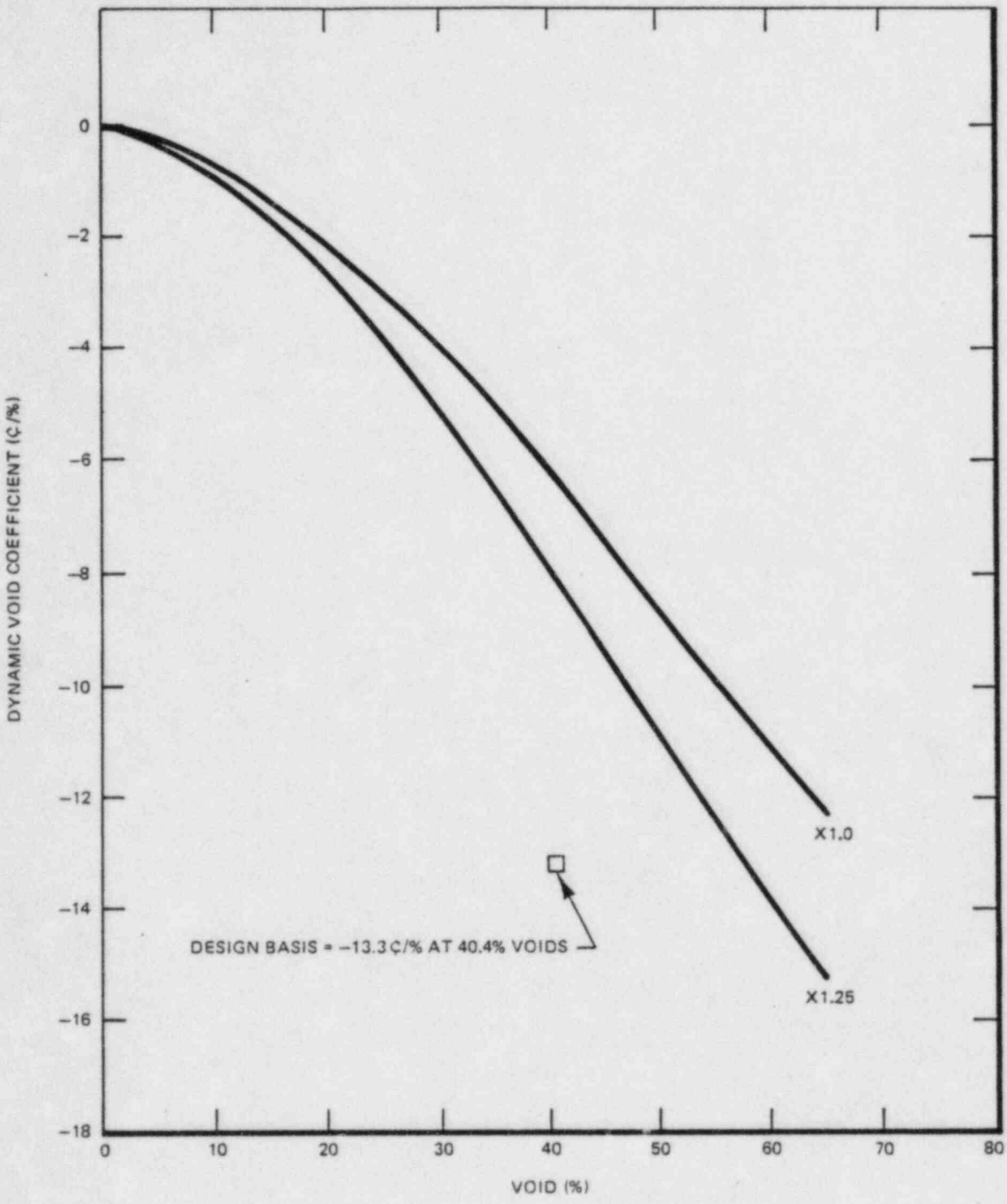

Figure 4.3-15 RIVER BEND STATION – FSAR DYNAMIC MODERATOR VOID REACTIVITY COEFFICIENT AS A FUNCTION OF PERCENT VOIDS AT END-OF-CYCLE

85-201-25

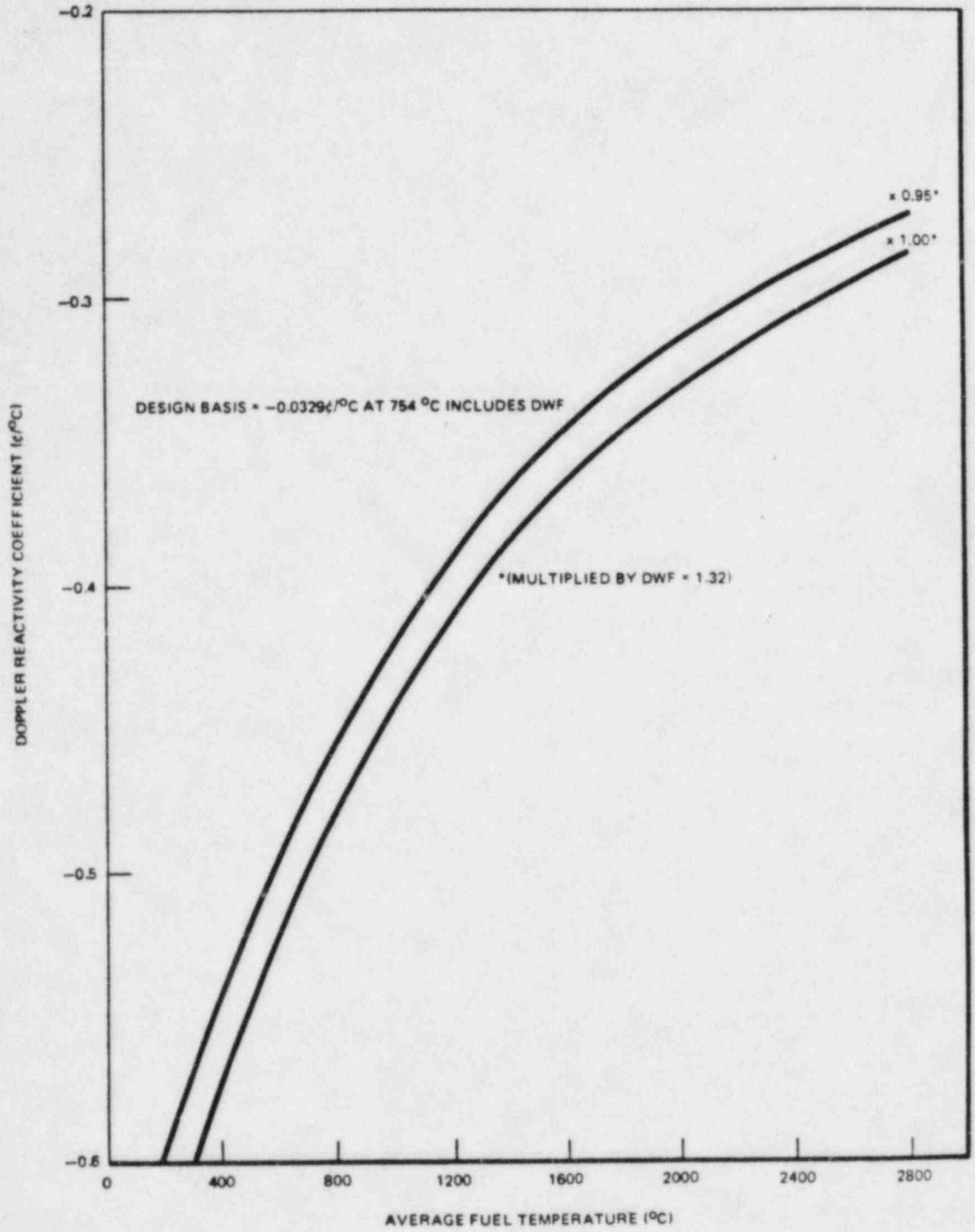

DWF = DOPPLER WEIGHTING FACTOR

Replace with attached

FIGURE 4.3-~~24~~ 16

DOPPLER REACTIVITY COEFFICIENT AS A FUNCTION OF AVERAGE FUEL TEMPERATURE, HOT OPERATING, END-OF-CYCLE-ONE

RIVER BEND STATION

FINAL SAFETY ANALYSIS REPORT

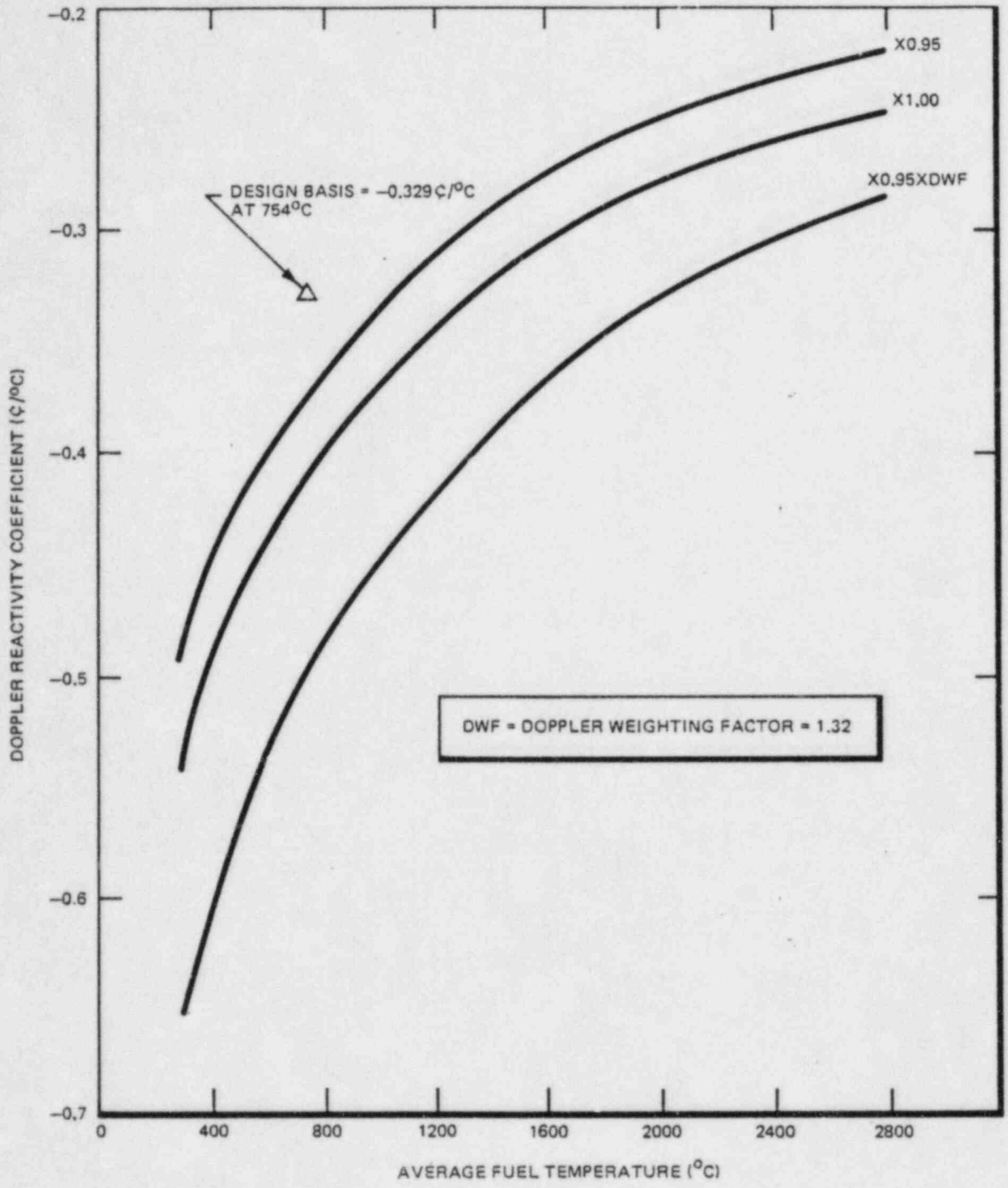

Figure 4.3-16 RIVER BEND STATION – FSAR DOPPLER REACTIVITY COEFFICIENT AS A FUNCTION OF AVERAGE FUEL TEMPERATURE, HOT OPERATING, END-OF-CYCLE-ONE

85-201-02

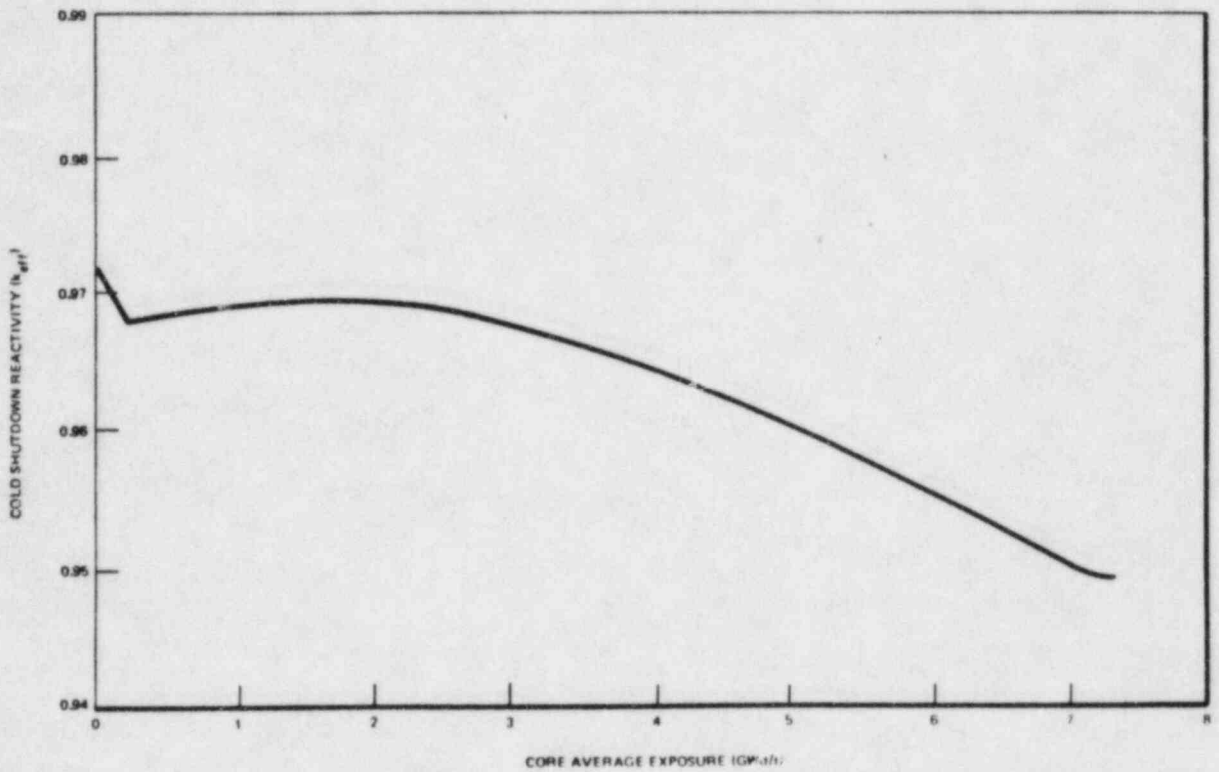

Replace with attached

FIGURE 4.3-25 17

COLD SHUTDOWN REACTIVITY MARGIN AS A FUNCTION OF EXPOSURE; STRONGEST ROD WITHDRAWN, NO XENON

RIVER BEND STATION

FINAL SAFETY ANALYSIS REPORT

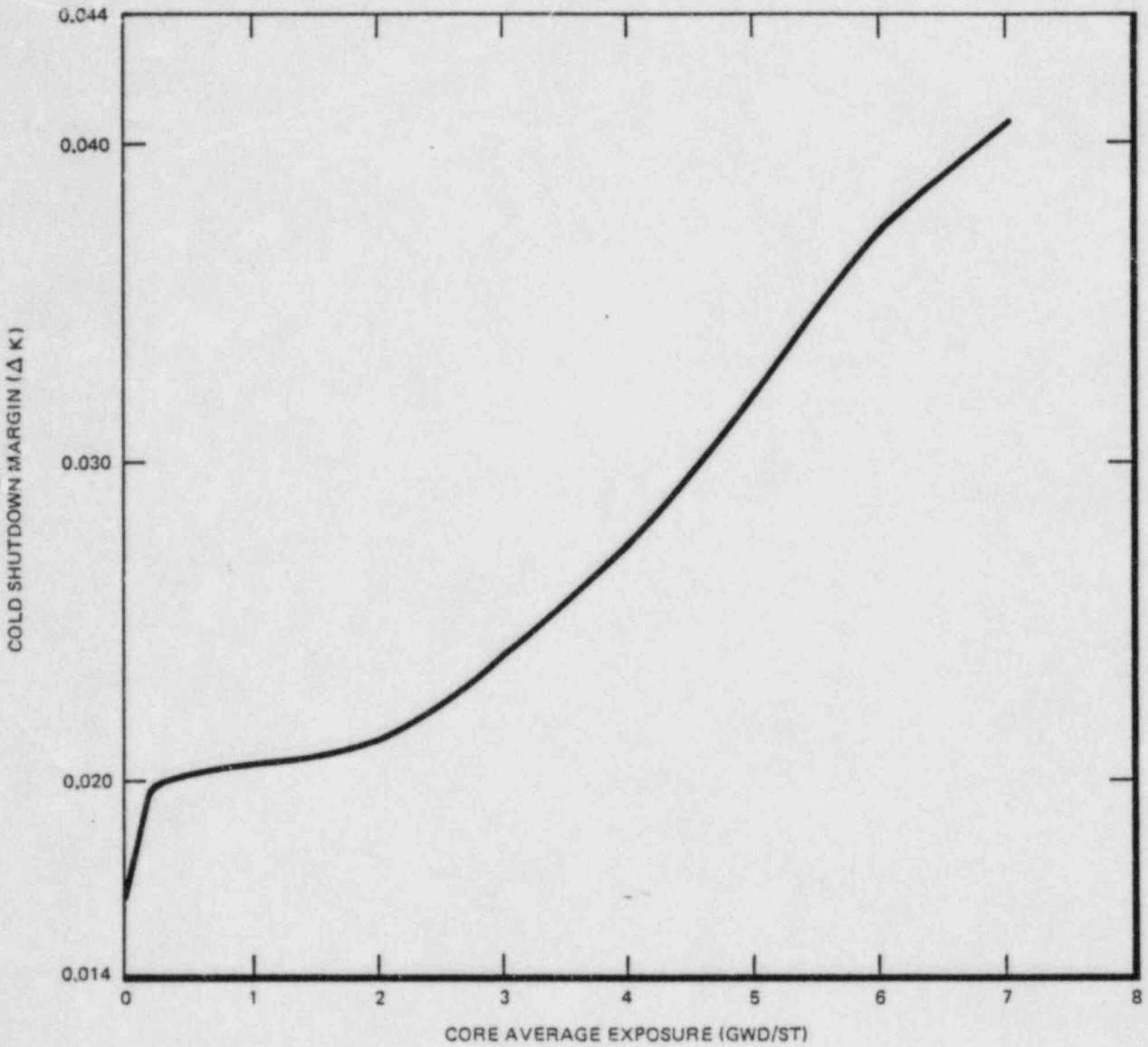

Figure 4.3-17 RIVER BEND STATION – FSAR COLD SHUTDOWN MARGIN AS A FUNCTION OF EXPOSURE; STRONGEST ROD WITHDRAWN, NO XENON

85-201-01

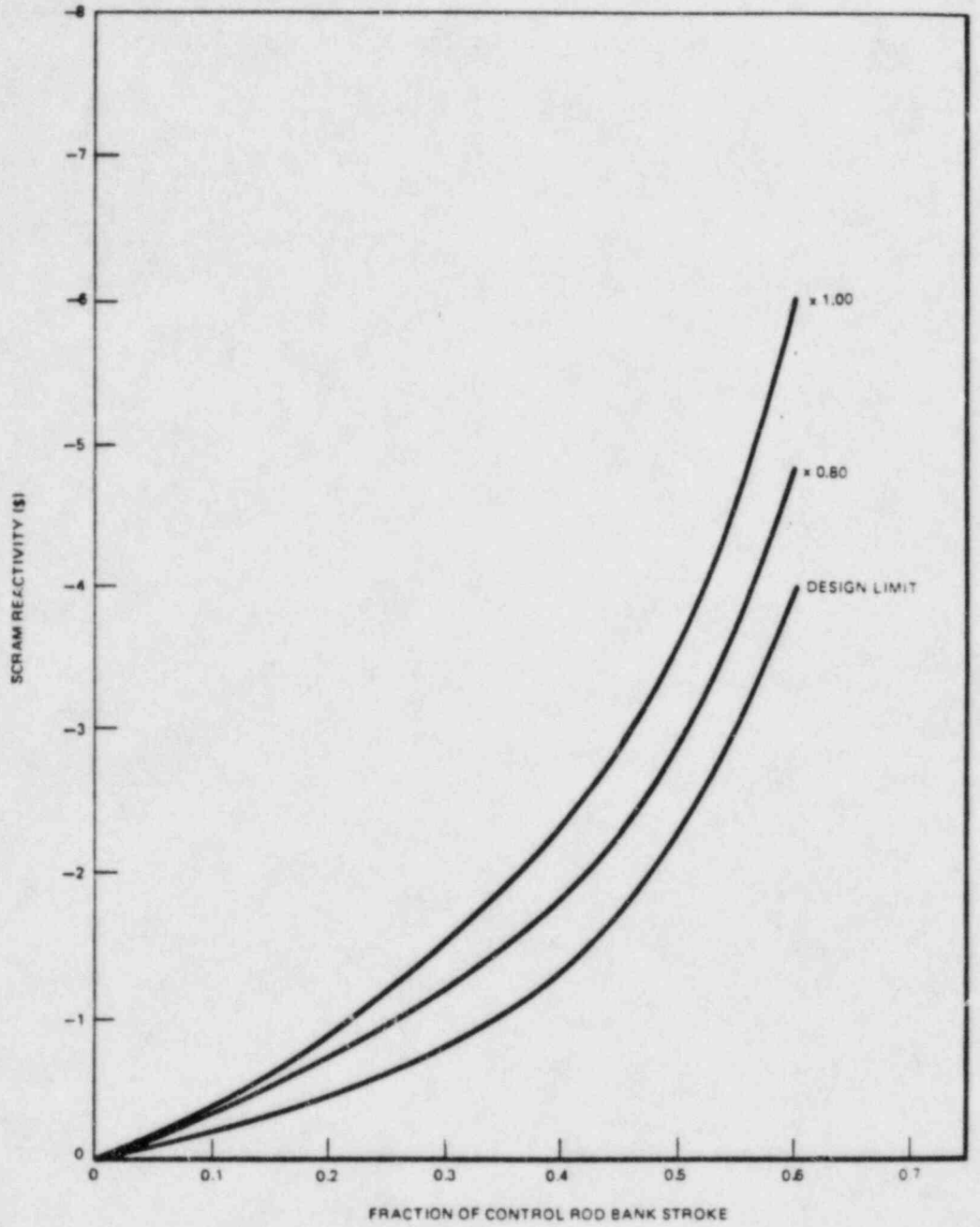

Replace with attached

FIGURE 4.3-~~26~~ 18

HOT OPERATING, EOC-1 SCRAM REACTIVITY ($) AS A FUNCTION OF CONTROL FRACTION

RIVER BEND STATION

FINAL SAFETY ANALYSIS REPORT

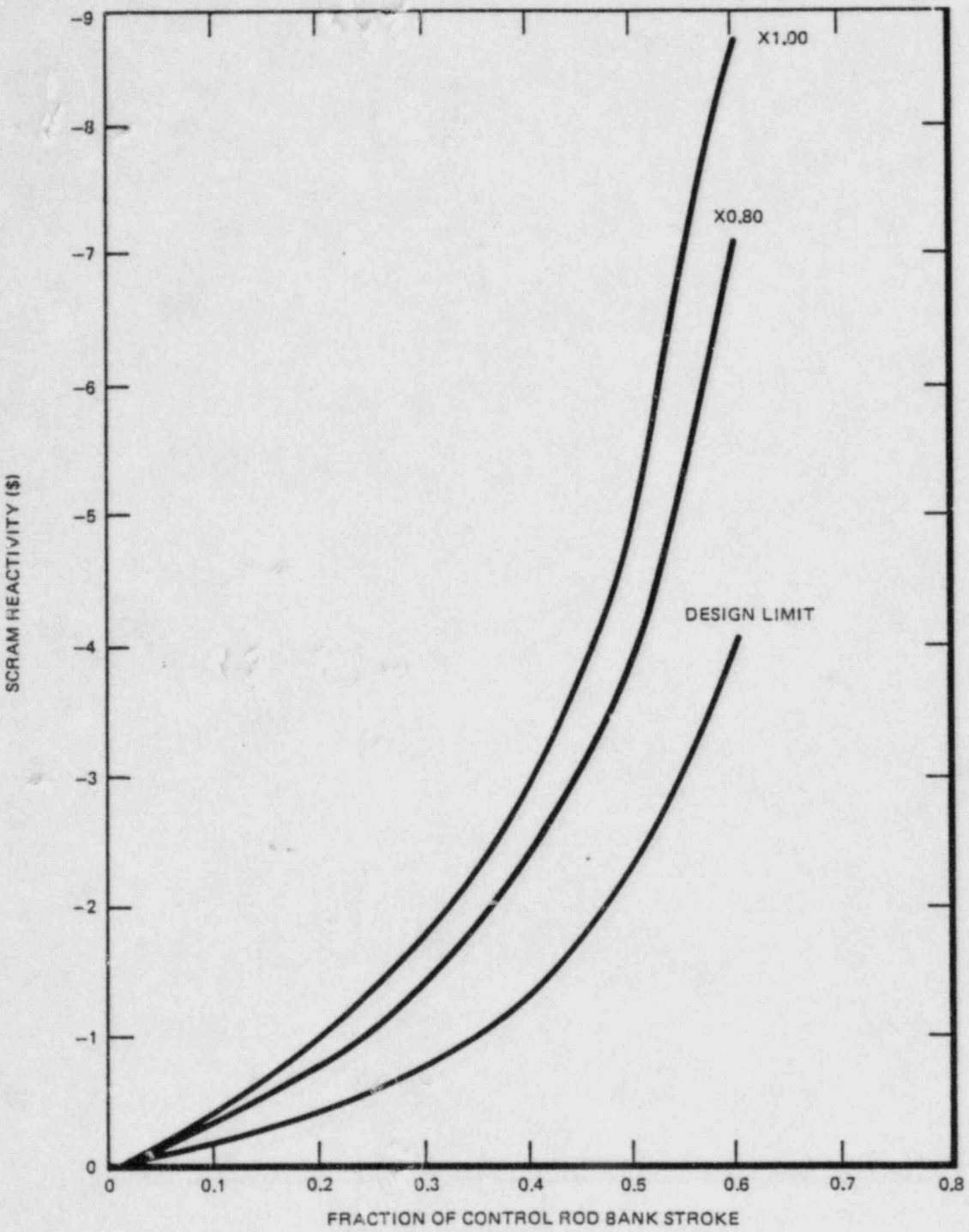

Figure 4.3-18 RIVER BEND STATION – FSAR HOT OPERATING, EOC-1 SCRAM REACTIVITY ($) AS A FUNCTION OF CONTROL FRACTION

85-201-03

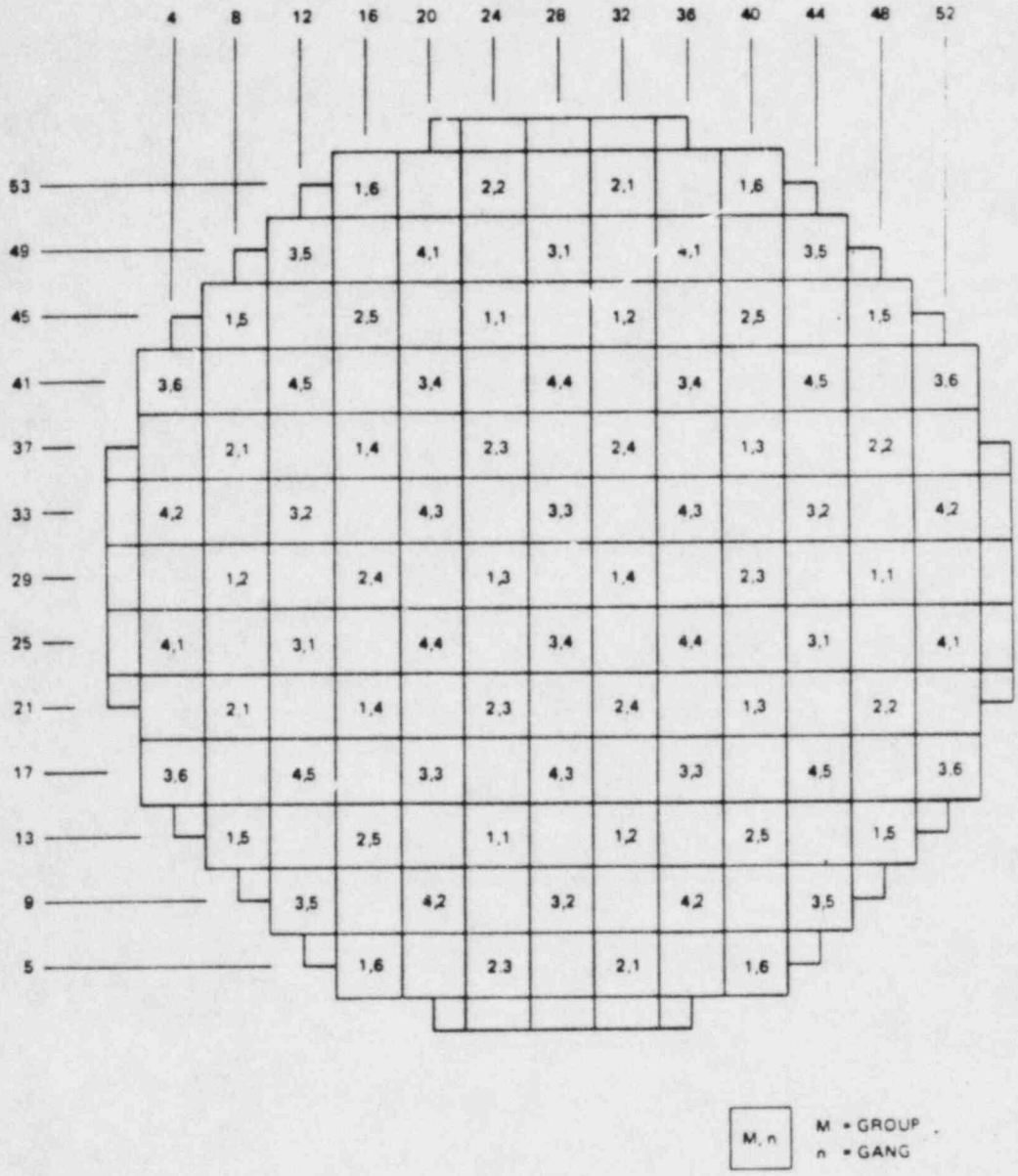

Replace with attached

FIGURE 4.3-27 19

BANKED POSITION WITHDRAWAL SEQUENCE RPCS - GROUPS 1 THROUGH 4, SEQUENCE A

RIVER BEND STATION

FINAL SAFETY ANALYSIS REPORT

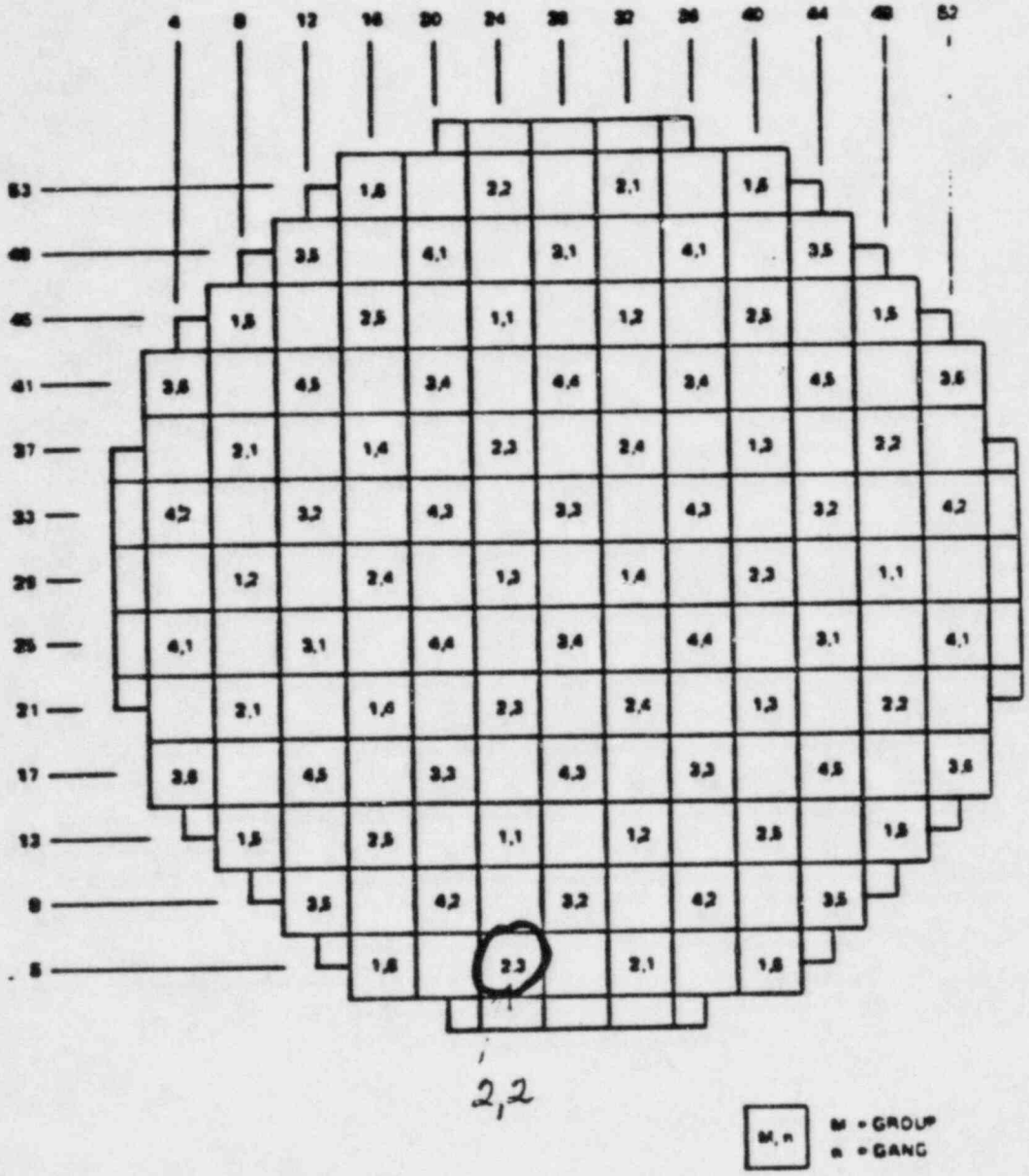

2,2

Ref. 73S HAC 9AF
Rev. 6

FIGURE 4.3-19

BANKED POSITION WITHDRAWAL SEQUENCE RPCS - GROUPS 1 THROUGH 4, SEQUENCE A

E.O.E.

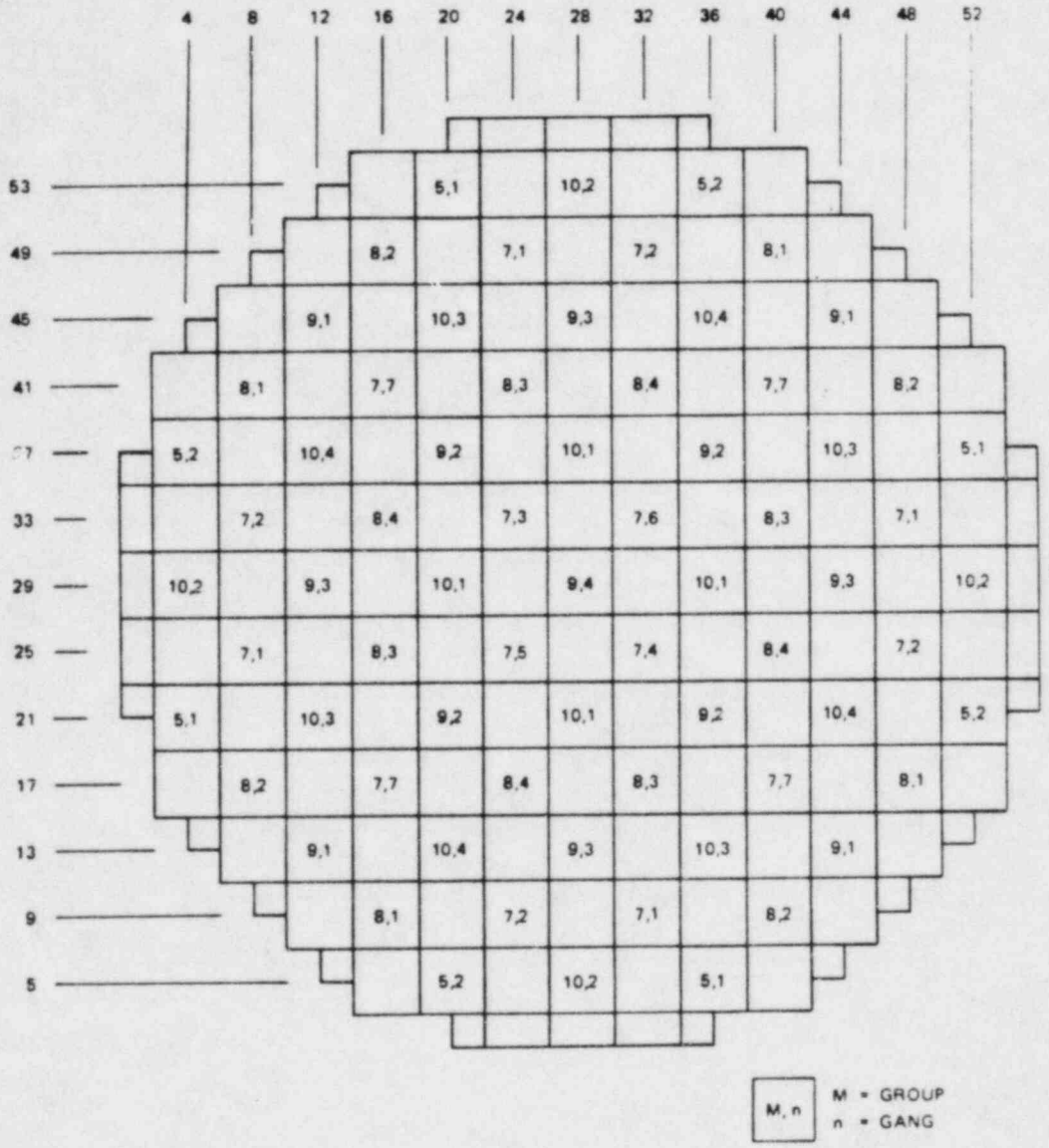

Replace with attached

FIGURE 4.3-~~28~~ 20

BANKED POSITION WITHDRAWAL SEQUENCE RPCS - GROUPS 5 THROUGH 10, SEQUENCE A

RIVER BEND STATION

FINAL SAFETY ANALYSIS REPORT

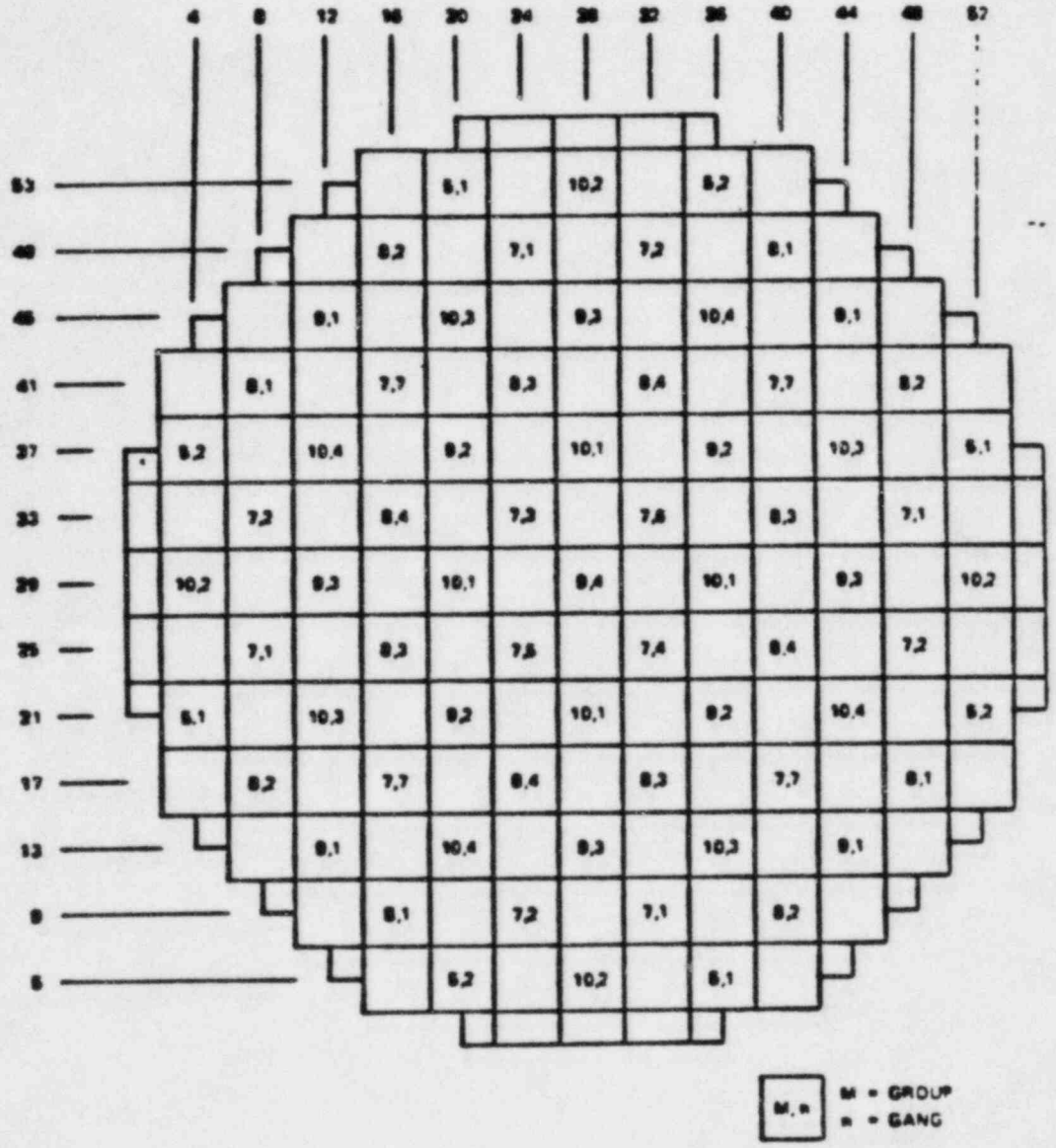

Dec 383HA669AF
Rev. 6

FIGURE 4.3-~~20~~

BANKED POSITION WITHDRAWAL SEQUENCE RPCS - GROUPS 5 THROUGH 10, SEQUENCE A

E.O.E.

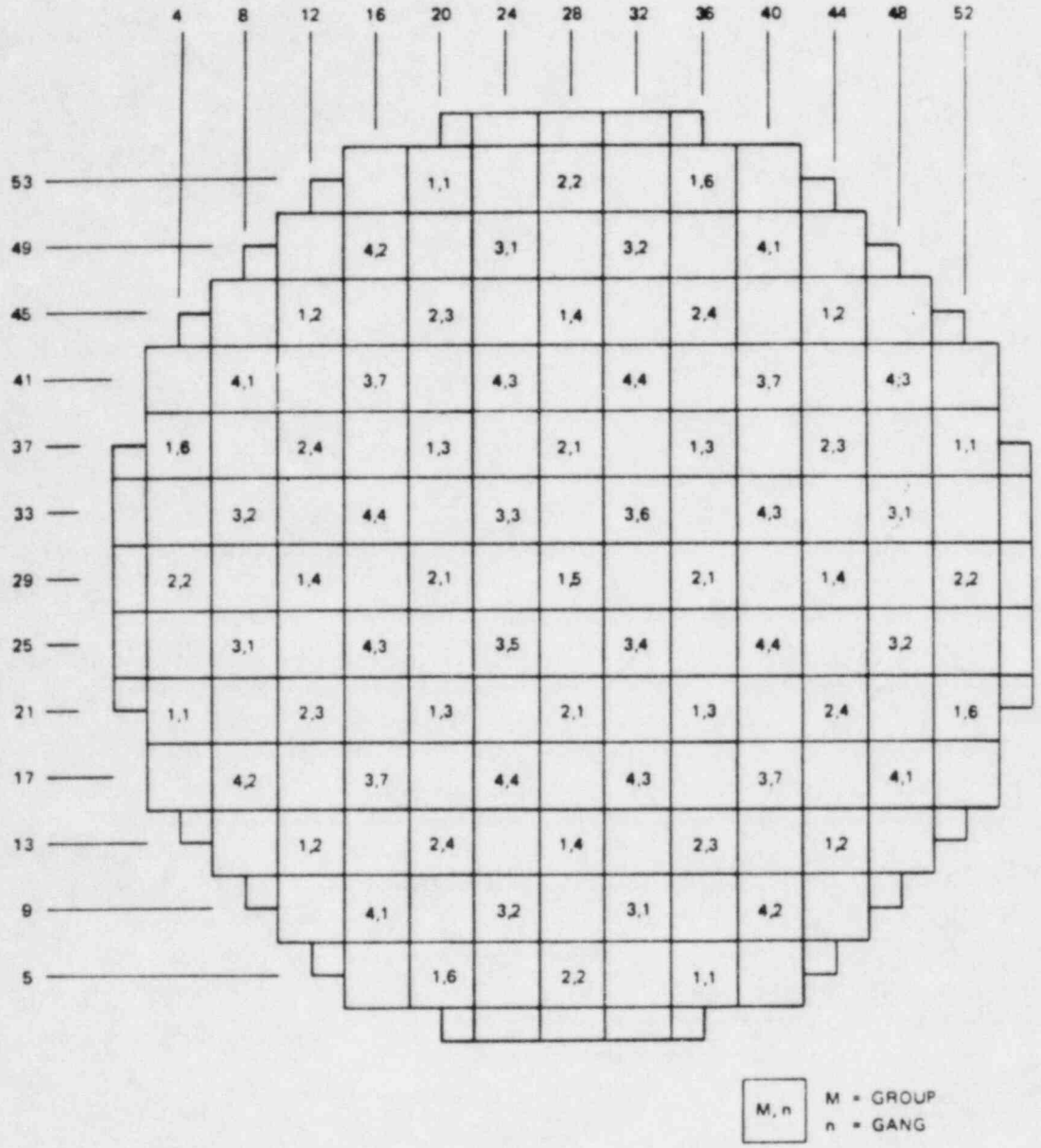

Replace with attached

FIGURE 4.3-~~29~~ 21

BANKED POSITION WITHDRAWAL SEQUENCE RPCS- GROUPS 1 THROUGH 4, SEQUENCE B

RIVER BEND STATION

FINAL SAFETY ANALYSIS REPORT

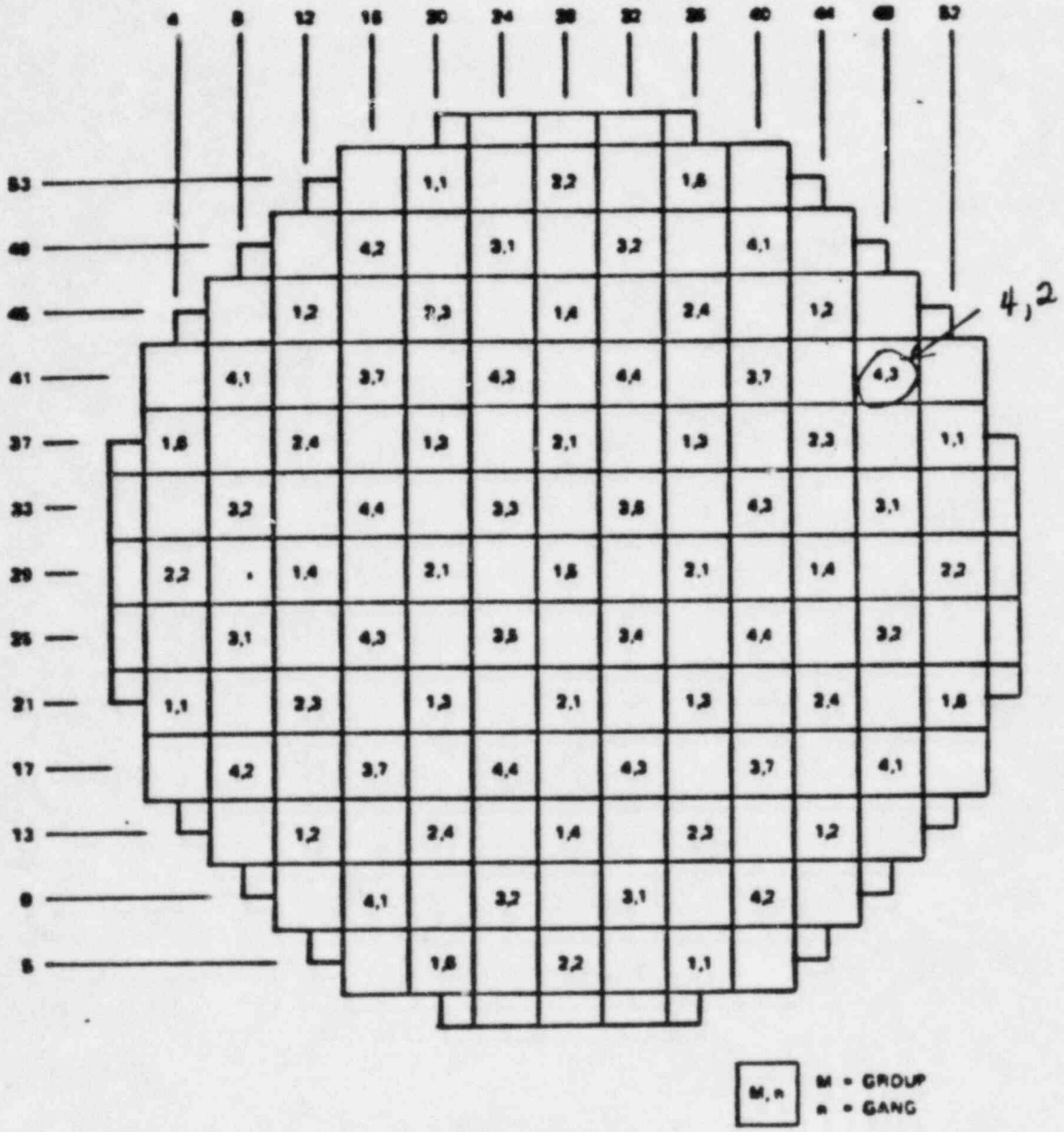

Doc. 553HA669AF

Rev. 6

E.O.E.

FIGURE 4.3-20

BANKED POSITION WITHDRAWAL SEQUENCE RPCS- GROUPS 1 THROUGH 4, SEQUENCE B

RIVER BEND STATION

FINAL SAFETY ANALYSIS REPORT

From 50 percent rod density to the low power set point (LPSP), groups 5-10 are to be withdrawn as follows: rod groups 5 and 6 are to be withdrawn to notch positions 00->N1->48. N1 is to be a flexible input which may vary from fuel cycle to fuel cycle.

Any group may be selected next; however, if rods in group 7 or 8 are moved first, rods in groups 9 and 10 cannot be moved until all rods contained in groups 5 and 6 and 7 or 8 are at notch position ≥N1. If rods in group 9 or 10 are moved first, rods in groups 7 and 8 cannot be moved until all rods contained in groups 5 and 6 and 9 or 10 are at notch position ≥N1. In this mode of operation, ganged rod operation is permitted.

Insert A

When the low power set point (LPSP) is reached, no further restrictions on rod movement are imposed. This set point is well above defined to be the point at which the rod drop accident consequences are no longer limiting and is determined to be at 20 percent power level. This power level is derived by measuring first stage turbine pressure using transmitters and alarm units. There are two channels of instruments which are redundant and separated divisionally. These trip functions are input to the proper rod activity control cabinet, and both instrument channels must trip to bypass the RPCS. These instruments are continuously monitored, and any instruments out of service or gross failure is alarmed and indicated in the main control room.

Insert B

From the LPSP on up in power, no restriction of rod motion is imposed until the high power set point (HPSP) is reached. From the HPSP (70 percent power level) to 100 percent power, rod withdrawals are restricted to prevent excessive change in the heat flux rate. A fixed number of notches is allowed for rod movement, and motion beyond this point is blocked.

Insert C

Shutdown follows the same rules previously stated but in reverse. The only difference is that an approach alarm, called the low power alarm point, is provided so that the operator may prepare valid rod positions for proper shutdown below the LPSP.

Because of the possibility of stuck rods, provisions are made by bypass failed inputs according to the following rules. Substitute rod positions may be entered into the RPCS providing:

1. Only one entry per channel per subgroup is allowed.

Insert A (page 7.6-16)

restrictions on rod movement to minimize the consequences of a rod drop accident are no longer imposed.

Insert B (page 7.6-16)

switch the RPCS to the rod withdrawal limiter mode.

Insert C (page 7.6-16)

The minimum setpoint of 20% power level is well below the analytical maximum for this setpoint. From the LPSP to the high power setpoint (HPSP), rod motion is limited to four (4) notches (two feet) and from the HPSP on up in power, rod motion is limited to two (2) notches (one foot). The HPSP, which has been determined to be at 70% power level, provides adequate margin from the analytical point at which the one foot restriction on rod motion is required.

actuations allow pneumatic pressure from the accumulator to act on the air cylinder operator and open the valve.

Operation of the SRV is initiated by high reactor vessel pressure. Redundant reactor vessel pressure channels are provided in each trip system which operate in a two-out-of-two configuration in order to prevent inadvertent SRV actuation. Each trip system provides the following capabilities:

1. Initiate operation of three groups of SRVs at the respective pressure set points. This feature automatically adjusts the relief capacity to the size of the overpressure condition. The reclose pressure set point (reset) for any group is separately adjusted, and adequate deadband is provided to eliminate rapid open/close operation and minimize system stresses.

2. Alter set points on five selected valves to minimize the number of valves that reopen following the initial pressure surge. In order to assure that no more than one relief valve reopens following a reactor isolation event, six SRV valves are provided with lower opening and closing set points. These set points override the normal set points following the initial opening of the relief valves and act to hold these valves open longer, thus preventing more than a single valve from reopening subsequently. This system logic is referred to as the low-low set point relief logic and functions to ensure that the containment integrity is not threatened on subsequent ADS actuations. This logic is armed when two or more valves are signaled to open from their normal relief pressure switches. At this time, the low-low set logic automatically seals itself into control of the six selected valves and actuates the annunciator. This logic remains sealed in until manually reset by the operator. (11)

   Since the valves have already opened from their original pressure relief signals, the low-low set logic acts to hold them open past their normal reclose point until the pressure decreases to a predetermined low-low set point. Thus these valves remain open longer than the other safety/relief valves. This extended relief capacity assures that no more than one valve reopens a second time. Also, the sealed-in logic provides the low-low set valves with new reopening set points which are

lower than than their original safety/relief set points. The "medium" low-low set valve acts as a backup for the "low" low-low set valve, should it mechanically fail. See Section 5.2.2 for further system description.

The low-low set logic is designed with redundancy and single failure criteria, i.e., no single electrical failure 1) prevents any low-low set valve from opening, or 2) causes inadvertent seal-in of low-low set logic.

The ~~six~~ five valves associated with low-low set are arranged in three independent secondary set point groups or ranges (low, medium, high). The low and medium pressure ranges consist of one valve each, having both reopen and reclose set points independently and uniquely adjustable. These are set considerably lower than their normal SRV set points. The remaining valves are individually controlled by new pressure switches which have an independently adjustable reclose set point. The normal SRV opening set points are slightly lower for this valve group though reclose is extended in the low-low set operating mode. 11

The pressure switches are arranged in two divisions for each low-low set valve. The single-failure criterion is thus met for this function.

The SRV system has two low-low set point logics, one in Division 1 and the other in Division 2. Either one can perform the low-low set function. Each valve has its own set of pressure switches. A key-locked switch which has a normal and a test position is provided for each division. The key is removable only in the normal position. When the key is inserted and switched to test, an annunciator alerts the operator of the test status of that division. In the test mode, all of the valves except the specific one under test remain responsive to the high reactor pressure signals should they occur. Indicator lights are switched in series with the solenoid coils on the low-low set valve to facilitate logic testing.

Manual system level initiation capability is included in each trip system. Remote manual switches are installed in the main control room. Lights in the main control room

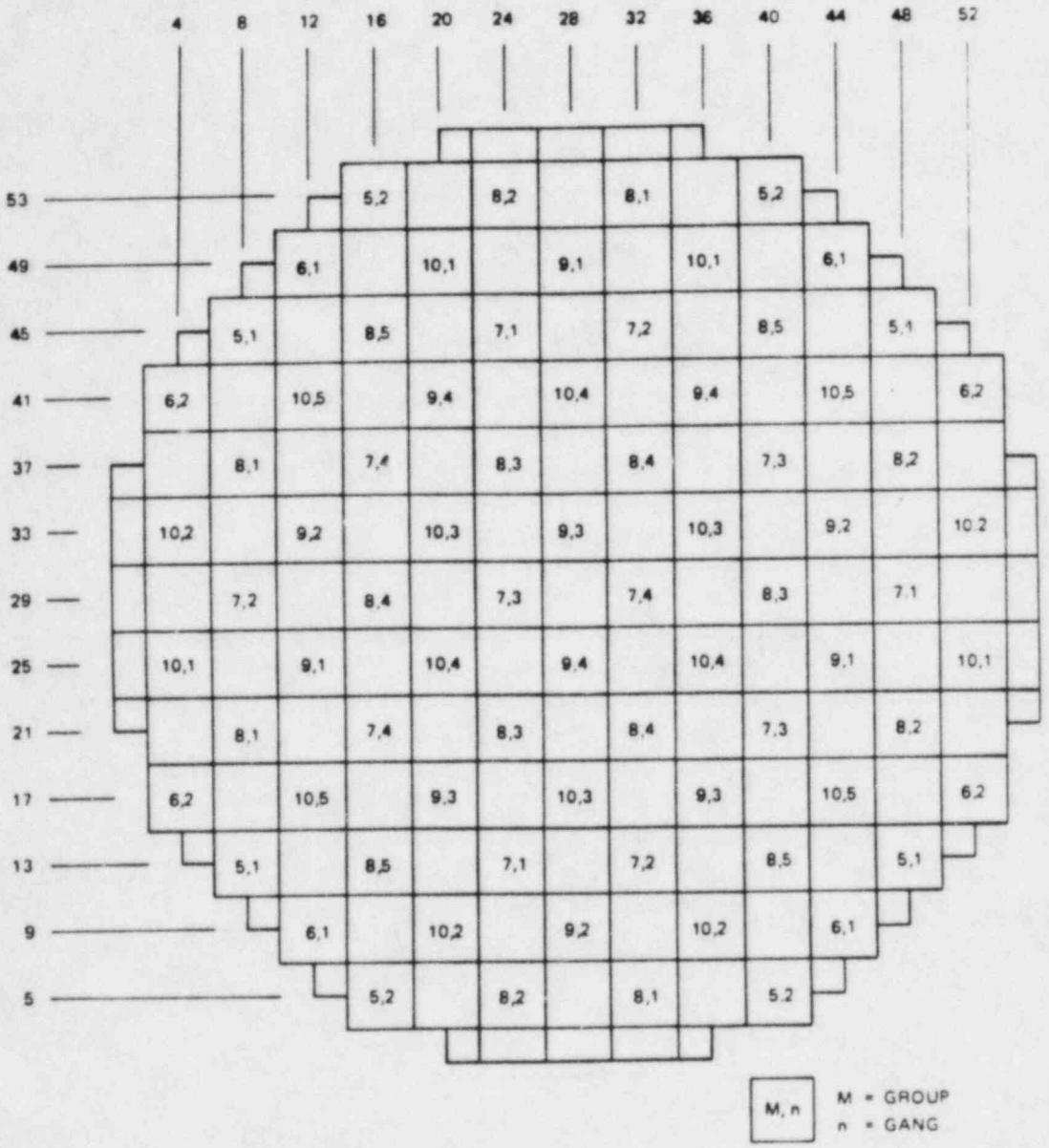

Replace with attached

FIGURE 4.3-~~30~~ 22

BANKED POSITION WITHDRAWAL SEQUENCE RPCS - GROUPS 5 THROUGH 10, SEQUENCE B

RIVER BEND STATION

FINAL SAFETY ANALYSIS REPORT

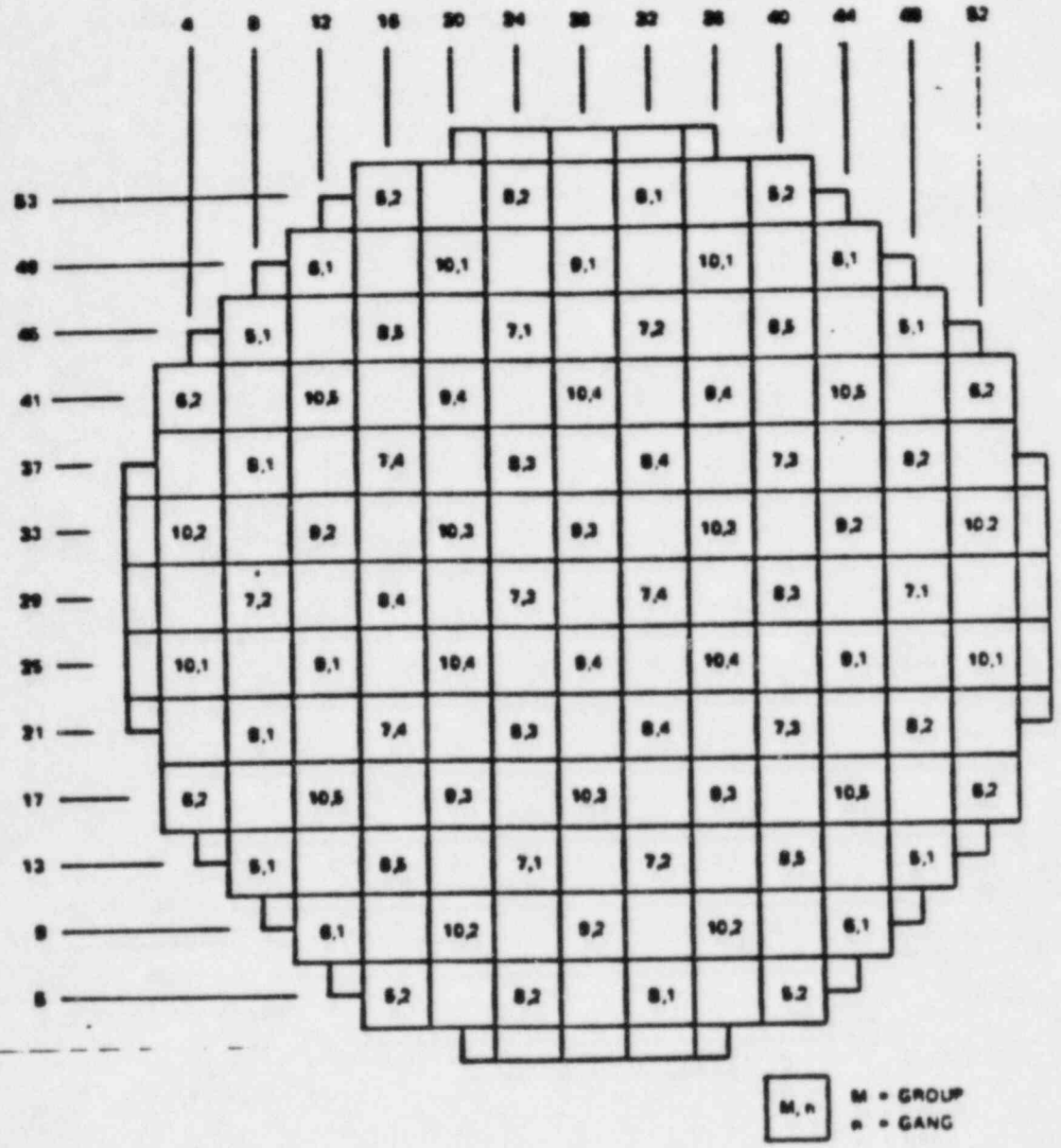

FIGURE 4.3-22

BANKED POSITION WITHDRAWAL SEQUENCE RPCS - GROUPS 5 THROUGH 10, SEQUENCE B

Doc. 383 HA 669 AF

Rev. 6

E.O.E.

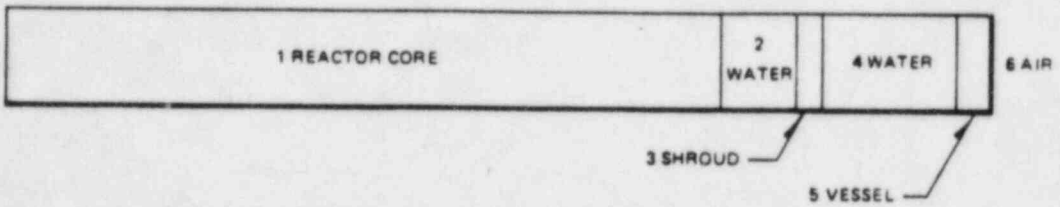

MATERIAL		RADIUS (in.)	MATERIAL	MATERIAL DENSITY
NO.	NAME			
1	REACTOR CORE	84.6	WATER	0.318 g/cm^3
			UO_2	2.334 g/cm^3
			ZIRCONIUM	0.978 g/cm^3
			304L STAINLESS STEEL	0.088 g/cm^3
2	WATER	91.0	WATER	0.74 g/cm^3
3	SHROUD	93.0	304L STAINLESS STEEL	FROM ASME SA240
4	WATER	109.0	WATER	0.74 g/cm^3
5	VESSEL	114.41	CARBON STEEL	FROM ASME SA533 GR.B,CL.1
6	AIR		AIR	1.3×10^{-3} g/cc

FIGURE 4.3-~~31~~ 23

MODEL FOR ONE-DIMENSIONAL TRANSPORT ANALYSIS OF VESSEL FLUENCE

RIVER BEND STATION
FINAL SAFETY ANALYSIS REPORT

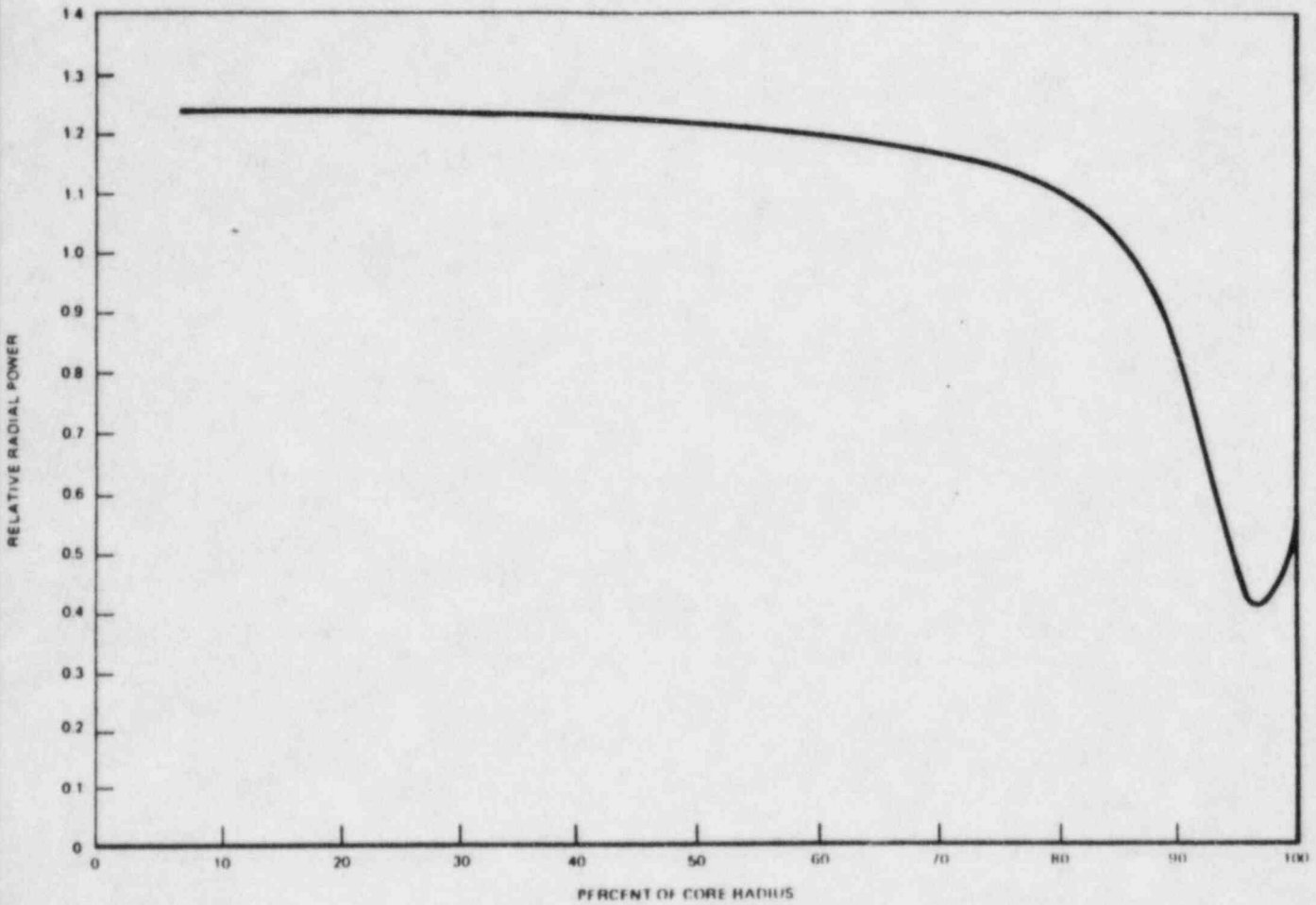

FIGURE 4.3-32 24

RADIAL POWER DISTRIBUTIONS
USED IN THE VESSEL
FLUENCE CALCULATIONS

RIVER BEND STATION
FINAL SAFETY ANALYSIS REPORT

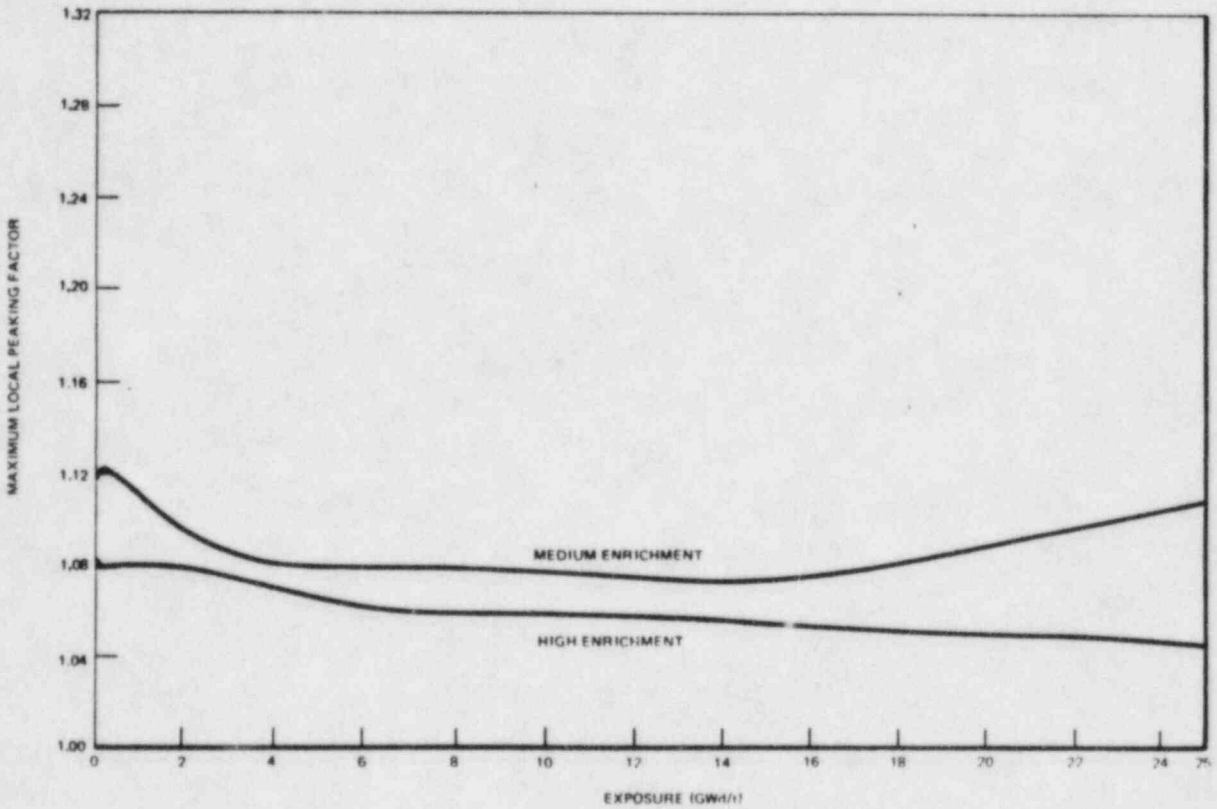

Deleted

FIGURE 4.3-14

VARIATION OF MAXIMUM LOCAL POWER PEAKING AS A FUNCTION OF EXPOSURE, DOMINANT FUEL TYPES, 40% VOIDS, UNCONTROLLED

THIS FIGURE IS GE COMPANY
PROPRIETARY AND IS SUBMITTED
UNDER SEPARATE PROPRIETARY COVER.

Deleted

FIGURE 4.3-15

UNCONTROLLED LOCAL POWER DISTRIBUTION AT 40% VOIDS AS A FUNCTION OF EXPOSURE-- HIGH ENRICHMENT DOMINANT FUEL TYPE (GE COMPANY PROPRIETARY)

THIS FIGURE IS GE COMPANY
PROPRIETARY AND IS SUBMITTED
UNDER SEPARATE PROPRIETARY COVER.

Deleted

FIGURE 4.3-16

UNCONTROLLED LOCAL POWER DISTRIBUTION AS A FUNCTION OF VOIDS AT BEGINNING OF CYCLE-- HIGH ENRICHMENT DOMINANT FUEL TYPE (GE COMPANY PROPRIETARY)

THIS FIGURE IS GE COMPANY
PROPRIETARY AND IS SUBMITTED
UNDER SEPARATE PROPRIETARY COVER.

Deleted

FIGURE 4.3-17

CONTROLLED LOCAL POWER DISTRIBUTION AT 40% VOID-- BEGINNING OF CYCLE-- HIGH ENRICHMENT DOMINANT FUEL TYPE (GE COMPANY PROPRIETARY)

THIS FIGURE IS GE COMPANY
PROPRIETARY AND IS SUBMITTED
UNDER SEPARATE PROPRIETARY COVER.

Deleted

FIGURE 4.3-18

UNCONTROLLED R-FACTOR
DISTRIBUTION AT 40% VOIDS--
BEGINNING OF CYCLE-- HIGH
ENRICHMENT DOMINANT FUEL TYPE
(GE COMPANY PROPRIETARY)

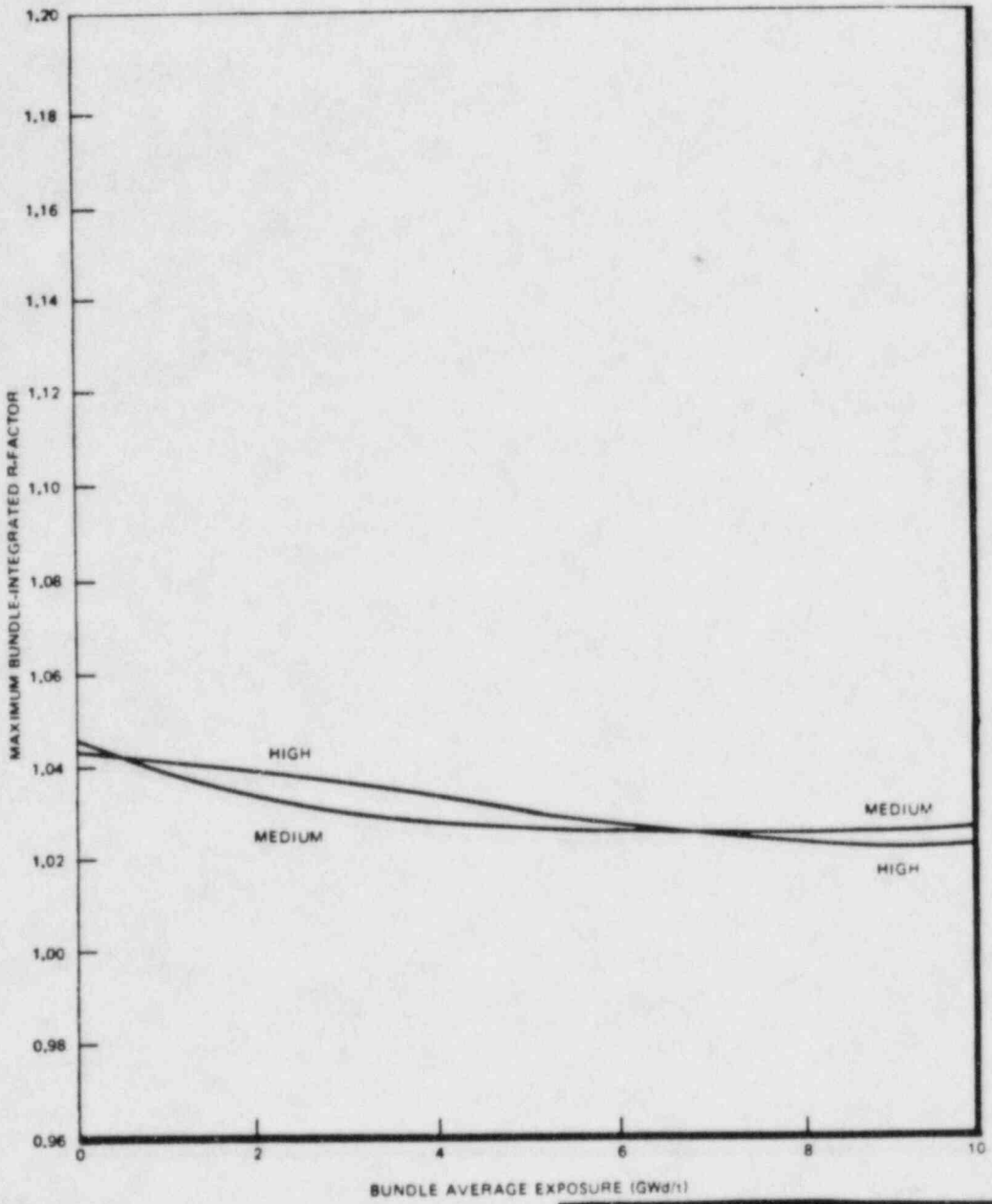

FIGURE 4.3-19

VARIATION OF THE MAXIMUM BUNDLE-INTEGRATED R-FACTOR AS A FUNCTION OF BUNDLE AVERAGE EXPOSURE FOR THE UNCONTROLLED HIGH ENRICHED BUNDLE AND THE MEDIUM ENRICHED BUNDLE

Deleted

RIVER BEND STATION
FINAL SAFETY ANALYSIS REPORT

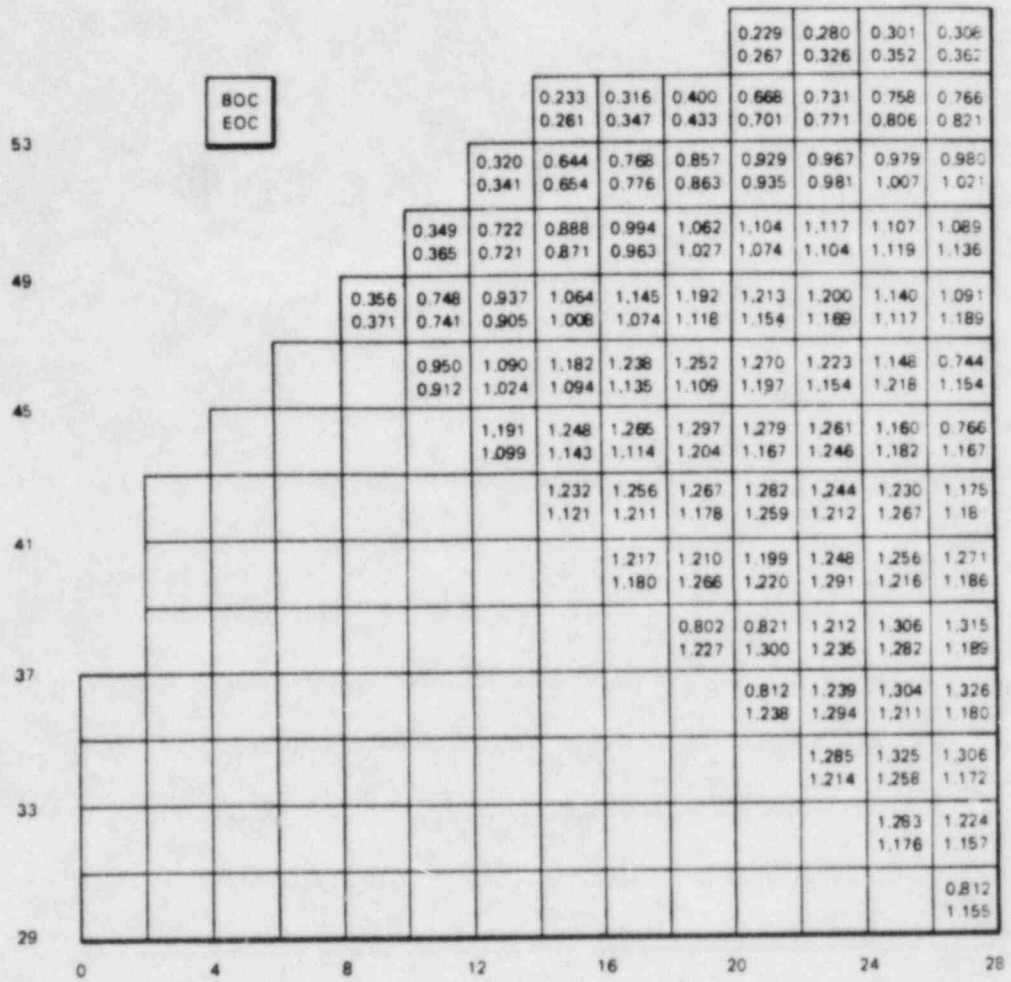

Deleted

FIGURE 4.3-20

RADIAL POWER FACTORS FOR BEGINNING-OF-CYCLE AND OPTIMAL END-OF-CYCLE CONDITIONS

RIVER BEND STATION

FINAL SAFETY ANALYSIS REPORT

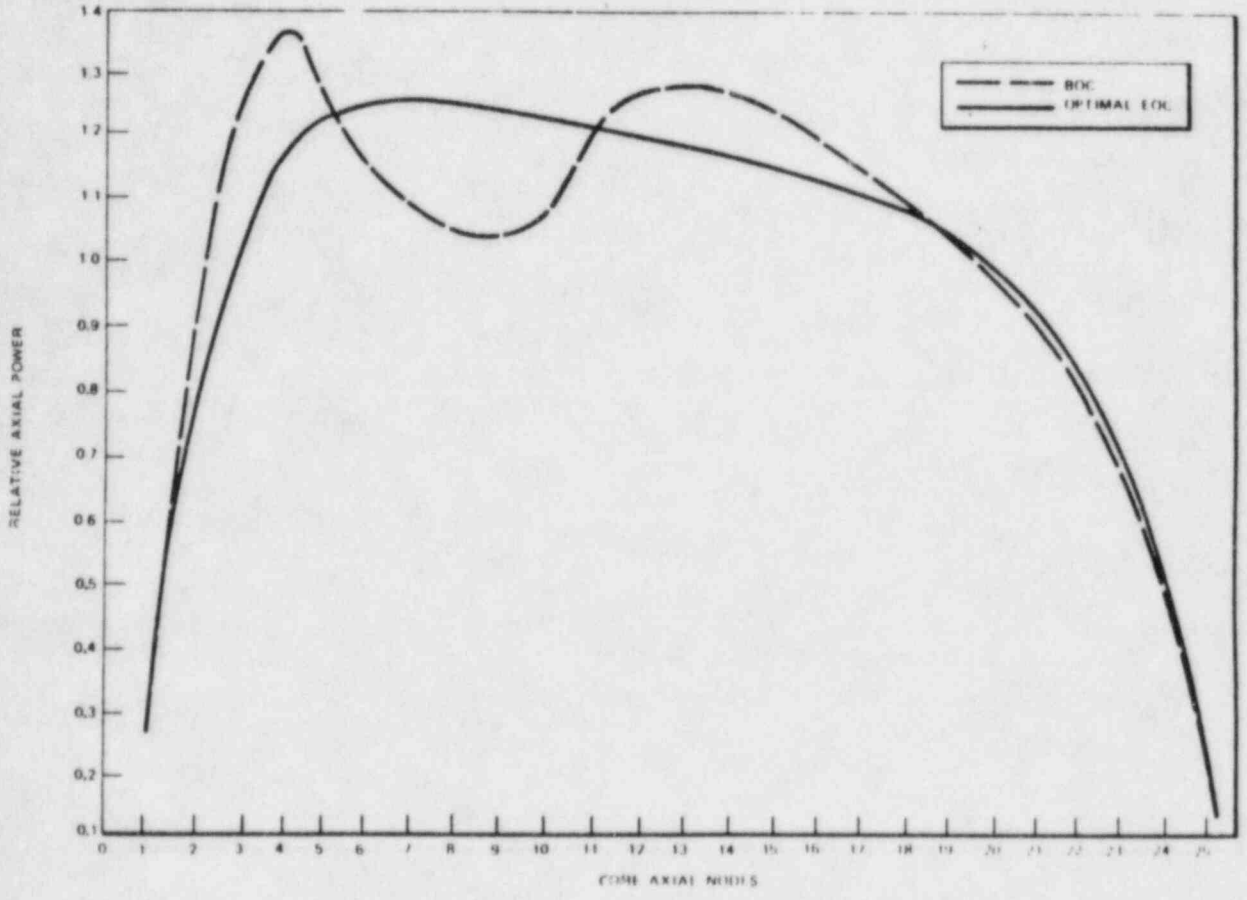

Deleted

FIGURE 4.3-21

BEGINNING OF CYCLE AND OPTIMAL END OF CYCLE CORE AVERAGE AXIAL POWER

RIVER BEND STATION
FINAL SAFETY ANALYSIS REPORT

TABLE 4.4-1

THERMAL AND HYDRAULIC DESIGN CHARACTERISTICS OF THE REACTOR CORE

	River Bend	Perry	Grand Gulf
General Operating Conditions			
Reference rated thermal output, Mwt	2,894	3,579	3,833
Design power level for engineered safety features, Mwt	3,015	3,758	4,025
Rated steam flow rate, at 420°F final feedwater temperature, millions lb/hr	12.453	15.400	16.49
Core coolant flow rate, millions lb/hr	84.5	104.0	112.5
Feedwater flow rate, millions lb/hr	12.428	15.367	16.46
System pressure, nominal in steam dome, psia	1,040	1,040	1,040
System pressure, nominal core design, psia	1,055	1,055	1,055
Coolant saturation temperature at core design pressure, °F	551	551	551
Average power density, kW/liter	52.4	54.1	54.1
Maximum LHGR, kW/ft	13.4	13.4	13.4
Average LHGR, kW/ft	5.7	5.9	5.9
Core total heat transfer area, sq ft	61,151	73,303	78,398
Maximum heat flux, Btu/hr-sq ft	361,600	361,600	361,600
Average heat flux, Btu/hr-sq ft	154,600	159,500	159,800
Design operating MCPR	1.20 1.18	1.20	1.20 1.18
Core inlet enthalpy at 420°F FFWT, Btu/lb	527.8	527.7	527.9

Hydraulic supply subsystem pressures can be observed from instrumentation in the main control room. Scram accumulator pressures can be observed on the nitrogen pressure gages.

4.6.3.1.1.4 Acceptance Tests

Criteria for acceptance of the individual CRD mechanisms and the associated control and protection systems will be incorporated in specifications and test procedures covering three distinct phases: 1) preinstallation, 2) after installation prior to startup, and 3) during startup testing.

The preinstallation specification will define criteria and acceptable ranges of such characteristics as seal leakage, friction, and scram performance under fixed test conditions which must be met before the component can be shipped.

The after installation, prestartup tests (Chapter 14) include normal and scram motion and are primarily intended to verify that piping, valves, electrical components, and instrumentation are properly installed. The test specifications will include criteria and acceptable ranges for drive speed, timer settings, scram valve response times, and control pressures. These tests are intended more to document system condition than system performance.

As fuel is placed in the reactor, the startup test procedure (Chapter 14) will be followed. The tests in this procedure are intended to demonstrate that the initial operational characteristics meet the limits of the specifications over the range of primary coolant temperatures and pressures from ambient to operating. The detailed specifications and procedures have not as yet been prepared but will follow the general pattern established for such specifications and procedures in BWRs presently under construction and in operation.

4.6.3.1.1.5 Surveillance Tests

The surveillance requirements for the CRD system are described as follows:

1. Sufficient control rods shall be withdrawn, following a refueling outage when core alterations are performed, to demonstrate with a margin of 0.28 percent Δk that the core can be made subcritical at any time in the subsequent fuel cycle with the strongest operable control rod fully withdrawn and all other operable rods fully inserted. $\Delta k/k$

2. Each partially or fully withdrawn control rod shall be exercised one notch at least once each week.

   In the event that operation is continuing with three or more rods valved out of service, this test shall be performed at least once each day.

   The weekly control rod exercise test serves as a periodic check against deterioration of the control rod system and also verifies the ability of the CRD to scram. If a rod can be moved with drive pressure, it may be expected to scram since higher pressure is applied during scram. The frequency of exercising the control rods under the conditions of three or more control rods valved out of service provides even further assurance of the reliability of the remaining control rods.

3. The coupling integrity shall be verified for each withdrawn control rod as follows:

   a. When the rod is first withdrawn, observe discernible response of the nuclear instrumentation; and

   b. When the rod is fully withdrawn the first time, observe that the drive will not go to the overtravel position.

   Observation of a response from the nuclear instrumentation during an attempt to withdraw a control rod indicates indirectly that the rod and drive are coupled. The overtravel position feature provides a positive check on the coupling integrity, for only an uncoupled drive can reach the overtravel position.

4. During operation, accumulator pressure at the normal operating value shall be verified. | 18

   Experience with CRD systems of the same type indicates that verification of accumulator pressure is sufficient to assure operability of the accumulator portion of the CRD system. | 18

5. At the time of each major refueling outage, each operable control rod shall be subjected to scram time tests from the fully withdrawn position.

Experience indicates that the scram times of the control rods do not significantly change over the time interval between refueling outages. A test of the scram times at each refueling outage is sufficient to identify any significant lengthening of the scram times. However, an additional test of at least 10% of the control rods, on a rotating basis, will be performed at least once per 120 days of power operation.

4.6.3.1.1.6 Functional Tests

The functional testing program of the CRDs consists of the 5 yr maintenance life and the 1.5 times design life test programs as described in Section 3.9.4.4.

There are a number of failures that can be postulated on the CRD but it would be very difficult to test all possible failures. A partial test program with postulated accident conditions and imposed single failures is available.

The following tests with imposed single failures have been performed to evaluate the performance of the CRDs under these conditions.

1. Simulated ruptured scram line test
2. Stuck ball check valve in CRD flange
3. HCU drive down inlet flow control valve (V122) failure
4. HCU drive down outlet flow control valve (V120) failure
5. CRD scram performance with V120 malfunction
6. HCU drive up outlet control valve (V121) failure
7. HCU drive up inlet control valve (V123) failure
8. Cooling water check valve (V138) leakage
9. CRD flange check valve leakage
10. CRD stabilization circuit failure
11. HCU filter restriction
12. Air trapped in CRD hydraulic system
13. CRD collet drop test
14. Control rod qualification velocity limiter drop test

Additional postulated CRD failures are discussed in Sections 4.6.2.3.2.2.1 through 4.6.2.3.2.2.11.

4.6.3.2 Control Rod Drive Housing Supports

CRD housing supports are removed for inspection and maintenance of the CRDs. The supports for one control rod can be removed during reactor shutdown, even when the reactor is pressurized, because all control rods are then inserted. When the support structure is reinstalled, it is inspected for correct assembly with particular attention to

TABLE 5.2-5

SYSTEMS WHICH MAY INITIATE DURING OVERPRESSURE EVENT

System	Initiating/Trip Signal(s)[1]
Reactor Protection System	Reactor trips "OFF" with High Flux
RCIC	"ON" with Reactor Water Level at L2
	"OFF" with Reactor Water Level at L8
HPCS	"ON" with Reactor Water Level at L2
	"ON" with High Drywell Pressure at 2 psig
	"OFF" with Reactor Water Level at L8[2]
Recirculation System	Pumps trip "OFF" with Reactor Water Level at L2
	Pumps trip to Low Frequency M/G set at L3
	"OFF" with Reactor Pressure at 1125 psig
RWCU system	"OFF" with Reactor Water Level at L2

---

[1] Vessel level trip settings are shown on Fig. 5.3-2.

[2] HPCS system continues to inject into the reactor if level L8 and a high drywell pressure signal exist.

steel is less than 100°F and the calculated peak neutron fluence E 1MEV at 1/4 T of the reactor vessel is not more than 5×10^{18} n/cm^2. The proposed withdrawal schedule is in accordance with 10CFR50, Appendix H. | 11 13

First capsule - 10 yr (one-fourth service life)
Second capsule - 30 yr (three-fourths service life)
Third capsule - standby

Fracture toughness testing of irradiated capsule specimens is to be in accordance with requirements of 10CFR50, Appendix H.

5.3.1.6.2 Neutron Flux and Fluence Calculations

A description of the methods of analysis is contained in Sections 4.1.4.5 and 4.3.2.8.

The peak fluence of 1/4 T depth of the vessel beltline material is 5×10^{18} n/cm^2 after 40 yr of service. All predictions of radiation damage to the reactor vessel beltline material were made using peak fluence values. |

5.3.1.6.3 Predicted Irradiation Effects on Vessel Beltline Materials

Estimated maximum changes in RT_{NDT} (initial reference temperature) as a function of the end-of-life (EOL) fluence at the 1/4 T depth of the vessel beltline materials are listed in Table 5.3-1. The predicted peak EOL fluence at the 1/4 T depth of the vessel beltline is 5×10^{18} n/cm^2 after 40 yr of service. Transition temperature changes and changes in upper shelf energy were calculated in accordance with the rules of Regulatory Guide 1.99. Reference temperature were established in accordance with 10CFR50, Appendix G and NB-2330 of the ASME Code. | 11

The lead factors for each surveillance capsule are 0.58 vessel i.d. and 0.86 1/4 T. Due to the geometry, the lead factors for all three capsule specimens will be the same. | 11

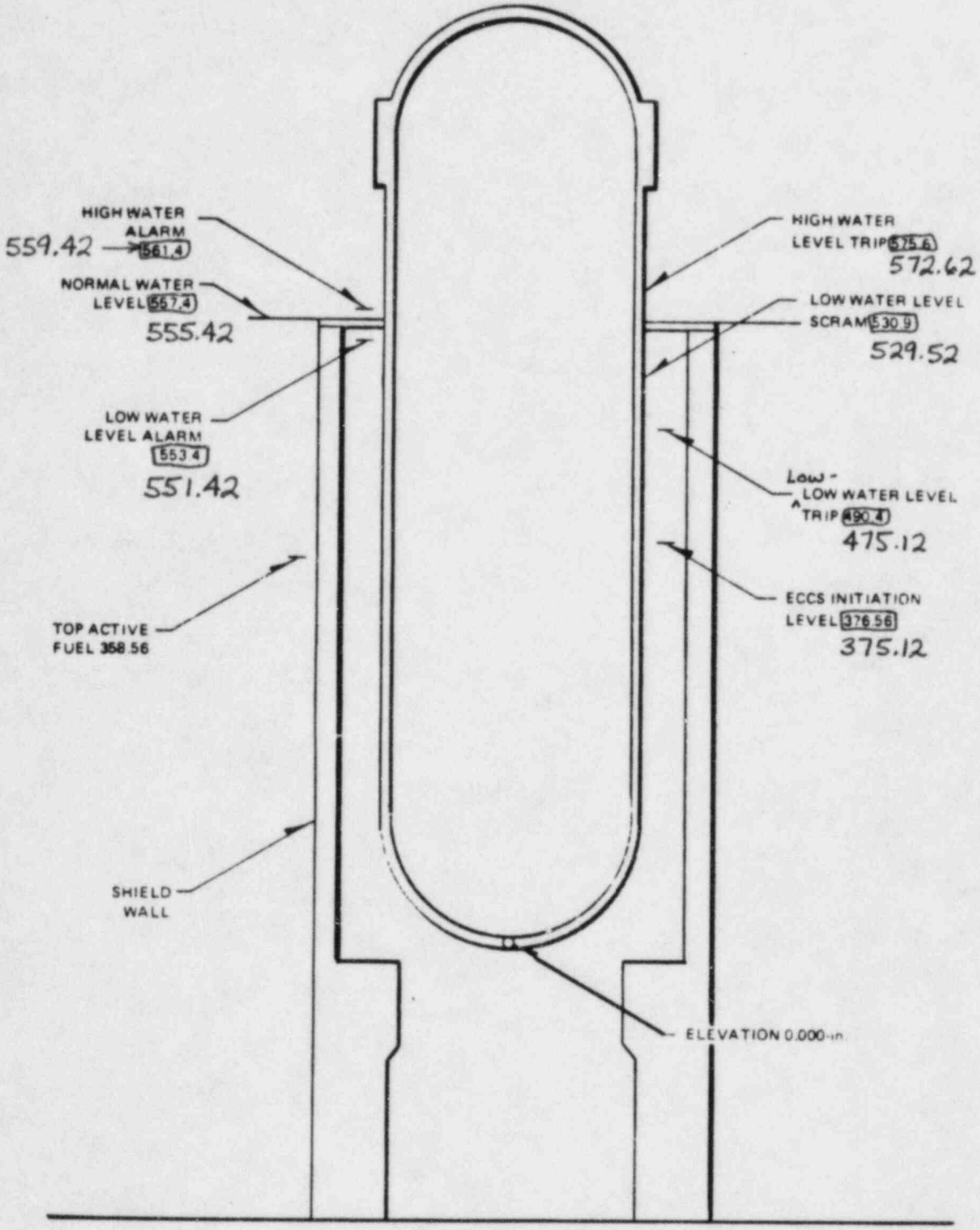

FIGURE 5.3-2

REACTOR VESSEL NOMINAL WATER LEVEL TRIP AND ALARM ELEVATIONS

RIVER BEND STATION

FINAL SAFETY ANALYSIS REPORT

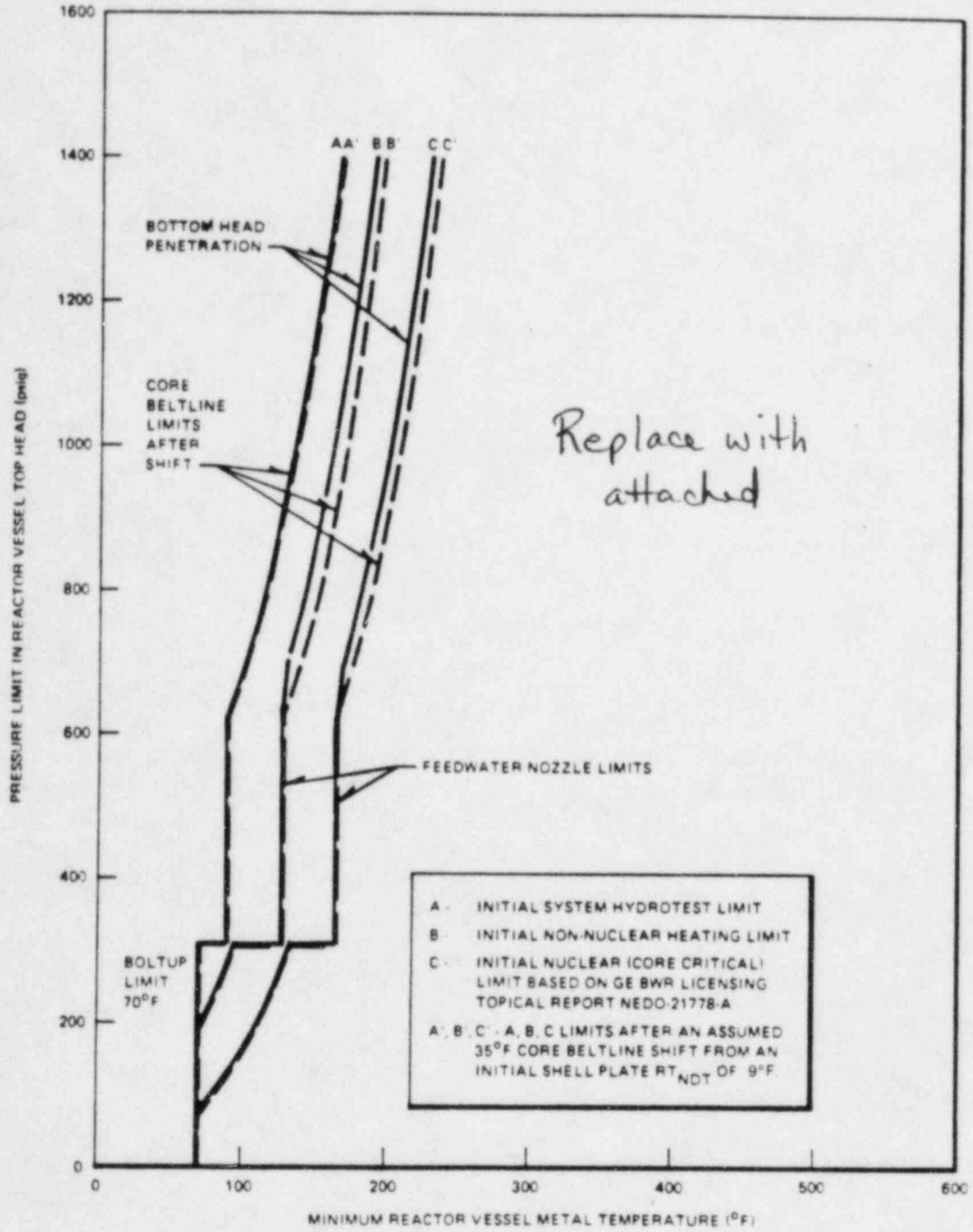

Replace with attached

NOTE:
CURVES A, B & C ARE PREDICTED TO APPLY AS THE LIMITS FOR 20 YEARS (16EFPY) OF OPERATION.

FIGURE 5.3-4

MINIMUM TEMPERATURES REQUIRED VERSUS REACTOR PRESSURE

RIVER BEND STATION
FINAL SAFETY ANALYSIS REPORT

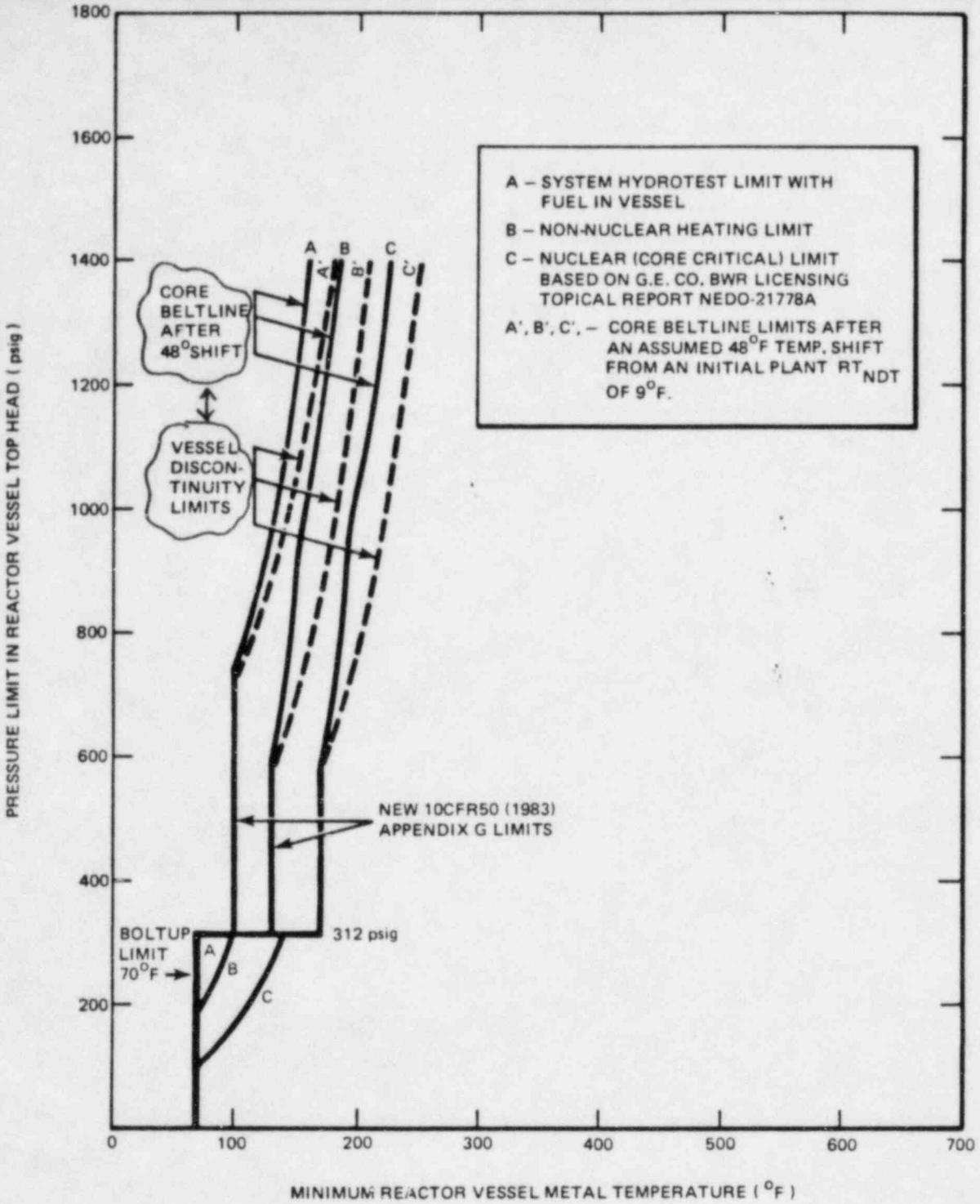

NOTE: CURVES A, B & C ARE PREDICTED TO APPLY AS THE LIMITS FOR 11 YEARS (8.8 EFPY) OF OPERATION.

FSAR FIGURE 5.3-4

MINIMUM TEMPERATURE REQUIRED VS REACTOR PRESSURE

If 2 hr are used for flushing, the minimum time required to reduce vessel coolant temperature to 212°F is depicted by Fig. 5.4-10.

The design basis for the most limiting single failure for the RHR system (shutdown cooling mode) is that one exchanger loop is lost and the plant is then shutdown using the capacity of a single RHR heat exchanger and related service water capability. Fig. 5.4-11 shows the nominal time required to reduce vessel coolant temperature to 212°F using one RHR heat exchanger.

RHR lines in the upper containment pool (Figure 5.4-13) are used in conjunction with the shutdown cooling mode of the RHR during refueling operations when the reactor pressure vessel head is removed. In this alignment, reactor water is pumped from one of the recirculation loops through the RHR system heat exchangers and back to the RPV through the RHR flow distribution spargers located in the upper containment pool. This flow path provides nonlateral flow loads on the fuel during fuel movement. Operation of the RHR in this alignment is initiated and terminated by the operator. 3

5.4.7.1.1.2 Low Pressure Coolant Injection Mode

The functional design basis for the LPCI mode is to pump a total of 5,050 gpm of water per loop using the separate pump loops from the suppression pool into the core region of the vessel, when the vessel pressure is 20 psi over drywell pressure. Injection flow commences at 225 psi vessel pressure above drywell pressure.

The initiating signals are: low vessel water level less than or equal to 1.0 ft above the active core or drywell pressure high greater than or equal to 2.0 psig. The pumps attain rated speed in 27 sec and injection valves fully open in 37 sec.

5.4.7.1.1.3 Suppression Pool Cooling Mode

The functional design basis for the suppression pool cooling mode is that it has the capacity to ensure that the suppression pool temperature immediately after a LOCA event with subsequent blowdown through either the SRVs or the vents does not exceed 170°F and anytime after the blowdown does not exceed 185°F. 3 5

5.4.7.1.1.4 Reactor Steam Condensing Mode

The functional design basis for the reactor steam condensing mode is that the heat exchanger in one loop of the RHR system, in conjunction with the RCIC turbine, is able to

Blowdown Flow and Energy Rates (Recirculation Pump Suction Line Break)

Fig. 6.2-31 shows the effect of changes in the reactor blowdown flow rate on peak drywell pressure differential. Nominal blowdown (Table 6.2-6) is calculated from the Moody frictionless flow model. The Moody flow rate is about 40 percent above experimental data and is, therefore, conservative[5,6].

Level Swell Time (Main Steam Line Break)

Fig. 6.2-32 shows the effect of changes in the reactor level swell time on peak drywell pressure differential. Nominal reactor level swell time is 1.05 sec and is calculated by the method described in Reference 1. This method is essentially the same as that given in Appendix B of GE Topical Report NEDO-10329[7], which agrees with the experimental data contained in the same report.

Initial Suppression Pool Temperature

Fig. 6.2-33 shows the effect of changes in the initial suppression pool temperature on peak containment pressure. The temperature used in the containment analysis is 100°F, which is the maximum normal operating suppression pool temperature. Suppression pool temperature is a plant operating parameter that is continuously monitored and subject to a technical specification limit.

Decay Heat Rate

Fig. 6.2-34 shows the effect of changes in the decay heat rate on peak containment pressure. The decay heat rate used in the FSAR analysis is calculated from Branch Technical Position ASB 9-2[12], with the following positive uncertainties:

Reactor Cooling Time (t)	Uncertainty (%)
$t<10^3$ sec	+20
10^3 sec $\leq t \leq 10^7$ sec	+10
$t>10^7$ sec	+10

15

Containment Unit Cooler Heat Transfer Coefficient

The sensitivity of the peak containment atmosphere pressure to changes in the containment unit cooler heat transfer coefficient is discussed in Section 6.2.2 and shown on Fig. 6.2-35.

In the long-term, fission product decay heat continues to be absorbed by the suppression pool. Unless this energy is removed from the suppression pool, an unacceptably high containment pressure eventually results. The suppression pool cooling mode of the RHR system is used to remove heat from the suppression pool and to limit the long-term, post-LOCA containment internal pressure and suppression pool temperature to less than 15 psig and 185°F, respectively.

In order to evaluate the adequacy of the RHR system, the following sequence of events is assumed to occur:

1. With the reactor initially at 102 percent of rated thermal power (2,952 MWt), a recirculation pump suction line DER occurs.

2. A loss of offsite power occurs and one standby diesel generator fails to start and remains out of service during the entire transient. This is the most limiting single failure.

3. Only three ECCS pumps are functional following the postulated loss of offsite power and standby diesel generator failure. The Division II standby diesel generator supplying two of the LPCI pumps is assumed to have failed, so that the three operating pumps serve the LPCS, LPCI, and the HPCS. Section 6.3 describes the ECCS equipment.

4. After 30 minutes, the plant operators actuate the RHR heat exchanger in the active suppression pool cooling loop in order to start containment heat removal. This involves shutting down the LPCS pump and starting up an additional standby service water pump.

Once the suppression pool cooling mode has been established, no further operation action is required.

When calculating the long-term, post-LOCA containment pressure and suppression pool temperature, it is assumed that the initial suppression pool and RHR standby service water temperature are at their maximum normal operating values of 100°F and 95°F, respectively. This assumption maximizes the heat sink temperature to which the containment heat is rejected and thus maximizes the suppression pool temperature and containment pressure responses.

In addition, the RHR heat exchanger and containment unit cooler are assumed to be in a fully fouled condition during

TABLE 6.3-2 (Cont)

B.2	LPCS system		
	Vessel pressure at which flow may commence	265 psid (vessel to drywell)	
	Minimum rated flow at vessel pressure	4900 gpm 113 psid (vessel to drywell)	
	Initiating Signals		
	Low water level or High drywell pressure	1.0 ft above top of active fuel 2.0 psig	15
	Minimum allowed (runout) flow	5500 gpm	15
	Maximum allowed delay time from initiating signal to pump at rated speed	27 sec	
	Pressure at which injection valve may open	450 psia	
	Injection valve fully open Greater of a) sec after DBA b) sec after pressure permissive	 40 27	15
B.3	HPCS		
	Vessel pressure at which flow may commence	1177 psia	
	Minimum rated flow available at vessel pressure	467 gpm @ 1177 psid 1400 gpm @ 1147 psid 5010 (4900) gpm @ 200 psid (vessel to pump suction)	

For each fuel load, high-high flux trip inputs from each source range monitor (SRM) are combined with IRM and APRM trips to produce a noncoincident reactor NMS trip. Following each fuel loading, this noncoincident trip is removed.

The NMS logic contacts for IRM and APRM can be bypassed by selector switches located in the main control room. APRM channels A, C, E, and G bypasses are controlled by one selector switch and channels B, D, F, and H bypasses are controlled by a second selector switch. Each selector switch can bypass only one APRM channel at one time.

IRM channels A, C, E, and G and channels B, D, F, and H are bypassed in the same manner as the APRM channels.

Bypassing either an APRM or an IRM channel does not inhibit the NMS from providing protective action when required.

(1) Intermediate Range Monitors (IRM)

The IRM channels monitor neutron flux between the upper portion of the SRM range and the lower portion of the APRM range. The IRM detectors are positioned in the core remotely from the main control room.

The IRM is divided into two groups of four IRM channels. Two IRM channels are associated with each of the trip channels of the RPS. The arrangement of IRM channels allows only one IRM channel in each group to be bypassed at one time.

Each IRM channel includes four trip circuits. One trip circuit is used as an instrument trouble trip. It operates on three conditions: 1) when the high voltage drops below a preset level, 2) when one of the modules is not plugged in, or 3) when the OPERATE-CALIBRATE switch is not in the OPERATE position. Each of the other trip circuits is specified to trip when preset downscale or upscale levels are reached.

The reactor mode switch determines whether IRM trips are effective in initiating a reactor scram. With the reactor mode switch in REFUEL or STARTUP, an IRM upscale or inoperative trip signal actuates an NMS trip of the RPS. Only one of the IRM channels must trip to initiate an NMS trip of the associated RPS trip channel.

After the first trip channel is reset, the second trip channel is tripped manually and so forth for the four manual scram switches. In addition to main control room annunciator and computer printout indications, scram group indicator lights verify that the trip actuator contacts have opened and interrupted power to the scram solenoids.

The single rod scram test, which verifies capability of each rod to scram. It is accomplished by operating two toggle switches on the hydraulic control unit for the particular CRD. Timing traces can be made for each rod scrammed.

The sensor test involves applying a test signal to each RPS sensor or trip unit in turn and observing the trip channel trip results. The test signals can be applied to the processing sensing instrumentation (pressure and differential pressure) through calibration taps.

A test of individual scram discharge instrument volume water level sensors can be performed during full power operation by valving out the sensor and injecting water into a test tap. At plant shutdown, the level transmitters may be calibrated by introducing a fixed volume of water into the discharge instrument volume and observing that all level transmitters operate at the specified trip points.

During plant operation, the operator can set the turbine stop valve or MSIV closure logic test switch in test position and actuate the other valve which completes the respective channel trip with annunciation and computer logging. The operator can then confirm that the MSIV and turbine stop valve limit switches operate during valve motion, from full open to full closed and vice versa, by comparing the time that the RPS channel trip occurs with the time that the valve position indicator lights in the main control room signal that the valve is fully open and fully closed. This test does not confirm the exact set point, but does provide the operator with an indication that the limit switch operates between the limiting positions of the valve. During reactor shutdown, calibration of the MSIV and turbine stop valve limit switch set point at a valve position of less than or equal to 10 percent closure is possible by physical observation of the valve stem. 8 and 5 percent respectively

During reactor operation, a test and calibration of the individual EHC oil line pressure sensors associated with TCV closure when the plant is operating above 40 percent of rated power may be accomplished by valving one sensor out-of-service at a time and introducing a test pressure input.

(d) Steam Bypass Operation

Fast opening of the steam bypass valves during turbine trips or generator load rejections requires coordinated action with the turbine control system. When the TCVs are under pressure control, no bypass steam flow is demanded; conversely, when the turbine speed-load demand falls below the pressure regulation demand, a net bypass flow demand is computed. During turbine or generator trip events resulting in fast-closure of the turbine stop or control valves, the TCV demand is immediately tripped to zero as an anticipatory response, causing the bypass steam flow demand to equal the initial pressure regulation demand.

(e) Loss of Turbine Control System Power

Turbine controls and valves are designed so that the turbine stop and control valves close upon loss of control system power or hydraulic pressure.

7.7.1.5 Refueling Interlocks

1. Refueling Interlocks Function

The purpose of the refueling interlocks is to restrict the movement of control rods and the operation of refueling equipment. This reinforces operational procedures that prevent the reactor from becoming critical during refueling operations.

2. Refueling Interlocks Operation

The refueling interlocks circuitry senses the condition of the refueling equipment and the control rods to prevent the movement of the refueling equipment or withdrawal of control rods (rod block). Redundant circuitry is provided to sense the following conditions:

1. All rods inserted
2. Refueling platform positioned near or over the core
3. Refueling platform hoists (fuel grapple, frame-mounted hoist, trolley-mounted hoist) fuel loaded (monorail)
4. Reactor mode switch in REFUEL position.

The indicated conditions are combined in logic circuits to satisfy all restrictions on refueling equipment operations

and control rod movement (Table 7.7-1). A two-channel circuit indicates that all rods are in. The rod-in condition for each rod is established by the closure of a magnetically operated reed switch in the rod position indicator probe. The rod-in switch is generated. Both channels must indicate "all-rods-in" to allow refueling equipment to be used.

During refueling operations, no more than one control rod is permitted to be withdrawn; this is enforced by a redundant logic circuit that uses the all-rods-in signal and a rod selection signal from the RC&IS to prevent the selection of a second rod for movement with any other rod not fully inserted. Control rod withdrawal is prevented by comparison between the A and B portions of the RC&IS rod position with a subsequent rod withdrawal block if necessary. With the mode switch in the REFUEL position, the circuitry prevents the withdrawal of more than one control rod and the movement of the loaded refueling platform over the core with any control rod withdrawn.

Operation of refueling equipment is prevented by interrupting the power supply to the equipment. The refueling platform is provided with two mechanical switches attached to the platform, which are tripped open by a long stationary ramp mounted adjacent to the platform rail. The switches open before the platform or any of its hoists are physically located over the reactor vessel to indicate the approach of the platform toward its position over the core.

Load cell readout is provided for all hoists. Indicators display given hoist loads directly to the operator. Load sensing is by hydraulic load cells that use demineralized water as the operating fluid. Associated interlock and load functions are performed by pressure switches that sense the pressure generated by the hydraulic load cells.

The three hoists on the refueling platform are provided with switches that open when the hoists are fuel loaded. The switches open at a load weight that is lighter than that of a single fuel assembly. This indicates when fuel is loaded on any hoist.

The rod block interlocks and refueling platform interlocks provide two independent levels of interlock action. The interlocks which restrict operation of the platform hoist and grapple provide a third level of interlock action since they would be required only after a failure of a rod block and refueling platform interlock.

The fuel grapple hoist interlocks with the rod block circuitry and refueling platform drive circuitry as well as hoist power. The monorail-mounted and frame-mounted auxiliary hoists interface with hoist power only.

interlock is provided to avoid accidental paralleling. There is no sharing of the HPCS power system with other standby diesel generators.

The HPCS power system loads consist of the HPCS pump/motor and associated auxiliaries, motor-operated valves, one standby service water pump, and miscellaneous auxiliary loads. Table 8.3-3 shows the Division III loads.

The HPCS pump motor is a General Electric 4kV vertical induction motor rated at 2500 hp. The vertical pump was manufactured by the Borg-Warner Byron-Jackson Pump Division. It is rated at 5,125 gpm with 945 ft of head and its motor has a maximum shaft bhp of 2,500 at 1,780 rpm.

The HPCS electric system is capable of performing its function when subjected to the effects of design bases natural phenomena. It is designed in accordance with Seismic Category I and housed in a Seismic Category I structure.

The detailed description of the fuel oil storage and transfer system associated with the HPCS diesel generator unit is described in Section 9.5.4. Fuel for the HPCS diesel engine is provided in a separate day tank and in a storage tank. The day tank permits a minimum of 1 hr of operation at rated load. The combined capacity of the day tank and the storage tank permits the HPCS diesel engine to operate at continuous rated load conditions for at least 7 days.

The engine air starting system contains two complete sets of starting components, either of which is capable of starting the engine. Each set of components consists of dual air start motors, air relay valve, solenoid valve, air receivers, and air compressor assembly. One of the compressors for the HPCS diesel generator is electric motor driven, and the other is diesel engine driven. Both compressors are capable of automatic start and stop and are controlled by pressure switches to maintain required pressure in the air receivers. The two air starting systems are redundant, independent, and arranged so that failure of start in one system causes automatic transfer to the other system. to will not jeopardize starting of the diesel generator by the other system.

Manual controls are provided to permit the operator to select the most suitable distribution path from the power

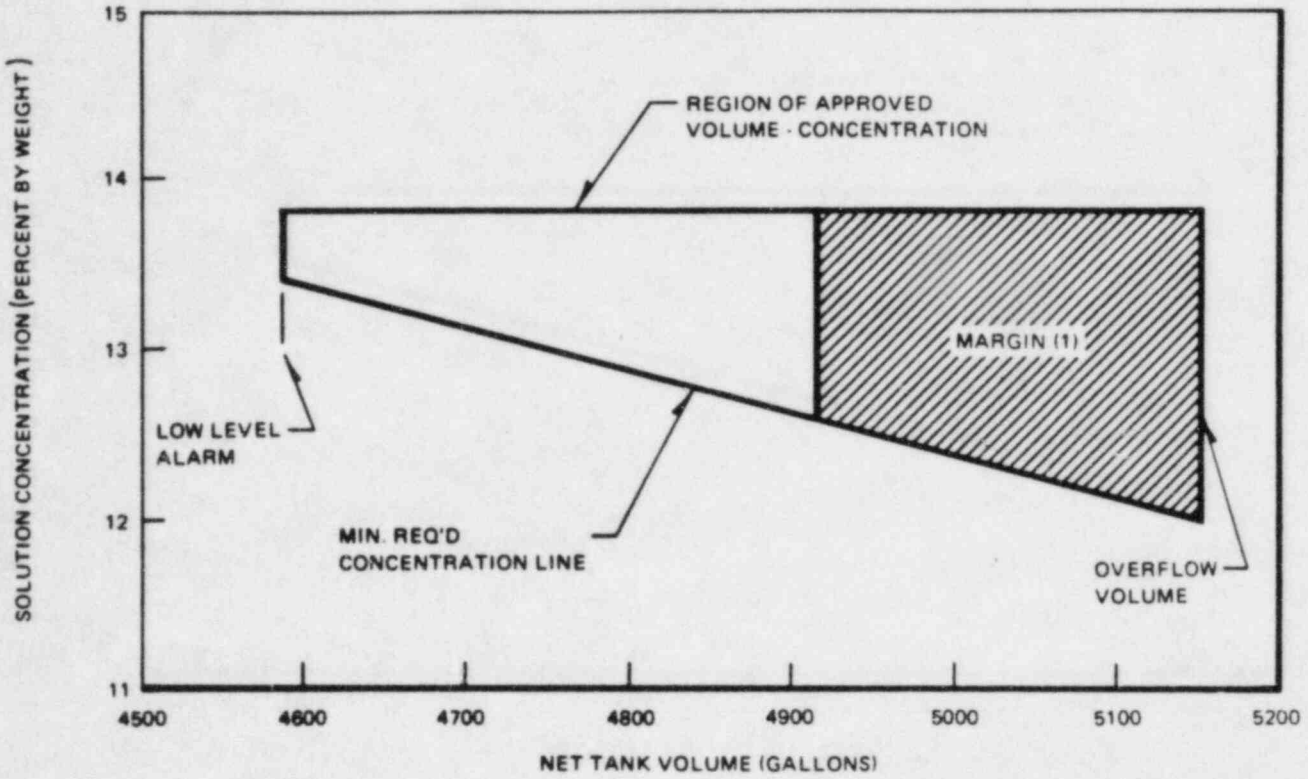

NOTE(1)
G.E. RECOMMENDS 6 IN. OF MARGIN BETWEEN MAXIMUM OPERATING AND OVERFLOW LEVELS

Replace with attached

FIGURE 9.3-14

SODIUM PENTABORATE
($Na_2B_{10}O_{16}\cdot 10H_2O$) VOLUME / CONCENTRATION REQUIREMENTS

RIVER BEND STATION
FINAL SAFETY ANALYSIS REPORT

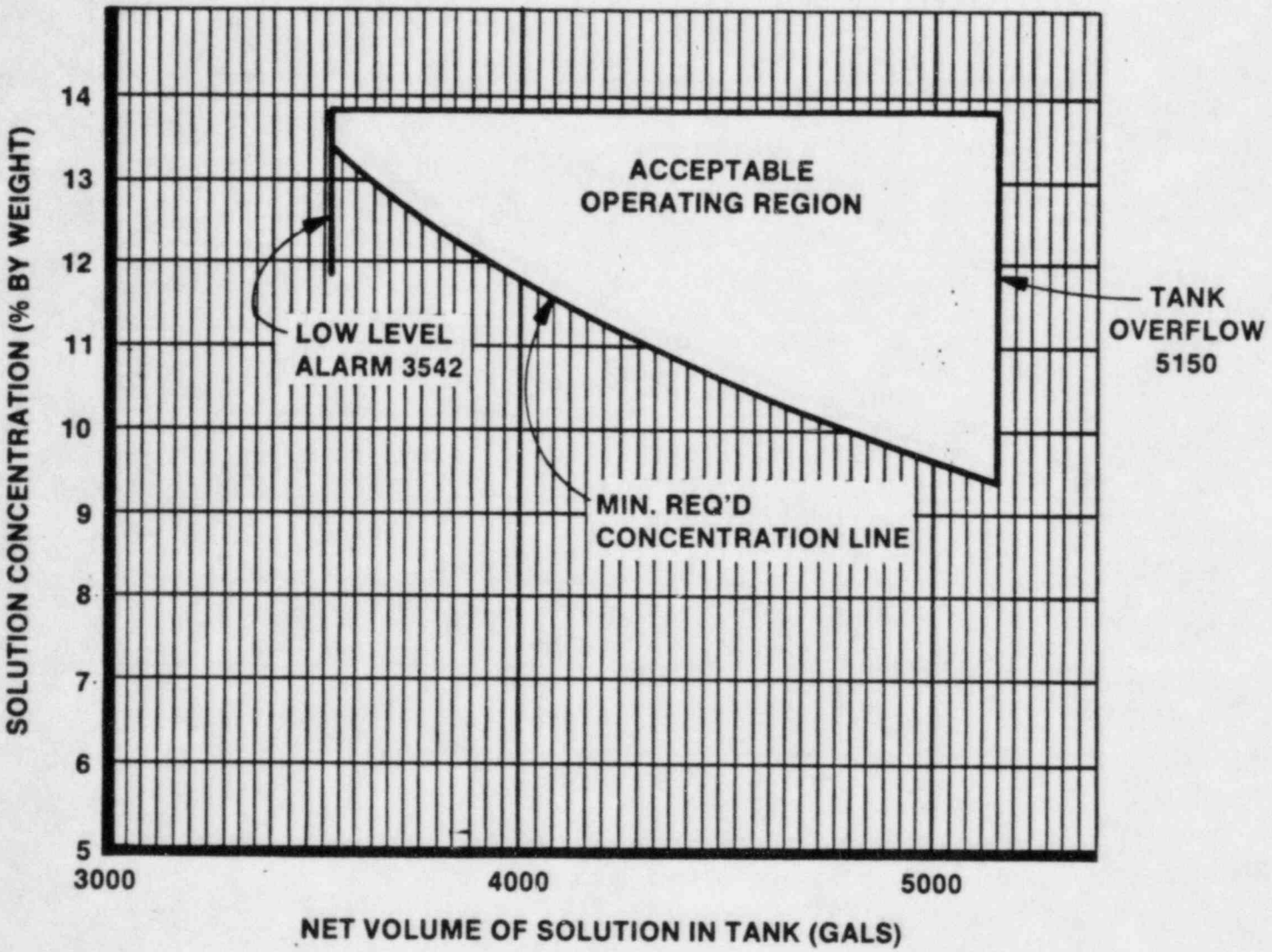

FSAR FIGURE 9.3-14
SODIUM PENTABORATE SOLUTION VOLUME/CONCENTRATION REQUIREMENTS

2. During operation mode, the cooling water leakage will result in a drop of water pressure and activate a "Low Cooling Water Pressure" alarm.

3. During the operating mode, persistent leakage will also cause a rise in the cooling temperature and a "High Water Temperature" alarm will annunciate at local panel. These will alert the operator to the system toruble and operating procedures will be followed to take corrective action. 11

4. Lube oil leakage into the cooling water system will result in a drop of pressure and will be alarmed as a "Low Lube Oil Pressure" alarm at the local panel.

9.5.6 Diesel Generator Starting System (DGSS)

The DGSS for the standby diesel generators and the High Pressure Core Spray (HPCS) diesel generator is shown in Fig. 9.5-2b and 9.5-2d. 14

9.5.6.1 Design Bases

The DGSS is designed in accordance with the following criteria:

1. Each emergency diesel generator is provided with a separate and independent compressed-air starting system.

2. The components of the DGSS essential to the starting of a diesel engine are designed to Safety Class 3, and Seismic Category I requirements. The components of the DGSS are housed within the diesel generator building which is a Seismic Category I structure capable of protecting the system from extreme natural phenomena, such as earthquakes, tornados, hurricanes, and floods.

3. The DGSS is designed so that a single failure of any active or passive component, assuming a loss of offsite power, cannot result in the loss of more than one diesel generator starting system train. 5

4. Piping which forms integral part of the diesel engine is designed in accordance with ANSI Piping Code B31.1. The remainder of the piping is designed in accordance with ASME III, Class 3. The air receivers associated with the DGSS are designed and constructed in accordance with the requirements of ASME Code, Section III, Class 3.

5. Each redundant DGSS train is capable of providing the standby diesel generator with eight starts (five of them are 10 sec starts) from two air receivers without recharging the associated air receivers.

6. The HPCS diesel generator air start subsystem has sufficient capacity to start the diesel generator within 10 seconds five times without recharging, when operated in its normal configuration using both redundant trains through all air start motors, and when initially charged to 215 psig. ~~At this pressure the diesel-driven air compressor is automatically operated to replenish the air supply to 250 psig.~~ 13 15 13

7. The DGSS will be evaluated for the consequences of moderate energy line breaks in accordance with the guidelines given in Section 3.6. The moderate energy lines installed in the diesel generator room are the air start piping and components, and the standby service water piping and components. There are no high energy lines which could affect the system. 7

9.5.6.2 System Description

9.5.6.2.1 Standby Diesel Generators

Each DGSS for each standby diesel generator consists of the following major components and associated piping, valves, and controls:

1. Two starting air compressors (nonsafety-related)

in the distributors causes spool valves to engage and follow the profile of the air starting cams on the ends of the camshaft. The cam profiles are so designed that at least one spool valve is always in position to emit a pilot signal to the proper cylinder, causing that cylinder's air starting valve to admit 250 psig air into the combustion chamber, forcing the piston down to rotate the crankshaft. As the engine rotates, timed and sequenced pilot air signals are emitted, starting 5 deg before top dead center and ending at 115 deg after top dead center. When the starting signal is cut off, the spool valves lift off the cam.

9.5.6.2.2 HPCS Diesel Generator

The DGSS for the HPCS diesel generator consists of the following major components and the associated piping, valves, and controls:

1. Two starting air compressors
2. Two starting air dryers
3. Two starting air receivers (64 cu ft each)
4. Two starting air motors.

There are two independent air starting systems. The air supply system contains one receiver in each redundant system. Each system has one air compressor for charging air into the air receivers. One of the air compressors is electric motor driven and the other is diesel engine driven.

1. The electric motor-driven air compressor is powered from the HPCS bus. It is automatically started when the air pressure in the receiver drops below 225 psig and shuts off when the air pressure reaches 250 psig.

245

2. The diesel-driven air compressor is air-cooled and supplied by a 2 1/2-gallon, engine-mounted, fuel tank. It is automatically started when the air pressure in the receiver drops below 215 psig and shuts off when the air pressure reaches 250 psig. The exhaust for the engine discharges to atmosphere within the HPCS DG exhaust silencer missile enclosure.

11

225

245

The air supply train with a diesel-driven air compressor thus provides a backup for the electric motor-driven air compressor train. The diesel-driven air compressor is

13

15

started by a 125-V dc motor which is connected to the 125-V dc standby bus C and associated battery chargers (Fig. 8.3-6). Additional discussion of instrumentation requirements for the air compressors is provided in Section 9.5.6.5. The air receivers are equipped with safety/relief valves which operate at 270 psig. Both air compressors are provided with intake air filters. 250

Each air starting system has two rotary vane air motors. On receipt of the engine start signal, a normally closed solenoid valve opens and air flows to the piston for the pinion gear of the lower motor. The entry of air moves the pinion gear forward to engage with the engine ring gear. Movement of the pinion gear uncovers a port, allowing air pressure to be released to the upper motor pinion gear piston which, in turn, engages its pinion gear with the engine ring gear. Full engagement of the upper pinion gear permits air flow to the air valve which, in turn, opens the air starting valve and releases the main starting air

energy standby service water piping installed in the diesel generator building are evaluated in accordance with the guidelines given in Section 3.6 to assure that the ability of the DGSS to perform its safety function is not impaired. Detailed results will be provided in Appendix 3C. | 7 | 11

During normal plant operation, compressed air for each diesel is stored in an individual starting system. The starting system for each diesel is comprised of redundant starting trains. The system for the standby diesel generator stores sufficient air in each redundant train to start the engine eight times without operation of the compressors. The system for the HPCS diesel generator has adequate air storage capacity to start the engine five consecutive times without recharging when operated in its normal configuration using both redundant trains through all air start motors, and when initially charged to ~~250~~ 245 psig. | 5 | 11

The starting air receivers (storage tanks) are provided with drains which are opened periodically to remove any moisture or oil carryover which may have accumulated from the starting air compressors. This minimizes the formation of

11.5.2.2.2 Off Gas Pretreatment Radiation Monitoring System

This system monitors radioactivity in the condenser off gas at the discharge of the delay pipe after it has passed through the off gas condenser and moisture separator. The monitor detects the radiation level which is attributable to the fission gases produced in the reactor and transported with steam through the turbine to the condenser.

A continuous sample is extracted from the off gas pipe via a sample line. It is then passed through a sample chamber and a sample panel before being returned to the suction side of the steam jet air ejector (SJAE). The sample chamber is a steel pipe which is internally polished to minimize plateout. It can be purged with room air to check detector response to background radiation by using a three-way solenoid operated valve. The valve is controlled by a switch located in the main control room. The sample panel measures and indicates sample line flow. A sensor and convertor (GM tube) is positioned adjacent to the vertical sample chamber and is connected to a radiation monitor in the main control room.

Nonsafety-related power is supplied from the 125-V dc bus B for the radiation monitor and recorder, and from a 120-V ac local bus for the sample and vial sampler panels.

The radiation monitor has four trip circuits: two upscale (high-high and high), one downscale (low), and one inoperative.

The trip outputs are used for alarm function only. Each trip is visually displayed on the radiation monitor and actuates a main control room annunciator: off gas high-high, off gas high, and off gas downscale/inoperative. High or low sample line flow measured at the sample panel actuates a main control room off gas sample high-low flow annunciator.

The radiation level output by the monitor can be directly correlated to the concentration of the noble gases by using the semiautomatic vial sampler panel to obtain a grab sample. To draw a sample, a serum bottle is inserted into a sample chamber, the sample lines are evacuated, and a solenoid-operated sample valve is opened to allow off gas to enter the bottle. The bottle is then removed and the sample is analyzed in the counting room with a multichannel gamma pulse height analyzer to determine the concentration of the various noble gas radionuclides. A correlation between the

these cases, the decay ratio for each controlled mode of response is less than or equal to 0.25. 5

b. The temperature measured by thermocouples on the discharge side of the valves returns to within 10°F of the temperature recorded before the valve was opened. If pressure sensors are available, they return to their initial states upon valve closure.

c. During the 250 psig functional test the steam flow through each relief valve, as measured by the initial and final bypass valve position, is not less than 10 percent of valve position under the average of all valve responses.

d. During the rated pressure test the steam flow through each relief valve, as measured by MWe, is not less than 0.5 percent of rated MWe less than the average of all the valve responses.

15

e. When the low-low pressure relief logic functions, the open/close actions of the SRVs occur within ±13 psi and ±20 psi, respectively, of their design points.

14.2.12.3.24 Test Number 27 - Turbine Trip and Generator Load Rejection 5

1. Test Objective

The purpose of this test is to demonstrate the response of the reactor and its control systems to protective trips in the turbine and generator.

2. Prerequisites

The appropriate preoperational tests have been completed; the FRC has reviewed and approved the test procedures and initiation of testing. All controls and interlocks are checked and instrumentation calibrated.

bundle is operating at or above the MCPR limit of 1.18 for the initial cycle and an estimated operating limit MCPR for subsequent cycles of 1.19. Maintaining MCPR greater than 1.06 for the initial cycle and 1.07 for subsequent cycles is a sufficient, but not necessary, condition to assure that no fuel damage occurs. This is discussed in Section 4.4.

For situations in which fuel damage is sustained, the extent of damage is determined by correlating fuel energy content, cladding temperature, fuel rod internal pressure, and cladding mechanical characteristics.

These correlations are substantiated by fuel rod failure tests and are discussed in Section 4.4 and Section 6.3.

15.0.3.3.2 Input Parameters and Initial Conditions for Analyzed Events

In general, the events analyzed within this section have values for input parameters and initial conditions as specified in Table 15.0-2. Analyses which assume data inputs different from these values are designated accordingly in the appropriate event discussion.

Add insert A (attached) →

15.0.3.3.3 Initial Power/Flow Operating Constraints

The analysis basis for most of the transient safety analyses is the thermal power at rated core flow (100 percent) corresponding to 105 percent nuclear boiler rated (NBR) steam flow. This operating point is the apex of a bounded operating power/flow map which, in response to any classified abnormal operational transients, yields the minimum pressure and thermal margins of any operating point within the bounded map. Referring to Fig. 15.0-1, the apex of the bounded power/flow map is point A, the upper bound is the design flow control line (104.2 percent rod line A-D), the lower bound is the zero power line H-J, the right bound is the rated core flow line A-H, and the left bound is the natural circulation line D-J.

The power/flow map A-D-J-H-A represents the acceptable operational constraints for abnormal operational transient evaluations.

Any other constraint which may truncate the bounded power/flow map must be observed, such as the recirculation valve and pump cavitation region, the licensed power limit and other restrictions based on pressure and thermal margin criteria. For instance, if the licensed power is 100 percent NBR, the power/flow map is truncated by the line

Insert A (for page 15.0-9)

The transient analyses for River Bend were performed using nuclear parameters representative of the End of Equilibrium Cycle (EOEC) nuclear characteristics for the core design before the Control Cell Core concept was adopted. Comparisons of the void coefficients and scram characteristics used for these analyses were made with those for the End of Cycle One (EOC1) characteristics of the Control Cell Core (CCC). These comparisons demonstrated that the analyses results described in this chapter for the EOEC, non-CCC are bounding relative to the EOC1, CCC reactor for all limiting transients and accidents.

The void co-efficients and scram curves were determined from the ODYN code output (see Section 15.1.2.3.1 for additional information on this model). The one-dimensional input to ODYN was obtained from the three-dimensional BWR Core Simulator Model (see Section 15.4.2.3.1 for additional description of this code). The void co-efficient for the original core at EOEC was found to be 42 % greater than that for the current design at EOC1, (-) 11.4¢/% rated void vs (-) 8.0¢/% rated voids, respectively.

The (negative) scram reactivity insertion, as shown on Figure 15.0-4, similarly favors the current CCC design at EOC1. Future cycle core loadings will be analyzed and presented in the plant's reload licensing submittal.

TABLE 15.0-2

INPUT PARAMETERS AND INITIAL CONDITIONS FOR TRANSIENTS

1. Thermal power level, MWt	
Warranted value	2,894
Analysis value	3,015
2. Steam flow, lb/hr	
Warranted value	12.45×10^6
Analysis value	13.07×10^6
3. Core Flow, lb/hr	84.5×10^6
4. Feedwater flow rate(1), lb/sec	
Warranted value	3,458
Analysis value	3,631
5. Feedwater temperature, °F	425
6. Vessel dome pressure, psig	1,045
7. Vessel core pressure, psig	1,056
8. Turbine bypass capacity, % NBR	10
9. Core coolant inlet enthalpy, Btu/lb	529.9
10. Turbine inlet pressure, psig	960
11. Fuel lattice	P 8x8R
12. Core average gap conductance, Btu/sec-ft²-°F	0.1892
13. Core leakage flow, %	11
14. Required MCPR operating limit	
First core	1.18
Reload core	1.19
15. MCPR safety limit	
First core	1.06
Reload core	1.07
16. Doppler coefficient (-) ¢/°F	
Analysis data(2)	0.132
17. Void coefficient (-) ¢/% rated voids	
Analysis data for power increase events(2)(4)	14.0
Analysis data for power decrease events(2)	4.0
18. Core average rated void fraction, %(2)	42.53
19. Scram reactivity, Analysis data(2)(4)	Fig. 15.0-2
20. Control rod drive speed, position versus time	Fig. 15.0-3
21. Jet pump ratio, M	2.47

TABLE 15.0-2 (Cont)

22. SRV capacity, % NBR @ 1,210 psig	109.4
Manufacturer	Crosby
Quantity installed	16
23. Relief function delay, sec	0.40
24. Relief function response	
Time constant, sec	0.10
25. Safety function delay, sec	0.0
26. Safety function response	
Time constant, sec	0.2
27. Set points for SRVs	
Safety function, psig	1175, 1185, 1195 1205, 1215
Relief function, psig	1125, 1135, 1145 1155
28. Number of valve groupings simulated	
Safety function, no.	5
Relief function, no.	4
29. SRV reclosure	
Set point - both modes (% of set point)	
Maximum safety limit (used in analysis)	98
Maximum operational limit	89
30. High flux trip, % NBR	
Analysis set point (122 x 1.042)	127.2
31. High pressure scram set point, psig	1,095
32. Vessel level trips, ft above bottom of separator skirt bottom	
Level 8 - (L8), ft	5.88
Level 4 - (L4), ft	4.03
Level 3 - (L3), ft	2.16 1.94
Level 2 - (L2), ft	(-) 1.217 2.86
33. APRM simulated thermal power trip, % NBR	
Analysis set point (114 x 1.042)	118.8
34. Time constant, sec	7
35. Nuclear characteristics used in ODYN simulations (4)	End of equilibrium cycle (EOEC)
36. Recirculation pump trip delay, sec	0.14
37. Recirculation pump trip inertia time constant for analysis, sec(3)	max 5.0 min 3.0

TABLE 15.0-2 (Cont)

38. Total steamline volume, ft³	3,275
39. Pressure set point of recirculation pump trip - psig (nominal)	1,135

(1) Includes control rod drive flow
(2) Applicable only for events analyzed using model described in Reference 1 to Section 15.1.
(3) The inertia time constant is defined by the expression:

$$t = \frac{2\pi J_o n}{g T_o}$$

where:

t = Inertia time constant (sec)
J_o = Pump motor inertia (lb-ft)
n = Rated pump speed (rps)
g = Gravitational constant (ft/sec)
T_o = Pump shaft torque (lb-ft)

(4) The transient analyses for RBS are based on End of Equilibrium Cycle nuclear parameters for a pre-Control Cell Core design. These analyses results described in Chapter 15 are bounding for limiting transients relative to the expected performance of the plant at End of Cycle 1 conditions for the Control Cell Core

Instrumentation for pressure sensing of the turbine inlet pressure is designed to be single failure proof for initiation of main steam isolation valve (MSIV) closure.

Reactor scram sensing, originating from limit switches on the MSIV, is designed to be single failure proof. It is therefore concluded that the basic phenomenon of pressure decay is adequately terminated. See Appendix 15A for a detailed discussion of this subject.

15.1.3.3 Core and System Performance

15.1.3.3.1 Mathematical Model

The nonlinear dynamic model described briefly in Section 15.1.1.3.1 is used to simulate this event.

15.1.3.3.2 Input Parameters and Initial Conditions

This transient is simulated by setting the controlling regulator output to a high value, which causes the turbine admission valves and the turbine bypass valves to open fully. Since the controlling and backup regulator outputs are gated by a high value gate, the effect of such a failure in the backup regulator would be exactly the same. A regulator failure with 130 percent steam flow demand was simulated as a worst case since 115 percent is the normal maximum flow limit.

A 5-sec isolation valve closure instead of a 3-sec closure is assumed when the turbine pressure decreases below the turbine inlet low pressure set point for main steam isolation initiation. This is within the specification limits of the valve and represents a conservative assumption.

15 Reactor scram is initiated when the isolation valves reach the 90 percent closed position. This is the maximum travel from the full open position allowed by design specification. |

This analysis has been performed, unless otherwise noted, with the plant conditions listed in Table 15.0-2.

15.1.3.3.3 Results

Fig. 15.1-4 shows graphically how the isolation valve closure stops vessel depressurization and produces a normal shutdown of the isolated reactor.

TABLE 15.1-3

SEQUENCE OF EVENTS FOR FEEDWATER CONTROLLER FAILURE, MAXIMUM DEMAND (FIGURE 15.1-3)

Time (sec)	Event
0	Initiate simulated failure of 130 percent upper limit on feedwater flow at a system design pressure of 1,065 psig
12.2	L8 vessel level set point initiates reactor scram and trips main turbine and feedwater pumps
12.21	RPT actuated by stop valve position switches
12.21	Main turbine bypass valves opened due to turbine trip
13.4	SRVs open due to high pressure
19.7	SRVs close
(20.3) >25 (est)	Water level dropped to low water level set-point (Level 2)
>150 (est)	RCIC and HPCS flow into vessel (not simulated)

TABLE 15.1-4

SEQUENCE OF EVENTS FOR PRESSURE REGULATOR FAILURE - OPEN TO 130% (FIGURE 15.1-4)

Time-sec	Event
0	Simulate steam flow demand to 130 percent
0.5	Main turbine bypass fully opens
8	Turbine control valves wide open
19	Low turbine inlet pressure trip initiates main steam isolation
19.5	MSIV closure initiates reactor scram
22.0	Vessel water level reaches L3 set point. Recirculation pumps trip to low frequency M/G sets.
24.2 (26 (est))	Vessel water level reaches L2 set point. Recirculation pumps trip due to Level 2 RPT signal
25.5(est)	SRVs open
30.5(est)	SRVs close
41.18	Group 1 SRVs open again to relieve decay heat
46.18	Group 1 SRVs close again
54.2 (>50) (est)	HPCS and RCIC flow enters vessel (not simulated)

TABLE 15.2-11

SEQUENCE OF EVENTS FOR LOSS OF NORMAL AND PREFERRED STATION SERVICE TRANSFORMERS (FIGURE 15.2-8)

Time (sec)	Event
0	Loss of normal and preferred station service transformers occurs.
0	Recirculation system pump motors are tripped.
0	Feedwater and condensate pumps are tripped.
2.00	Reactor scram and closure of MSIV occur due to loss of power to the solenoids.
5.10	SRVs open due to high pressure
10.12	SRVs close
12.10	Group 1 SRVs cycle open and close on pressure
21→12.23	Vessel water level reaches Level 2 set point
42.2 >45(est)	HPCS and RCIC flow enters vessel (not simulated)

TABLE 15.2-12

SEQUENCE OF EVENTS FOR LOSS OF ALL GRID CONNECTIONS (FIGURE 15.2-9)

Time (sec)	Event
(-)0.015 (approx.)	Loss of grid causes T-G to detect a loss of electrical load.
0	Turbine control valve fast closure is initiated.
0	T-G power-load unbalance (PLU) trip initiates main turbine bypass system operation.
0	Recirculation system pump motors are tripped.
0	TCV fast closure initiates a reactor scram trip.
0.07	TCVs closed.
0.11	Turbine bypass valves open.
1.33	SRVs open due to high pressure.
2.00	Closure of MSIV due to loss of power.
9.03	SRVs close.
19(est) ~~10.68~~	Vessel water level reaches Level 2 set point.
>45(est) ~~40.68 (est)~~	HPCS and RCIC flow enters vessel (not simulated).

TABLE 15.2-13

SEQUENCE OF EVENTS FOR LOSS OF ALL FEEDWATER FLOW (FIGURE 15.2-10)

Time (sec)	Event
0	Trip of all feedwater pumps initiated.
2.33	Vessel water level reaches level 4 and initiates recirculation flow runback.
4.88	Feedwater flow decays to zero.
8.71	Vessel water level (L3) trip initiates scram trip and recirculation pumps trip to low frequency M/G set.
12.97	Vessel water level reaches Level 2.
13.03 (est)	Recirculation pumps trip due to Level 2 RPT signal.
41.00 (est)	HPCS and RCIC flow enters vessel (not simulated).

control rod movements. In general, very few control rod maneuvers are performed in excess of 65 percent of the rated reactor power. A statistical approach, using appropriately conservative acceptance criteria, shows that consequences of the majority of RWEs are not significant.

15.4.2.2 Sequence of Events and Systems Operation

15.4.2.2.1 Sequence of Events

The sequence of events for this transient is presented in Table 15.4-1.

15.4.2.2.2 System Operations

While operating in the power range, i.e., greater than 20 percent of reactor power in a normal mode of operation, the reactor operator makes a procedural error and withdraws a control rod or gang of control rods continuously until the maximum worth RWL inhibits further withdrawal. The RWI utilizes rod position indications of the selected rod or gang as input.

During the course of this event, normal operation of plant instrumentation and controls is assumed, although no credit is taken for this except as described above.

No operation of any ESF is required during this event.

15.4.2.2.3 Single Failure or Single Operator Error

The effect of operator errors has been discussed above. It was shown that operator errors (which initiated this transient) cannot impact the consequences of this event due to the RCIS system. The RCIS system is designed to be single failure proof; therefore, termination of this transient is assured. See Appendix 15A for details.

15.4.2.3 Core and System Performance

15.4.2.3.1 Mathematical Model

The consequences of an RWE are calculated utilizing a three-dimensional, coupled nuclear-thermal-hydraulics computer program[2]. This model calculates the changes in power level, power distribution, core flow, and CPR under steady-state conditions, as a function of control blade position. For this transient, the time span of the for reactivity insertion is greater than the fuel thermal time constant and core-hydraulic transport times, so that the steady-state assumption is valid.

15.4.2.3.2 Input Parameters and Initial Conditions

The reactor core is assumed to be operating on MCPR and MLHGR technical specification limits prior to RWE initiation. A statistical analysis of the rod withdrawal error results (Reference 3) initiated from a wide range of operating conditions (exposure, power, flow, rod patterns, xenon conditions, etc.) has been performed, establishing allowable rod withdrawal increments applicable to all BWR/6 plants. These rod withdrawal increments were determined such that the design basis ΔCPR (change in the critical power ratio) for rod withdrawal errors initiated from the technical specification operating limit and mitigated by the RWL system provides a 95 percent probability at the 95 percent confidence level that any randomly occurring RWE does not result in a larger ΔCPR. MCPR was verified to be the limiting thermal performance parameter and therefore was used to establish the allowable withdrawal increments. The 1 percent plastic strain limit on the clad was always a less limiting parameter.

15.4.2.3.3 Results

The calculated results demonstrate that, should a rod or gang be withdrawn a distance equal to the allowable rod withdrawal increments, there exists a 95 percent probability at the 95 percent confidence level that the resultant ΔCPR is not greater than the design basis ΔCPR. Furthermore, the peak LHGR is substantially less than that calculated to yield 1 percent plastic strain for the fuel clad.

The results of the generic analyses in Reference 3 show that a control rod or gang can be withdrawn in increments of 12 in at power levels above 70 percent of rated, and 24 in at power levels ranging from 20-70 percent. See Section 15.4.1.2 for RWEs below 20 percent reactor power. The 20 percent and 70 percent reactor core power levels correspond to the low power set point (LPSP) and high power set point (HPSP) of the RWL.

15.4.2.3.4 Consideration of Uncertainties

The most significant area of uncertainty for this transient is the initial control rod pattern and the location of the rod or gang improperly selected and withdrawn. Because of the large number of combinations of control patterns and reactor states, all possible states cannot be analyzed. However, enough states have been evaluated so as to clearly establish the 95 percent probability/95 percent confidence level. Only high worth gangs were included in the

1. Transfer flow control to manual and reduce flow to minimum.

2. Identify cause of failure.

Reactor pressure is controlled as required, depending on whether a restart or cooldown is planned. In general, the corrective action would be to hold reactor pressure and condenser vacuum for restart after the malfunctioning flow controller has been repaired. The following is the sequence of operator actions expected during the course of the event, assuming restart. The operator should:

1. Observe that all rods are in.

2. Check the reactor water level and maintain above low-low level (L2) trip to prevent MSIVs from isolating. L1

3. Switch the reactor mode switch to the startup position.

4. Continue to maintain vacuum and turbine seals.

5. Transfer the recirculation flow controller to the manual position and reduce set point to zero.

6. Survey maintenance requirements and complete the scram report.

7. Monitor the turbine coastdown and auxiliary systems.

8. Establish a restart of the reactor according to the normal procedure.

15.4.5.2.2 Systems Operation

The analysis of this transient assumes and takes credit for normal functioning of plant instrumentation and controls, and the RPS. Operation of engineered safeguards is not expected.

15.4.5.2.3 The Effect of Single Failures and Operator Errors

Both these transients lead to a quick rise in reactor power level. Corrective action first occurs in the high flux trip which, being part of the RPS, is designed to single failure criteria. (See Appendix 15A for details.) Therefore,

shutdown is assured. Operator errors are not of concern here in view of the fact that automatic shutdown events follow so quickly after the postulated failure.

15.4.5.3 Core and System Performance

15.4.5.3.1 Mathematical Model

The nonlinear dynamic model described briefly in Section 15.1.1.3.1 is used to simulate this event.

15.4.5.3.2 Input Parameters and Initial Conditions

These analyses have been performed, unless otherwise noted, with plant conditions tabulated in Table 15.0-2.

In each of these transient events the most severe transient results when initial conditions are established for operation at the low end of the rated flow control rod line. Specifically, this is 56 percent NBR power and 37 percent core flow. The maximum stroking rate of the recirculation loop valves for a master controller failure driving two loops is limited by individual loop controls to 13 percent per sec; however, a conservative value of 13 percent per sec. is used in the analysis.
Maximum stroking rate of a single recirculation loop valve for a loop controller failure is limited by hydraulics to 30 percent per sec.

15.4.5.3.3 Results

15.4.5.3.3.1 Fast Opening of One Recirculation Valve

Figure 15.4-2 shows the analysis of a failure where one recirculation loop main valve is opened at its maximum stroking rate of 30 percent per sec.

The rapid increase in core flow causes a sharp rise in neutron flux initiating a reactor scram at approximately 0.97 sec. The peak neutron flux reached was 472 percent of NBR value, while the accompanying average fuel surface heat flux reaches 84 percent of NBR at approximately 1.8 sec. MCPR remains above the safety limit and fuel center temperature increases only 425°F. Reactor pressure is discussed in Section 15.4.5.4.

15.4.5.3.3.2 Fast Opening of Two Recirculation Valves

Figure 15.4-3 illustrates the failure where both recirculation loop main valves are opened at a maximum

15.4.7.3 Core and System Performance

15.4.7.3.1 Mathematical Model

A three-dimensional BWR simulator model is used to calculate the core performance resulting from this event. This model is described in detail in Reference 2.

Replace with attached insert

15.4.7.3.2 Input Parameters and Initial Conditions

The initial core consists of three bundle types with average enrichments that are high, medium, or low with correspondingly different gadolinia concentrations. The fuel bundle loading error involves interchanging a bundle of one enrichment with another bundle of a different enrichment. The following fuel loading errors can be conceived for an initial core:

1. A high-enriched bundle is misloaded into a low-enriched bundle location.

2. A medium-enriched bundle is misloaded into a low-enriched bundle location.

3. A low-enriched bundle is misloaded into a high-enriched bundle location.

4. A low-enriched bundle is misloaded into a medium-enriched bundle location.

5. A medium-enriched bundle is misloaded into a high-enriched bundle location.

6. A high-enriched bundle is misloaded into a medium-enriched bundle location.

Since all low-enriched bundles are located on the core periphery, the two possible fuel loading errors consisting of the misloading of high- or medium-enriched bundles into a low-enriched bundle location (i.e., Types 1 and 2 from above) are not significant. In these cases, the higher reactivity bundles are moved to a region of lower importance resulting in an overall improvement in performance.

The third type of fuel loading error, as identified above, results in largest enrichment mismatch. However, it does not result in an unacceptable operating consequence. Consider a fuel bundle loading error at beginning-of-cycle (BOC) with the low-enriched bundle (which should be loaded at the periphery) interchanged with a high-enriched bundle

Insert on page 15.4-15

15.4.7.3.2 Input Parameters and Initial Conditions

The initial core consists of five bundle types with average enrichments in the range of high, medium, and low with correspondingly different gadolinia concentrations. The fuel bundle loading error involves interchanging a bundle of one enrichment range with another bundle of a different enrichment range.

A series of fuel loading errors are done by interchanging bundles of different enrichment range in the core. The fuel bundle loading error with greatest impact in thermal margin occurs when a 2.78 percent enriched bundle is interchanged with a 0.94 percent enriched bundle located in the center of the core and away from an LPRM. These bundles have the largest K infinity difference for uncontrolled state at all exposures in the cycle. After the loading errors are made and have gone undetected, the operator assumes that the mislocated bundle is operating at the same power as the instrumented bundles in the mirror image location and operates the plant until end of cycle (EOC). For

the purpose of conservatism, it is assumed that the mirror image bundle is on thermal limits as recorded by the LPRM. As a result of placing the instrumented bundle on limits, the mislocated bundle violates the technical specification operating MCPR limit. However, it does not exceed the MCPR safety limit.

located adjacent to an LPRM and predicted to have the highest LHGR and/or lowest CPR in the core. After the loading error has occurred and has gone undetected, it is assumed, for purposes of conservatism, that the operator uses a control pattern that places the limiting bundle in the four bundle array containing the misplaced bundle, on thermal limits as recorded by the LPRM. As a result of loading the low-enriched bundle in an improper location, the average power in the four bundles decreases. Normally, the reading of the LPRM shows a decrease in thermal flux due to the decreased power; however, in this case an increase in the thermal flux occurs due to decreased neutron absorption in the low-enriched bundle. The effects of the softer neutron spectrum due to the decreased thermal absorption are larger than the power depression effect of the lower fission rate resulting in a net increase in instrument reading. Thus, a fuel loading error of this kind does not result in undetected reductions in thermal margins during power operations.

The fourth and fifth types of fuel loading errors are of the same kind (lower enrichment into higher enrichment) as the third type, and also do not result in a nonconservative operating error.

The fuel bundle loading error with greatest impact on thermal margin is of the sixth type which occurs when a high-enriched bundle is interchanged with a medium-enriched bundle located away from an LPRM. Since the medium- and high-enrichment bundles have a corresponding medium and high gadolinia content, the maximum reactivity difference occurs at end of cycle (EOC) where the gadolinia is burned out. After the loading errors are made and have gone undetected, the operator assumes that the mislocated bundle is operating at the same power as the instrumented bundles in the mirror image location and operates the plant until EOC. For the purpose of conservatism, it is assumed that the mirror image bundle is on thermal limits as recorded by the LPRM. As a result of placing the instrumented bundle on limits, the mislocated bundle violates the technical specification operating MCPR limit.

A summary of input parameters for this analysis is given in Table 15.4-6.

15.4.7.3.3 Results

Results of analyzing the worst fuel bundle loading error are reported in Table 15.4-7. As can be seen, MCPR remains well above the point where boiling transition would be expected

15.4.9.2.3 Effect of Single Failures and Operator Errors

Systems mitigating the consequences of this event are RCIS and APRM scram. The RCIS is designed as a redundant system network and therefore provides single failure protection. The APRM scram system is designed to single failure criteria. Therefore, termination of this transient within the limiting results discussed below is assured.

No operator error (in addition to the one that initiates this event) can result in a more limiting case since the RPS automatically terminates the transient.

Appendix 15A provides a detailed discussion on this subject.

15.4.9.3 Core and System Performance

15.4.9.3.1 Mathematical Model

The analytical methods, assumptions, and conditions for evaluating the excursion aspects of the CRDA are described in detail in References 4, 5, and 6. They are considered to provide a realistic yet conservative assessment of the associated consequences. The data presented in Reference 1 shows that the RCIS banked position mode reduces the control rod worths to the degree that the detailed analyses presented in References 4, 5, and 6 or the bounding analyses presented in Reference 7 are not necessary. References 1, 4, 5, and 6 provide sensitivity studies indicating large margins in peak enthalpy for rod worths below 1 percent Δk. Since this margin is sufficiently large that changes in Doppler coefficients, scram curves, reactivity insertion shape, etc, will not significantly reduce this margin, no unique bounding analysis is needed. Compliance checks are instead made to verify that the maximum rod worth does not exceed 1 percent Δk. 11

If this criterion is not met, then the bounding analysis is performed. The rod worths are determined using the BWR simulator model[2]. Detailed evaluations, if necessary, are made using the methods described in References 4, 5, and 6.

15.4.9.3.2 Input Parameters and Initial Conditions

The core at the time of CRDA is assumed to be at the point in cycle which results in the highest incremental rod worth, to contain no xenon, to be in a hot-startup condition, and to have the control rods in sequence A at 50 percent rod density (groups 1-4 withdrawn). Removing xenon, which competes well for neutron absorptions, increases the

TABLE 15.4-1

SEQUENCE OF EVENTS FOR
ROD WITHDRAWAL ERROR IN POWER RANGE

Elapsed Time	Event
0	Core is operating on thermal limits with a typical control rod pattern.
0	Operator selects and withdraws a single rod or gang of rods continuously.
~1 sec	The local power in the vicinity of the withdrawn rod (or gang) increases. Total core power output increases.
~4* sec	RWL blocks further withdrawal.
~25 sec	Core stabilizes at slightly higher core power level.

*Based on a 1.0-foot RWL increment.

TABLE 15.4-6

INPUT PARAMETERS AND INITIAL CONDITIONS FOR FUEL BUNDLE LOADING ERROR

	Input Parameters	Initial Conditions
1.	Power, % rated	100
2.	Flow, % rated	100
3.	MCPR operating limit (est)	~~1.20~~ 1.18
4.	MLHGR operating limit, kw/ft	13.4
5.	Core exposure	End of cycle

NOTE: Core conditions are assumed to be normal for a hot, operating core at EOC.

TABLE 15.4-7

RESULTS OF MISPLACED BUNDLE ANALYSIS

1.	MCPR limit	(1.20) 1.18 |
2.	MCPR with misplaced bundle	(1.10) 1.08 |
3.	ΔCPR for event	0.10
4.	LHGR limit	13.4
5.	LHGR with misplaced bundle	14.7
6.	ΔLHGR for event	1.3

TABLE 15.4-10

INCREMENT WORTH OF THE MOST REACTIVE ROD USING A BANK POSITION WITHDRAWAL SEQUENCE(1)

Core Condition (MWD/T)	Control Rod Group(2)	Banked At Notch	Control Rod (I,J)	Drops From-To	Increase In k_{eff}
0.0	7	00	(24,33)	00-04	0.00034
0.0	7	04	(24,33/49)	00-08	0.00249 0.0012
0.0	7	08	(24,33/49)	00-12	0.00383 0.0032
0.0	7	12	(24,33/49)	00-48	0.00426 0.0079
0.0	7	48	(24,33/49)	00-48	0.00266 0.0005

---

(1) The following assumptions were made to ensure that the rod worths were conservatively high for the BPWS:
a. BCC 1, 0.0 GWD/St Average Exposure
b. Hot startup
c. No xenon
d. Rod groups 1-6 withdrawn
e. Sequence A

(2) For definition of rod groups, see Reference 1.

15.6.5.2 Sequence of Events and Systems Operation

15.6.5.2.1 Sequence of Events

The sequence of events associated with this accident is shown in Table 6.3-1 for core system performance and Table 6.2-11 for barrier (containment) performance.

Following the pipe break and scram, the MSIVs begin closing on the low-low level signal. The low-low water level or high drywell pressure signal initiate HPCS and LPCS systems at time 0 plus approximately 30 sec. Since automatic actuation and operation of the ECCS is a system design basis, no operator actions are required for the accident. However, the operator should perform the following described actions.

The operator should, after assuring that all rods have been inserted at time 0 plus approximately 10 sec, determine plant condition by observing the annunciators. After observing that the ECCS flows are initiated, the operator should check that the diesel generators have started and are on standby condition. When possible (less than half an hour later), the operator should initiate operation of the RHR system heat exchangers in the suppression pool cooling mode and give instructions to put the service water systems in service. After the RHR system and other auxiliary systems are in proper operation, the operator should monitor the hydrogen concentration in the drywell for proper activation of the recombiner and mixer, if necessary.

15.6.5.2.2 Systems Operations

Accidents that could result in the release of radioactive fission products directly into the containment are the results of postulated nuclear system primary coolant pressure boundary pipe breaks. Possibilities for all pipe breaks sizes and locations are examined in Sections 6.2 and 6.3, including the severance of small process system lines, the main steam lines upstream of the flow restrictors, and the recirculation loop pipelines. The most severe nuclear system effects and the greatest release of radioactive material to the containment result from a complete circumferential break of one of the two recirculation loop pipelines. The minimum required functions of any reactor and plant protection system are discussed in Sections 6.2, 6.3, 7.3, 7.6, and 8.3, and Appendix 15A.

15.6.6.2.3 The Effect of Single Failures and Operator Errors

The feedwater line break outside the containment is a special case of the general LOCA break spectrum considered in detail in Section 6.3. The general single-failure analysis for LOCAs is discussed in detail in Section 6.3.3.3. For the feedwater line break outside the containment, since the break is isolatable, either the RCIC or the HPCS can provide adequate flow to the vessel to maintain core cooling and prevent fuel rod clad failure. A single failure of either the HPCS or the RCIC would still provide sufficient flow to keep the core covered with water. See Section 6.3 and Appendix 15A for detailed description of analysis.

15.6.6.3 Core and System Performance

15.6.6.3.1 Qualitative Summary

The accident evaluation qualitatively considered in this section is considered to be a conservative and envelope assessment of the consequences of the postulated failure (i.e., severance) of one of the feedwater piping lines external to the containment. The accident is postulated to occur at the input parameters and initial conditions as given in Table 6.3-2.

15.6.6.3.2 Qualitative Results

The feedwater line break outside the containment is less limiting than either the steam line break outside the containment (analysis presented in Sections 6.3 and/or 15.6.4), or the feedwater line break inside the containment (analysis presented in Sections 6.3.3 and 15.6.5). It certainly is far less limiting than the DBA (the recirculation line break analysis presented in Sections 6.3.3 and 15.6.5).

The reactor vessel is isolated on low-low water level and the RCIC and/or the HPCS restores the reactor water level to the normal elevation. The fuel is covered throughout the transient, and there are no pressure or temperature transients sufficient to cause fuel damage.

initiate on low-low water level and

15.6.6.3.3 Consideration of Uncertainties

This event was conservatively analyzed and uncertainties were adequately considered (Section 6.3).

TABLE 15.6-8

SEQUENCE OF EVENTS FOR FEEDWATER LINE BREAK OUTSIDE CONTAINMENT

Time (sec)	Event
0	One feedwater line breaks
0+	Feedwater line check valves isolate the reactor from the break
<30	At low low-water reactor level RCIC and HPCS initiate, MSIV closure and reactor scram initiate, and the recirculation pumps trip
2 min (approx)	The SRVs open and close and maintain the reactor vessel pressure at approximately 1,100 psig
1 to 2 hr	Normal reactor cooldown procedure established

5 (approx.) Reactor scram on low water level

<30 HPCS and RCIC start on low-low water level, L2, and are expected to maintain the water level above the low-low-low level, L1, trip and eventually restore it to the normal elevation